Mathematical Modeling of Creep and Shrinkage of Concrete

Edited by
Zdeněk P. Bažant
Professor of Civil Engineering
Northwestern University, Evanston,
Illinois, USA

In collaboration with
International Union of Research and Testing Laboratories
for Materials and Structures (RILEM) and
U.S. National Science Foundation

A Wiley–Interscience Publication

JOHN WILEY AND SONS
Chichester · New York · Brisbane · Toronto · Singapore

Mathematical Modeling of Creep and Shrinkage of Concrete
Edited by Z. Bažant

Chapter 2

Material Models for Structural Creep Analysis[†]

2.1 INTRODUCTION

Creep and shrinkage of concrete is an intricate phenomenon, and a constitutive equation which is both generally applicable and realistic is difficult to formulate. Before the computer era, this task was not really an issue because no structural analysis problems could be solved with a sophisticated constitutive model. After 1970, however, large computer codes that could accept a complicated constitutive model became available. Yet nothing useful could be done with these large codes if a good constitutive model was unavailable. Thus, computers have been providing an impetus for development of realistic constitutive relations for concrete creep and shrinkage, and tremendous progress has taken place during the last fifteen years.

The purpose of this chapter is to review the progress, spell out the fundamental concepts, and emphasize some recent developments that are just becoming ready for computational applications. Since two comprehensive reviews of a similar nature appeared several years ago (ASCE, 1982; Bažant, 1982b), the subjects discussed in depth in these reviews will be covered concisely, while the most recent developments, such as the modeling of creep at variable humidity, will be covered in more detail.

2.2 CONCRETE AS AGING VISCOELASTIC MATERIAL

2.2.1 Compliance function

The total strain of a uniaxially loaded concrete specimen at age t may be subdivided as

$$\begin{aligned}\varepsilon(t) &= \varepsilon_E(t) + \varepsilon_C(t) + \varepsilon_S(t) + \varepsilon_T(t) = \varepsilon_E(t) + \varepsilon''(t) \\ &= \varepsilon_E(t) + \varepsilon_C(t) + \varepsilon^0(t) = \varepsilon_\sigma(t) + \varepsilon^0(t)\end{aligned} \tag{2.1}$$

in which $\varepsilon_E(t)$ is the instantaneous strain, which is elastic (reversible) if the stress is

[†] Principal author: Z. P. Bažant. Prepared by RILEM TC69 Subcommittee 2, the members of which were Z. P. Bažant (Chairman), J. Dougill, C. Huet, T. Tsubaki, and F. Wittmann.

small, $\varepsilon_C(t)$ is the creep strain, $\varepsilon_S(t)$ is the shrinkage (or swelling), $\varepsilon_T(t)$ is the thermal expansion (or dilatation), $\varepsilon^0(t)$ is the stress-independent inelastic strain, $\varepsilon''(t)$ is the inelastic (stress-dependent) strain, and $\varepsilon_\sigma(t)$ is the stress-produced strain, also called the mechanical strain. Strain $\varepsilon_E(t)$ is reversible (recoverable) immediately after the moment of loading. Later, however, it is irreversible due to ageing caused by hydration, as well as by other time-dependent changes in the microstructure; see Section 1.3.

According to these strain definitions, measurement of creep generally requires two identical specimens subjected to exactly the same environmental histories, one specimen being loaded and the other (the companion specimen) being load-free. The difference between the deformations of these two specimens defines the mechanical strain, consisting of creep plus the instantaneous (elastic) deformation.

In this section, we consider only creep at constant stress. By measuring strains of test specimens loaded to different stress levels, and plotting the creep isochrones, representing the curves of stress versus strain for various fixed load durations (see Fig. 2.1), one finds that within the service stress range, i.e. for stresses less than about 0.4 of the strength, these curves are approximately linear. Thus,

$$\varepsilon(t) = \sigma J(t, t') + \sigma^0(t) \tag{2.2}$$

in which σ represents the uniaxial stress, ε is the axial strain, t is the time, normally chosen to represent the age of concrete, and $J(t, t')$ is the compliance function (often also called the creep function); this function represents the strain (elastic plus creep) at time t caused by a unit constant uniaxial stress that has been acting since time t'. Within the linear range, the creep at uniaxial stress is completely characterized by function $J(t, t')$. The typical shape of this function is sketched in Fig. 2.1. The compliance function is often expressed as a sum of the elastic (instant) compliance $1/E(t')$ and the creep compliance $C(t, t')$ (also called the specific creep), i.e.

$$J(t, t') = \frac{1}{E(t')} + C(t, t') = \frac{1 + \phi(t, t')}{E(t')} \tag{2.3}$$

where $E(t')$ is the elastic modulus characterizing the instantaneous deformation at age t', and $\phi(t, t') = E(t')J(t, t') - 1$ is the ratio of the creep deformation to the initial elastic deformation, called the creep coefficient. The values of ϕ for long times such as 30 years usually lie between 1 and 6, with 2.5–3 as typical values. The long-time values of the shrinkage strain, included in ε^0 (Eq. 2.2), are normally between 0.0002 and 0.0008.

The values of the compliance function and shrinkage are influenced by many factors, which may be divided into intrinsic and extrinsic. The intrinsic factors are those that become fixed when the concrete is cast; they include the concrete mix parameters, such as the aggregate fraction, the elastic modulus of aggregate, the

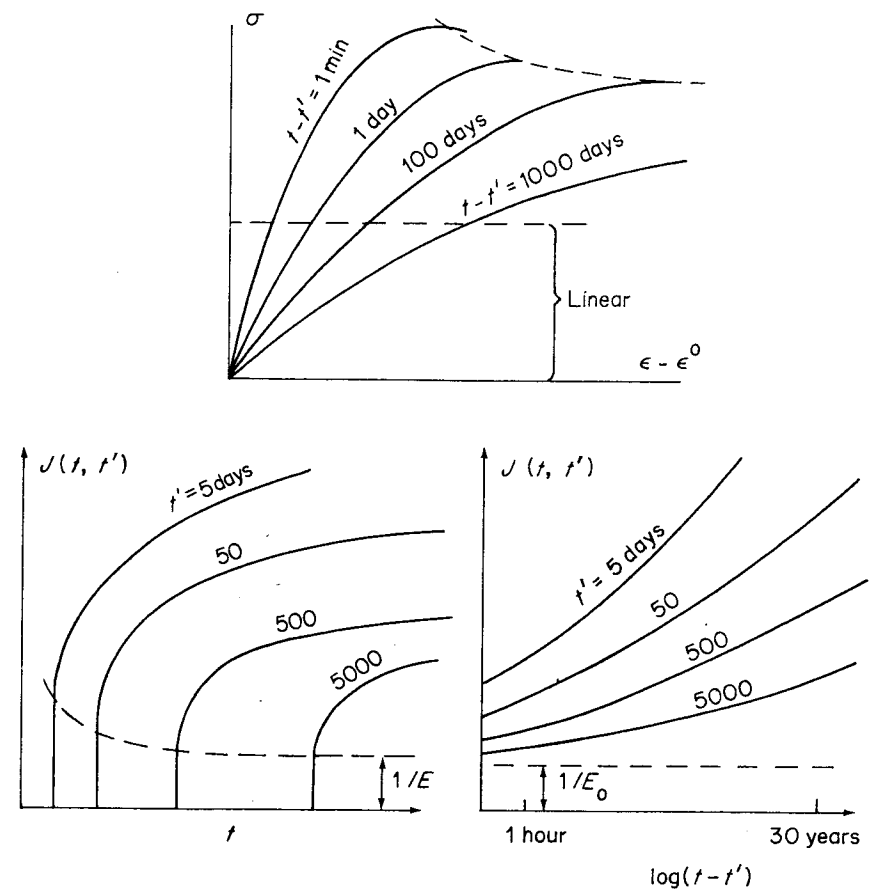

Figure 2.1 Creep isochrones (top), and compliance curves for various ages t' at loading (bottom)

cement content, the water–cement ratio, and the maximum aggregate size, as well as the design strength. The extrinsic factors are those that can be changed externally after the concrete has been cast; they include temperature and the specific water content (including their histories), the age when loading begins, the degree of hydration, etc. The mathematical expressions for the compliance function and the influencing factors will be discussed in more detail in Section 2.5 and in the meantime it will be assumed that the compliance function $J(t, t')$ is known, being given either by an analytical formula, or a graph, or a table of values (Fig. 2.2).

An important property of the compliance function of concrete is that it is a function of two variables, the current age, t, and the age at loading t' (Fig. 2.1). It is a salient characteristic of concrete that the compliance function cannot be considered as a function of one variable, i.e. the time-lag $t - t'$, as is customary in

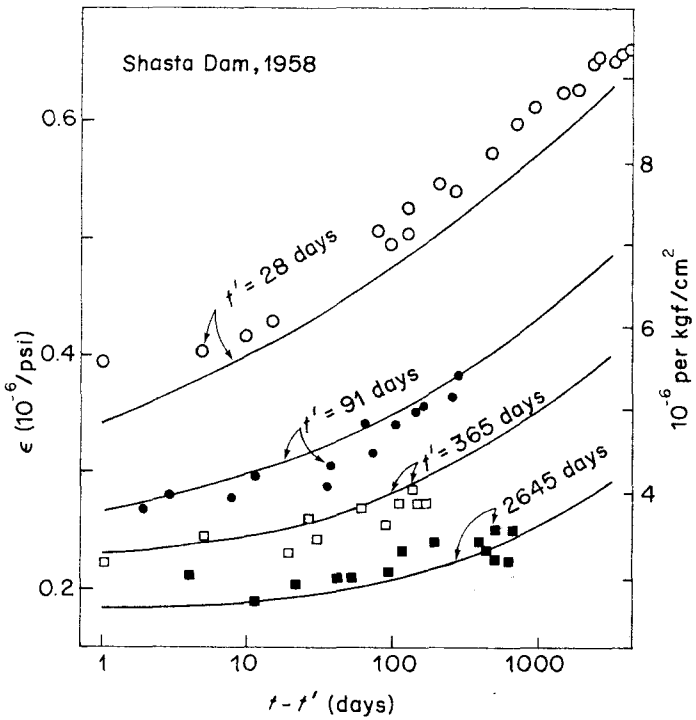

Figure 2.2 Compliance data measured concrete cylinders by Hanson and Harboe, and curves obtained after smoothing with ageing Maxwell chain. (after Bažant and Wu, 1974b, Hanson (1953) and Hanson and Harboe (1958)

classical viscoelasticity for other materials, e.g. polymers. The ageing is a considerable obstacle to analytical solutions of structural problems, and necessitates that most real problems have to be solved by numerical methods.

2.2.2 Principle of superposition

As a consequence of creep and shrinkage, the stress in redundant structures usually varies with time even if the load is constant. The calculation of creep caused by variable stress is greatly facilitated by the principle of superposition. This principle is usually assumed to apply to concrete within the service stress range, and its use in design is permitted by contemporary building codes and recommendations of engineering societies. The principle of superposition, which is equivalent to the hypothesis of linearity of the constitutive equation that relates the stress and strain histories, states that the response to a sum of two stress (or strain) histories is the sum of the responses to each of them taken separately. According to this principle, the strain caused by stress history $\sigma(t)$ may be obtained by decomposing the history into small increments $d\sigma(t')$ applied at

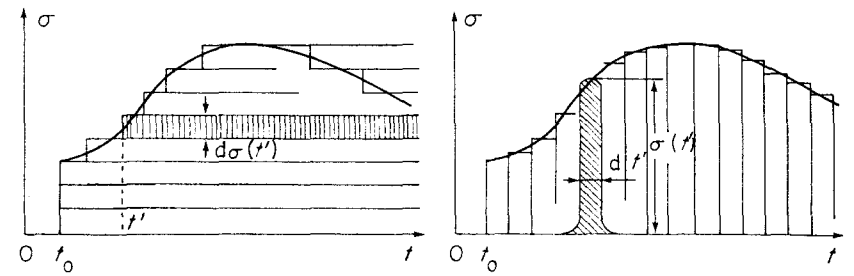

Figure 2.3 Decomposition of stress history into stress steps (left) or stress impulses (right)

times t', and summing (as illustrated in Fig. 2.3) the corresponding strains which equal $d\sigma(t')$, $J(t,t')$ on the basis of Eq. (2.2):

$$\varepsilon(t) = \int_0^t J(t,t')\,d\sigma(t') + \varepsilon^0(t) \tag{2.4}$$

This equation is a general uniaxial constitutive relation defining concrete as an ageing viscoelastic material. The integral in this equation should be understood as the Stieltjes integral, which is preferable to the usual Riemann integral since it applies not only for continuous but also discontinuous stress histories. When $\sigma(t)$ is continuous, we may substitute $d\sigma(t') = [d\sigma(t')/dt']\,dt'$ which yields the usual (Riemann) integral. For each finite sudden jump $\Delta\sigma(t_j)$ at time t_j, the term $J(t,t_j)\Delta\sigma(t_j)$ is implied by the Stieltjes integral and must be added to the Riemann integral. The principle of superposition (Eq. 2.4) was proposed by Boltzmann (1876) for non-ageing materials, and by Volterra (1913) for ageing materials. Equation (2.1) was introduced for concrete by McHenry (1943).

The principle of superposition (Eq. 2.4) yields accurate predictions only under the following conditions:

1. The stresses are within the service stress range, i.e. less than about 0.4 of the strength.
2. Unloading, i.e. strain of decreasing magnitude, does not take place (although the stress may decrease, as in relaxation).
3. There is no significant change in moisture content distribution during creep.
4. There is no large sudden stress increase long after the initial loading (this is the least important condition).

In practice, the superposition principle is often used even when conditions (2)–(4) are violated; however, the predictions may then be rather crude. It may be noted that the proportionality property for creep under constant stress (Eq. 2.2) appears to have a broader applicability than the principle of superposition (cf. Section 2.4.1). It may be also noted that a certain simple non-linear generalization of the principle of superposition extends the applicability range significantly; see Addendum to this chapter.

Substituting $d\sigma(t') = [d\sigma(t')/dt']dt'$ and integrating by parts, one may transform Eq. (2.4) to the following equivalent form, introduced for concrete by Maslov (1941):

$$\varepsilon(t) = \frac{\sigma(t)}{E(t)} + \int_0^t L(t,t')\sigma(t')\,dt' + \varepsilon^0(t) \tag{2.5}$$

in which $L(t,t') = -\partial J(t,t')/\partial t'$. Geometrically, this equation means that the stress history is decomposed into vertical strips each of which is considered as an impulse function of stress (Dirac δ-function); see Fig. 2.3. Thus, $L(t,t')$ represents the strain at time t caused by a unit stress impulse at time t' and is called the stress impulse memory function.

Differentiating Eq. (2.4), we see that the strain rate is expressed by the history integral,

$$\dot{\varepsilon}(t) = \frac{\dot{\sigma}(t)}{E(t)} + \int_0^t \frac{\partial J(t,t')}{\partial t}\,d\sigma(t') \tag{2.6}$$

where superior dots denote time derivatives.

The principle of superposition may be equivalently expressed in terms of the relaxation function, $R(t,t')$ (also called the relaxation modulus), which represents the uniaxial stress σ at time t caused by a unit constant axial strain imposed at time t' and held constant afterwards. Imaging the strain history $\varepsilon(t)$ to be decomposed into small strain increments $d\varepsilon(t')$ imposed at times t', the principle of superposition means that the responses to these increments, given as $R(t,t')\,d\varepsilon(t')$, may be superimposed. This yields the constitutive relation of ageing viscoelasticity in the form

$$\sigma(t) = \int_0^t R(t,t')[d\varepsilon(t') - d\varepsilon^0(t')] \tag{2.7}$$

in which the shrinkage (and thermal expansion) increments $d\varepsilon^0(t')$ must be subtracted from $d\varepsilon(t')$ since, by definition, they produce no stress.

The typical relaxation function of concrete is plotted in Fig. 2.4. Note again that it is a function of two variables t and t', and cannot be expressed as a function

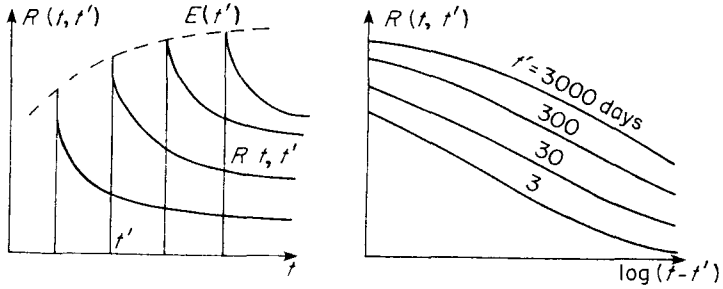

Figure 2.4 Curves of the relaxation function for various ages t' at strain imposition

of one variable, the time-lag $t - t'$, as is customary in classical viscoelasticity of non-ageing materials.

When the strain history is given, Eq. (2.4) represents a Volterra integral equation for the strain history $\varepsilon(t)$. By solving this equation for the strain history specified as a step function (a constant unit strain imposed at age t'), one may calculate the stress histories for various t' (relaxation curves), and thus obtain the relaxation function. For realistic forms of $J(t,t')$, this solution must be carried out numerically. Conversely, Eq. (2.7) represents a Volterra integral equation for $\varepsilon(t)$. By solving this equation for the stress history in the form of a step function, i.e. a constant unit stress applied at age t', one may calculate the individual creep curves, which together define the compliance function. Equation (2.7) is said to be the resolvent of Eq. (2.4) and vice versa. Functions $J(t,t')$ and $R(t,t')$, called the kernels of the integral equations, are complementary to each other, and if one of them is specified the other one follows.

For the creep functions typical of concrete, the relaxation function may be approximately calculated from Bažant and Kim's formula (Bažant and Kim, 1979):

$$R(t,t') = \frac{1-\Delta_0}{J(t,t')} - \frac{0.115}{J(t,t-1)}\left(\frac{J(t-\Delta,t')}{J(t,t'+\Delta)} - 1\right) \tag{2.8}$$

in which $\Delta = (t-t')/2$, $\Delta_0 \simeq 0.008$, and times must be given in days. Compared to the exact solution of the Volterra integral equation, the error of this formula is normally within 1 per cent of the initial value of the relaxation curve. A comparison of this formula with the accurately calculated relaxation curves is shown in Fig. 2.5 based on Bažant and Kim (1979) (with a correction by Chiorino *et al.* 1984, p. 150). Also plotted is the estimate $R(t,t') \simeq 1/J(t,t') = E_{\text{eff}}$ = effective modulus, which is often used in classical, non-ageing viscoelasticity. For no ageing, the use of E_{eff} yields good results, but not if ageing is present as Fig. 2.5 confirms. Development of an approximate formula for $R(t,t')$ was also proposed by Chiorino *et al.* (1972) and others.

Although Eqs (2.4) and (2.7) are equivalent, description of concrete creep behaviour in terms of the relaxation function is adopted rarely. The principal reason is that good experimental data on $R(t,t')$ (Hansen, 1964; Ross, 1958a; Harboe *et al.* 1958; Hanson, 1953; Klug and Wittman, 1970; Rostasy *et al.* 1972; Davies *et al.* 1957) are much more limited, since the relaxation tests are not as easy to carry out as the creep tests. However, for certain types of problems it is advantageous to first determine $R(t,t')$ from $J(t,t')$ and then carry out the structural analysis on the basis of $R(t,t')$.

There is solid experimental evidence (e.g. Hanson and Harboe, 1958; Hanson, 1953) showing that the conversion of creep function into the relaxation function according to the principle of superposition is quite accurate, provided that simultaneous drying or wetting does not cause significant deviations from linearity and the stress is not high; see Fig. 2.6.

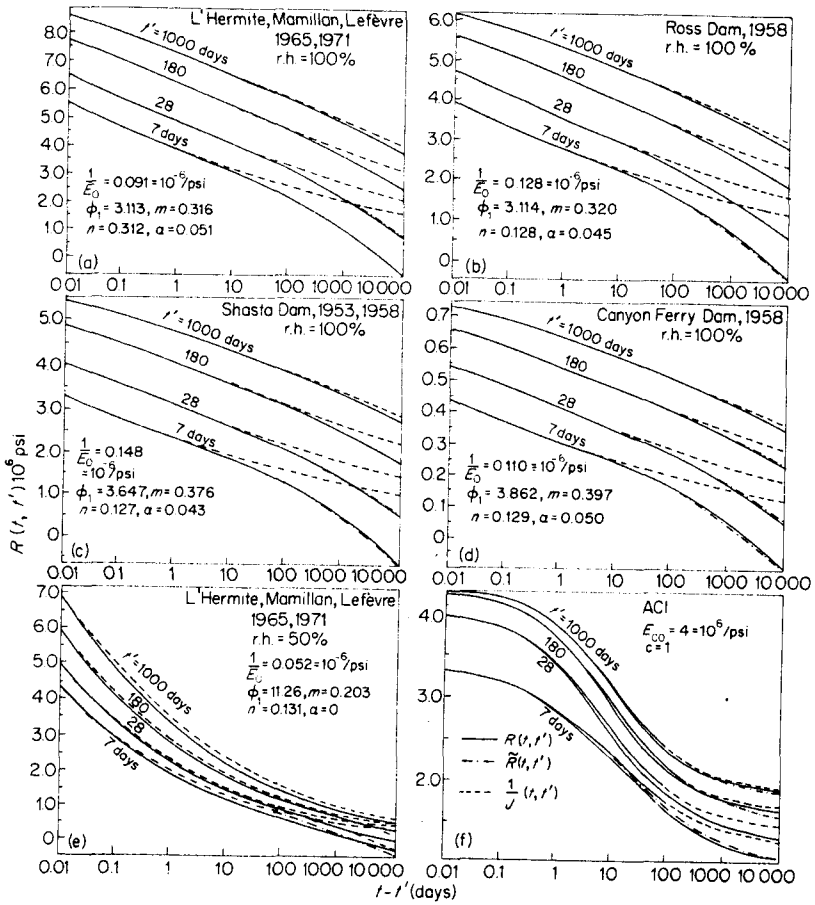

Figure 2.5 Comparison of approximate formula for relaxation function (dash-dot lines) with exact solution of relaxation function (solid lines) for various ages t' at loading, obtained from a smooth compliance function fitted to various data (a–e) or determined from ACI 1971 model (f). Dashed lines show effective modulus predictions. Where indistinguishable, dashed and dash-dot lines coincide with solid lines. (after Bažant and Kim, 1979; data from L'Hermite, Mamillan and Lefèvre, 1965, supplemented by private communication, Mamillan, 1971).

Multiaxial generalization of all the preceding relations is obtained easily, by virtue of the fact that the material is essentially isotropic. Based on the hypothesis of linearity (principle of superposition), Eqs (2.4) and (2.5) are generalized as

$$\boldsymbol{\varepsilon}(t) = \int_0^t \mathbf{B} J(t,t')\, \mathrm{d}\boldsymbol{\sigma}(t') + \boldsymbol{\varepsilon}^0(t) \tag{2.9}$$

or as

$$\boldsymbol{\varepsilon}(t) = \mathbf{B}\frac{\sigma(t)}{E(t)} + \int_0^t \mathbf{B} L(t,t')\boldsymbol{\sigma}(t')\, \mathrm{d}t' + \boldsymbol{\varepsilon}^0(t') \tag{2.10}$$

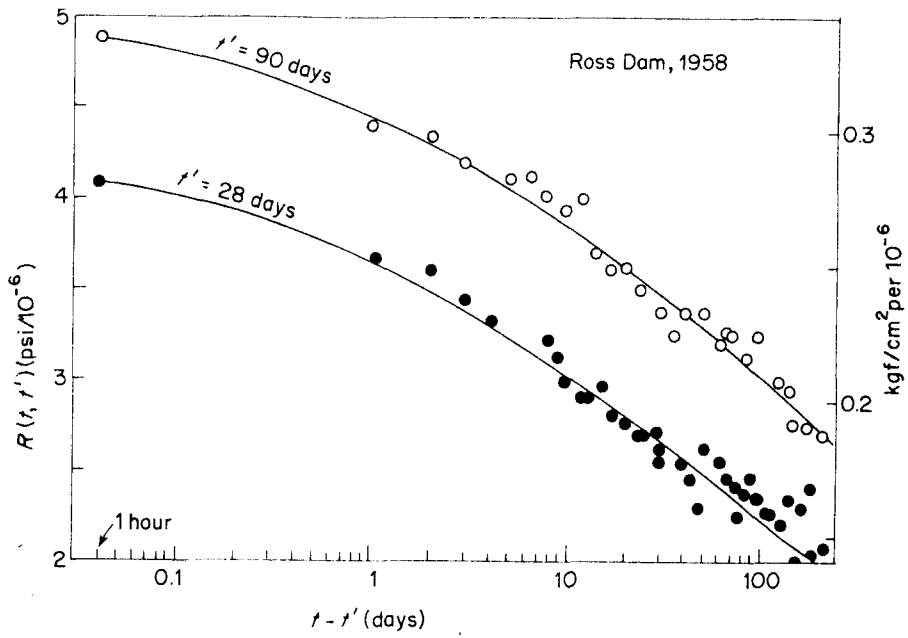

Figure 2.6 Relaxation measurements on concrete cylinders by Hanson (1953) and Harboe *et al.* (1958), compared to exact relaxation function curves for various ages t' at loading, calculated by superposition principle from smoothed compliance function measurements (one of the best proofs that the superposition principle correctly predicts relaxation; after Bažant and Wu, 1974b)

in which

$$\boldsymbol{\sigma} = (\sigma_{11}, \sigma_{22}, \sigma_{33}, \sigma_{12}, \sigma_{23}, \sigma_{31})^{\mathrm{T}}, \qquad \boldsymbol{\varepsilon} = (\varepsilon_{11}, \varepsilon_{22}, \varepsilon_{33}, \varepsilon_{12}, \varepsilon_{23}, \varepsilon_{31})^{\mathrm{T}},$$

$$\boldsymbol{\varepsilon}^0 = (\varepsilon^0, \varepsilon^0, \varepsilon^0, 0, 0, 0)^{\mathrm{T}}$$

and

$$\mathbf{B} = \begin{bmatrix} 1 & -\nu & -\nu & 0 & 0 & 0 \\ & 1 & -\nu & 0 & 0 & 0 \\ & & 1 & 0 & 0 & 0 \\ & & & 1+\nu & 0 & 0 \\ & & & & 1+\nu & 0 \\ & & & & & 1+\nu \end{bmatrix} \tag{2.11}$$

The numerical subscription of σ and ε denote the components of the stress and strain tensors in cartesian coordinates $x_i (i = 1, 2, 3)$, superscript T denotes the transpose of a matrix, and ν is the Poisson ratio generalized for viscoelastic behaviour, with $\nu(t,t)$ representing the elastic Poisson ratio at age t.

In the service stress range, and under the conditions stated above, the test data on shear creep (torsion) and biaxial creep (McDonald, 1972; York, 1970; Arthanari, 1967; Neville and Dilger, 1973, 1981; Meyer, 1969; Illston, 1972, etc.)

approximately agree with the additivity of the responses to various multiaxial stresses implied in Eq. (2.9).

Most generally, the Poisson ratio in Eq. (2.11) could be a function, $\nu = \nu(t, t')$. However, it so happens that at constant humidity (basic creep) this ratio is almost constant (approximately $\nu \simeq 0.18$), and then matrix **B** can be moved in front of the integrals in Eq. (2.9). However, when creep during variable moisture content is considered and is described by means of a mean compliance for the entire cross-section (Section 2.5.4), then the corresponding apparent overall Poisson ratio of the cross-section is quite variable and can drop almost to zero (Bažant and Wu, 1974a). Unfortunately, no unique function $\nu(t, t')$ then exists, since the evolution of ν depends on the humidity history and the cross-section size. Moreover, matrix **B** then takes, strictly speaking, the form of a compliance matrix for anisotropic materials.

The multiaxial stress–strain relations may also be written without matrix symbolism, as separate relations for the volumetric components and for the deviatoric components of the stress and strain tensors (Bažant, 1975, 1982b; ASCE, 1982). These equations are similar to Eqs (2.4) and (2.5), the uniaxial compliance function $J(t, t')$ being replaced by the volumetric compliance function $J^{V}(t, t') = 3(1 - 2\nu)J(t, t')$ and by the deviatoric compliance function $J^{D}(t, t') = 2(1 + \nu)J(t, t')$. The matrix formulation in Eqs (2.9) and (2.10) relates more directly to the way finite element programs are written.

Sometimes it is convenient to define creep operator $\underline{\mathbf{E}}^{-1}$ and relaxation operator $\underline{\mathbf{E}}$ by writing Eqs (2.4) and (2.7) in the forms $\boldsymbol{\varepsilon} = \underline{\mathbf{E}}^{-1}\boldsymbol{\sigma} + \boldsymbol{\varepsilon}^{0}$ and $\boldsymbol{\sigma} = \underline{\mathbf{E}}(\boldsymbol{\varepsilon} - \boldsymbol{\varepsilon}^{0})$. The multiaxial generalizations are then simply written as

$$\boldsymbol{\varepsilon} = \mathbf{B}\underline{\mathbf{E}}^{-1}\boldsymbol{\sigma} + \boldsymbol{\varepsilon}^{0} \quad \text{or} \quad \boldsymbol{\sigma} = \mathbf{B}^{-1}\underline{\mathbf{E}}(\boldsymbol{\varepsilon} - \boldsymbol{\varepsilon}^{0}) \tag{2.12}$$

in which

$$\mathbf{B}^{-1} = \frac{E(1-\nu)}{(1+\nu)(1-2\nu)}\begin{bmatrix} 1, & \nu/(1-\nu), & \nu/(1-\nu), & 0, & 0, & 0 \\ & 1, & \nu/(1-\nu), & 0, & 0, & 0 \\ & & 1, & 0, & 0, & 0 \\ & & & \nu^{*}, & 0, & 0 \\ & & & & \nu^{*}, & 0 \\ & & & & & \nu^{*} \end{bmatrix},$$

$$\nu^{*} = \frac{1-2\nu}{2(1-\nu)} \tag{2.13}$$

The relaxation operator $\underline{\mathbf{E}}$ is the inverse of the creep operator $\underline{\mathbf{E}}^{-1}$. These operators can be manipulated according to the rules of linear algebra (with certain minor limitations, particularly the lack of commutativity, which is due to ageing). This property may be exploited to prove an extension of the elastic–viscoelastic analogy to ageing viscoelastic materials, which permits converting any equation of linear elasticity to an analogous equation for ageing creep (Mandel, 1958; Bažant, 1961b, 1966, 1975; Huet, 1980) (see also Chapter 3).

2.2.3 Differential-type constitutive relations

Numerical creep analysis of large structural systems may be greatly facilitated, and analytical solutions of some problems may be rendered possible, if the integral-type constitutive equations from the preceding section are converted to a differential-type form consisting of a system of first-order ordinary differential equations in time. Such a conversion is possible if the kernel $J(t, t')$ or $R(t, t')$ has the degenerate form, i.e. consists of a sum of products of functions of single variables t and t'. The most general forms of the degenerate kernels may be written as

$$J(t, t') = \sum_{\mu=1}^{N} \frac{1}{C_{\mu}(t')}\{1 - \exp[y_{\mu}(t') - y_{\mu}(t)]\} \tag{2.14}$$

$$R(t, t') = \sum_{\mu=1}^{N} E_{\mu}(t')\exp[y_{\mu}(t') - y_{\mu}(t)] \tag{2.15}$$

Here $C_{\mu}(t')$ and $E_{\mu}(t')$ are functions of one variable, called the reduced times. They may be considered as

$$y_{\mu}(t) = (t/\tau_{\mu})^{q_{\mu}} \qquad (\mu = 1, 2, \ldots, N) \tag{2.16}$$

in which q_{μ} are positive exponents $\leqslant 1$. Here τ_{μ} are constants called either the retardation times in the case of Eq. (2.14), or the relaxation times in the case of Eq. (2.15). The expansion in Eqs (2.14) and (2.15) represents a series of real exponentials, called the Dirichlet series (also called the Prony series) (Hardy and Riesz 1915, Lancosz 1964, Cost 1964, Schapery 1962, Williams 1964).

The expansion in Eq. (2.14) is normally made to include as its first term the instantaneous (elastic) part of the compliance function. This is achieved by choosing an extremely small first retardation time $\tau_1 (\mu = 1)$, e.g. $\tau_1 = 10^{-9}$ day. Then the first term of the series in Eq. (2.14) is in all practical situations almost exactly $1/C_1(t')$, which represents the instantaneous compliance, $C_1(t') = E(t')$. Using very small but non-zero τ_1 is more convenient for computer programming than writing in Eq. (2.14) a separate instantaneous term which differs from the other terms of the sum.

If the compliance function is given, it is not difficult to calculate functions $C_{\mu}(t')$ or $E_{\mu}(t')$ for which Eqs (2.14) or (2.15) are close approximations. The calculation procedure is discussed in detail in Bažant *et al.* (1981) and a simple computer program for this purpose is given in Bažant (1982) (and with a manual and examples in Ha, H., Osman, M. A. and Huterer, J. (1984), *User's Guide*).

For certain special forms of the compliance function, such as the double power law or the logarithmic law, explicit expressions for $C_{\mu}(t)$ exist; see Bažant and Wu (1973a), Bažant (1977, 1982b). In general, functions $C_{\mu}(t')$ or $E_{\mu}(t')$ can be calculated by the method of least squares. As for τ_{μ}, however, they cannot be calculated from measured creep data but must be suitably chosen in advance. (If calculation of τ_{μ} on the basis of the least-squares condition is attempted, a

system of ill-conditioned equations results.) The choice of τ_μ cannot be arbitary but must satisfy certain conditions. The values of τ_μ must not be spaced too sparsely in the $\log(t-t')$ scale, and they must cover the entire time range of interest, in particular, the smallest τ_μ must be such that $\tau_2 \leqslant 3\tau_{\min}$ and the largest τ_μ must be such that $\tau_N \geqslant 0.5\tau_{\max}$, in which $\tau_{\min}$ and $\tau_{\max}$ are the smallest and the largest time delay after instantaneous load application for which the response is of interest. Moreover, the smallest τ_μ must be sufficiently smaller than the age of concrete t_0 when the structure is first loaded; $\tau_2 \leqslant 0.1t_0$ (otherwise the irreversible effect of concrete ageing at small ages would be missed in calculations.

The τ_μ-values that give a close fit of given $J(t,t')$ data are not unique. Equally good fits of the given compliance function data can be obtained for many possible choices of τ_μ-values which are uniformly spaced in the logarithmic time scale and cover the entire time range of interest. This is, of course, the reason that an attempt to determine τ_μ from a least-squares condition leads to an ill-conditioned system of equations.

Exponents q_μ in Eq. (2.16) may be always chosen as 1, in which case

$$y_\mu(t) = t/\tau_\mu \tag{2.17}$$

However, the compliance function of concrete can be approximated with fewer terms in the sum of Eq. (2.14) when the value of q_μ is chosen as roughly 2/3 (Bažant and Chern, 1984c). In that case the spacing of τ_μ may be chosen according to the rule

$$\tau_\mu = 10^{1.q_\mu}\tau_{\mu-1} \qquad (\mu = 3,4,\ldots,N) \tag{2.18}$$

Although usually not the most efficient, the values of q_μ in Eq. (2.16) may be chosen as 1; then the reduced times are proportional to the actual time, i.e. $y_\mu(t) = t/\tau_\mu$ and

$$\tau_\mu = 10^{\mu-1}\tau_1 \qquad (\mu = 1,2,\ldots,N-1) \tag{2.19}$$

in which case the τ_μ values are spaced by decades in the log-time scale. The individual terms of the Dirichlet expansion are then exponential curves which have the shape indicated in Fig. 2.7(a), consisting of a spread-out step. It so happens that this step extends over only about one decade in the log-time scale. For this reason the number 10 in Eq. (2.19) or (2.18) cannot be replaced by a larger number, i.e. the τ_μ-values cannot be spaced apart farther than by decades. The approximation of the creep curve or relaxation curve may then be imagined as a sum of many spread-out steps as shown in Fig. 2.7(b) or 2.7(c).

The plot of $C_\mu(t)$ or $E_\mu(t)$ versus $\log\tau_\mu$ is called the retardation spectrum or the relaxation spectrum. Its example is plotted in Fig. 2.8.

The Dirichlet series expansion should be regarded only as an approximation to the compliance function, motivated by computational convenience, rather than as a fundamental law. The expansion contains unnecessarily many material parameters defining all the functions $C_\mu(t')$ or $E_\mu(t')$. The input for a computer

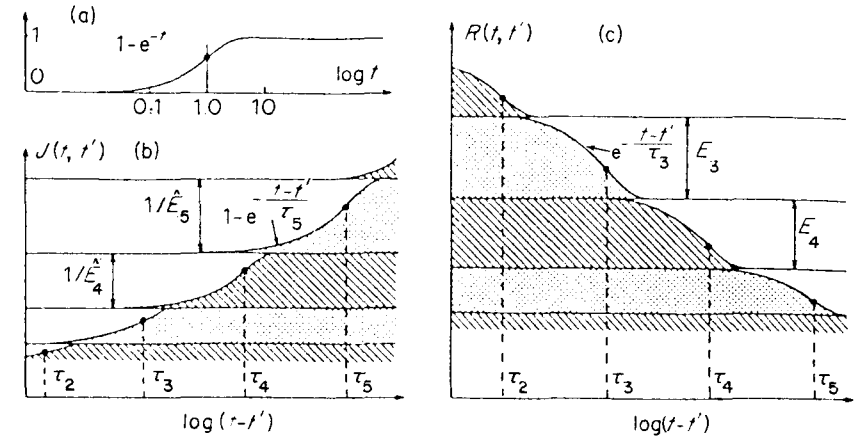

Figure 2.7 Approximation of compliance or relaxation function curve at fixed age t' at loading by a sum of exponentials (a—curve of a single exponential in log-time, b—decomposition of compliance curve, c—decomposition of relaxation curve)

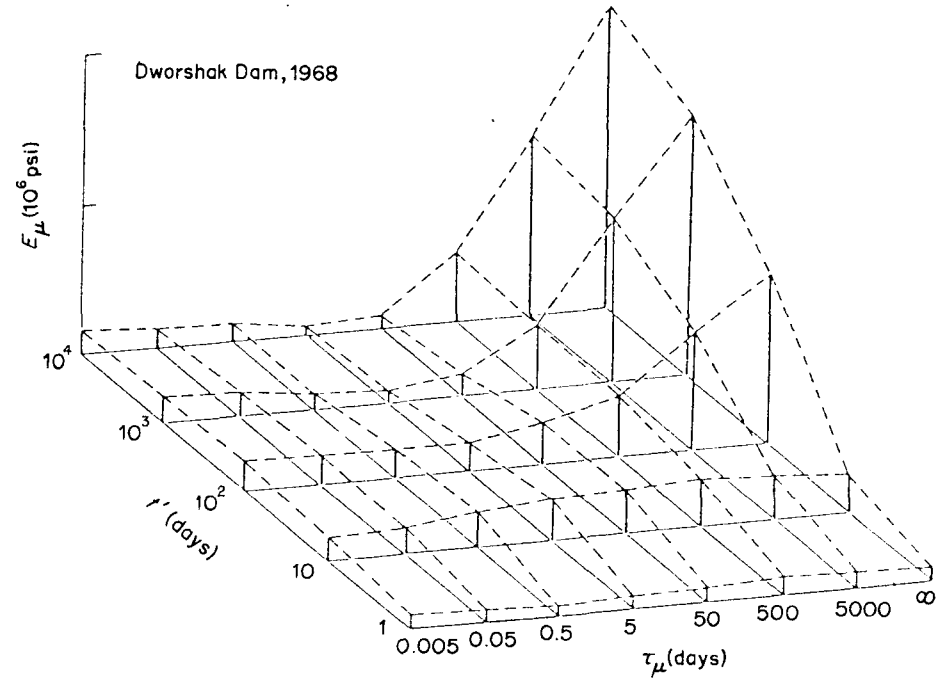

Figure 2.8 Example of relaxation spectra for various ages t' at loading, calculated from Dworshak Dam data shown in Fig. 2.24 (after Bažant and Wu, 1974b)

program should consist of the coefficients of a simple formula for $J(t,t')$, such as the log-double power law. The coefficients defining the Dirichlet series expansion should be generated from this formula by the computer (Bažant, 1982a; Day *et al.*, 1984).

As already mentioned, the purpose of the Dirichlet series expansion is to convert a constitutive equation of an integral type to one of a differential type. For an ageing material, this conversion is somewhat simpler when the relaxation function rather than the compliance function is used. Equation (2.7) with $R(t,t')$ given by Eq. (2.15) may be rewritten as

$$\boldsymbol{\sigma}(t) = \sum_{\mu=1}^{N} \boldsymbol{\sigma}_\mu(t) \tag{2.20}$$

in which

$$\boldsymbol{\sigma}_\mu(t) = \mathrm{e}^{-y_\mu(t)} \int_0^t \mathrm{e}^{y_\mu(t')} \mathbf{B}^{-1} E_\mu(t')[\mathrm{d}\boldsymbol{\varepsilon}(t') - \mathrm{d}\boldsymbol{\varepsilon}^0(t')] \tag{2.21}$$

Now, expressing the derivative $\mathrm{d}\boldsymbol{\sigma}_\mu/\mathrm{d}y_\mu$, we may verify that the column vectors $\boldsymbol{\sigma}_\mu$, called the partial stresses (internal variables), satisfy the differential equations

$$\dot{\boldsymbol{\sigma}}_\mu + \dot{y}_\mu(t)\boldsymbol{\sigma}_\mu = \mathbf{B}^{-1} E_\mu(t)(\dot{\boldsymbol{\varepsilon}} - \dot{\boldsymbol{\varepsilon}}^0) \tag{2.22}$$

Consider now the well-known Maxwell chain model (Fig. 2.9(b)), in which $\boldsymbol{\sigma}_\mu$ is interpreted as the stress in the μth Maxwell unit. The strain rate in the ageing spring is $\dot{\sigma}_\mu/E_\mu(t)$, and that in the dashpot is $\sigma_\mu/\eta_\mu(t)$, where η_μ represents the age-dependent viscosity of the μth dashpot. Summing these strain rates, we get $\mathbf{B}^{-1}(\dot{\boldsymbol{\varepsilon}} - \dot{\boldsymbol{\varepsilon}}^0) = (\dot{\boldsymbol{\sigma}}_\mu/E_\mu) + (\boldsymbol{\sigma}_\mu/\eta_\mu)$, which may be written as

$$\dot{\boldsymbol{\sigma}}_\mu + \frac{E_\mu(t)}{\eta_\mu(t)}\boldsymbol{\sigma}_\mu = \mathbf{B}^{-1} E_\mu(t)(\dot{\boldsymbol{\varepsilon}} - \dot{\boldsymbol{\varepsilon}}^0) \tag{2.23}$$

Comparing the coefficients of this equation with Eq. (2.22), we see that the spring moduli $E_\mu(t)$ of the Maxwell chain are identical to the functions $E_\mu(t)$ used in the

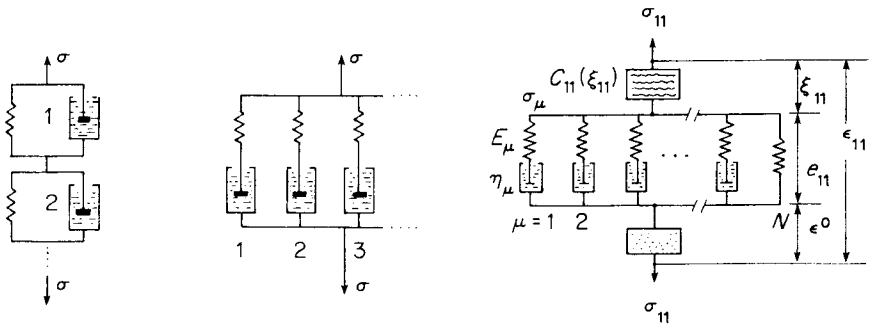

Figure 2.9 Kelvin chain model (left), Maxwell chain model (middle), and Maxwell chain model enhanced with cracking element on top and shrinkage element at bottom (right)

Dirichlet series expansions (Eq. 2.15), and that the viscosity of the μth dashpot is

$$\eta_\mu(t) = E_\mu(t)/\dot{y}_\mu(t) \tag{2.24}$$

In particular, for $y_\mu = (t/\tau_\mu)^q$ we have $\eta_\mu(t) = \tau_\mu^q E_\mu(t) t^{q-1}/q$ (Bažant and Chern, 1984c), and for $q = 1$ we have $\eta_\mu(t) = \tau_\mu E_\mu(t)$, a relation which has been used in most works so far.

The differential-type constitutive relation for concrete creep has also been termed the rate-type constitutive relation. However, the latter term is used by some authors in theoretical continuum mechanics (e.g. Truesdell) to refer to a different formulation in which $\dot{\sigma}$ is a function of $\varepsilon, \dot{\varepsilon}, \ddot{\varepsilon}, \ldots$.

A similar conversion to a differential-type form may be achieved for the Dirichlet series expansion of the compliance function (Eq. 2.14); see, e.g. Bažant (1971c, 1975, 1982b), Bažant and Chern (1984c), Bažant and Wu (1973b). The resulting differential-type constitutive law may be written as

$$\boldsymbol{\varepsilon}(t) = \sum_{\mu=1}^{N} \boldsymbol{\varepsilon}_\mu(t) + \boldsymbol{\varepsilon}^0(t) \tag{2.25}$$

with

$$\ddot{\boldsymbol{\varepsilon}}_\mu + \frac{E_\mu(t) + \dot{\eta}_\mu(t)}{\eta_\mu(t)}\dot{\boldsymbol{\varepsilon}}_\mu = \mathbf{B}\frac{\dot{\boldsymbol{\sigma}}}{\eta_\mu(t)} \tag{2.26}$$

and

$$\eta_\mu(t) = \frac{C_\mu(t)}{\dot{y}_\mu(t)}, \qquad E_\mu(t) = C_\mu(t) - \frac{C_\mu(t)}{\dot{y}_\mu(t)} \tag{2.27}$$

See Bažant and Chern (1984c). Equations (2.25)–(2.27) may be recognized as the differential-type constitutive equation based on the Kelvin or Kelvin–Voigt chain model Fig. 2.7(a). Indeed, the rate of stress in the μth spring is $E_\mu(t)\dot{\varepsilon}_\mu$, while the rate of stress in the μth dashpot is $\eta_\mu(t)\dot{\varepsilon}_\mu$. Setting the sum of these two stress rates equal to $\dot{\boldsymbol{\sigma}}$, we get Eq. (2.26).

Note that the differential equation for Kelvin chain (Eq. 2.26) is of the second order, while for a non-ageing material it is of the first order. This is a disadvantage in comparison to the differential-type formulation based on Maxwell (rather than Kelvin) chain, obtained from the Dirichlet series expansion of the relaxation function.

A further disadvantage of the Kelvin chain formulation is that, due to the presence of the minus sign, Eq. (2.27) can yield a negative spring modulus E_μ. Although this is not thermodynamically inadmissible (the thermodynamic restrictions apply only to the overall material moduli, not to the partial moduli E_μ), we then do not have a guarantee that thermodynamic restrictions are satisfied overall. This is certainly disturbing.

The Kelvin chain formulation may also be converted to a system of first-order differential equations.

$$\frac{\mathrm{d}\boldsymbol{\gamma}_\mu}{\mathrm{d}y_\mu} + \boldsymbol{\gamma}_\mu = \frac{\mathbf{B}}{C_\mu(t)}\frac{\mathrm{d}\boldsymbol{\sigma}}{\mathrm{d}y_\mu} \qquad (\mu = 1, 2, \ldots, n) \tag{2.28}$$

However, unlike ε_μ, the variables $\gamma_\mu(t)$ do not have any direct physical interpretation, merely defined by the relation $\dot{\gamma}_\mu = \dot{\varepsilon}_\mu + \dot{\sigma}/C_\mu(t)$. Nevertheless, the numerical step-by-step algorithm for the Kelvin chain model may be based on the first-order equation (Eq. 2.28) rather than the second-order equation (Eq. 2.26); see Bažant (1971c, 1975, 1982b), Bažant and Wu (1973b).

Variables $\boldsymbol{\sigma}_\mu$ or $\boldsymbol{\varepsilon}_\mu$ represent what is known in continuum thermodynamics as the internal variables, i.e. state variables that cannot be directly measured. (They were originally called by Biot (1955) the 'hidden' variables.) The current values of these variables characterize the effect of the past history of the material, thus replacing the history integral. Only a few current values of $\boldsymbol{\sigma}_\mu$ or $\boldsymbol{\varepsilon}_\mu$ are needed to sufficiently characterize a long past history, e.g. only four values suffice for the history from $t - t' = 1$ day until 10^4 days. Another term for $\boldsymbol{\sigma}_\mu$ is the hidden stresses or partial stresses, and for $\boldsymbol{\varepsilon}_\mu$ is the hidden strains or partial strains.

Fig. 2.10 shows that the unit creep curves (compliance function) according to the Maxwell chain model are smooth curves which can be made to fit very closely the test data; e.g., those of Pirtz (1968), Hanson (1953) and Harboe *et al.* (1958).

From the previous discussion it may be concluded that either the Maxwell chain or the Kelvin chain can approximate the integral-type creep law of ageing viscoelasticity with any desired accuracy. Therefore, these two models are mutually equivalent, and they must also be equivalent to any other spring-dashpot model. For non-ageing materials this was rigorously proven long ago by Roscoe (1950).

Certain subtle questions nevertheless remain in the case of ageing materials. It may happen that, for the same $J(t, t')$, the spring moduli and the dashpot viscosities are always positive for one model but could become negative in some time periods for another model. If this is disallowed, the rheologic models for ageing materials are not completely equivalent (Bažant, 1979).

The fact that the Kelvin chain model leads to a second-order differential equation and is more likely to give negative spring moduli or viscosities than the Maxwell model is caused by the fact that the equation for the ageing spring must be written as $\dot{\sigma}_\mu = E_\mu(t)\dot{\varepsilon}_\mu$, not as $\sigma_\mu(t) = E_\mu(t)\varepsilon_\mu$. The latter equation would be thermodynamically correct for a chemically softening material (e.g. dehydrating concrete at very high temperatures), while the former equation is required for a material that is chemically hardening, as is concrete due to hydration (see Section 2.4.4) (Bažant, 1966a, b, 1979).

Remark

After completion of the committee's work, Bažant discovered a new creep model for which a Kelvin chain with age-independent properties (constant E_μ) can be used. The age-dependence is taken into account separately, by certain transformations of time-dependent variables. This new model appears to be much more efficient and better justified physically than the existing models just described; see the Addendum to this chapter.

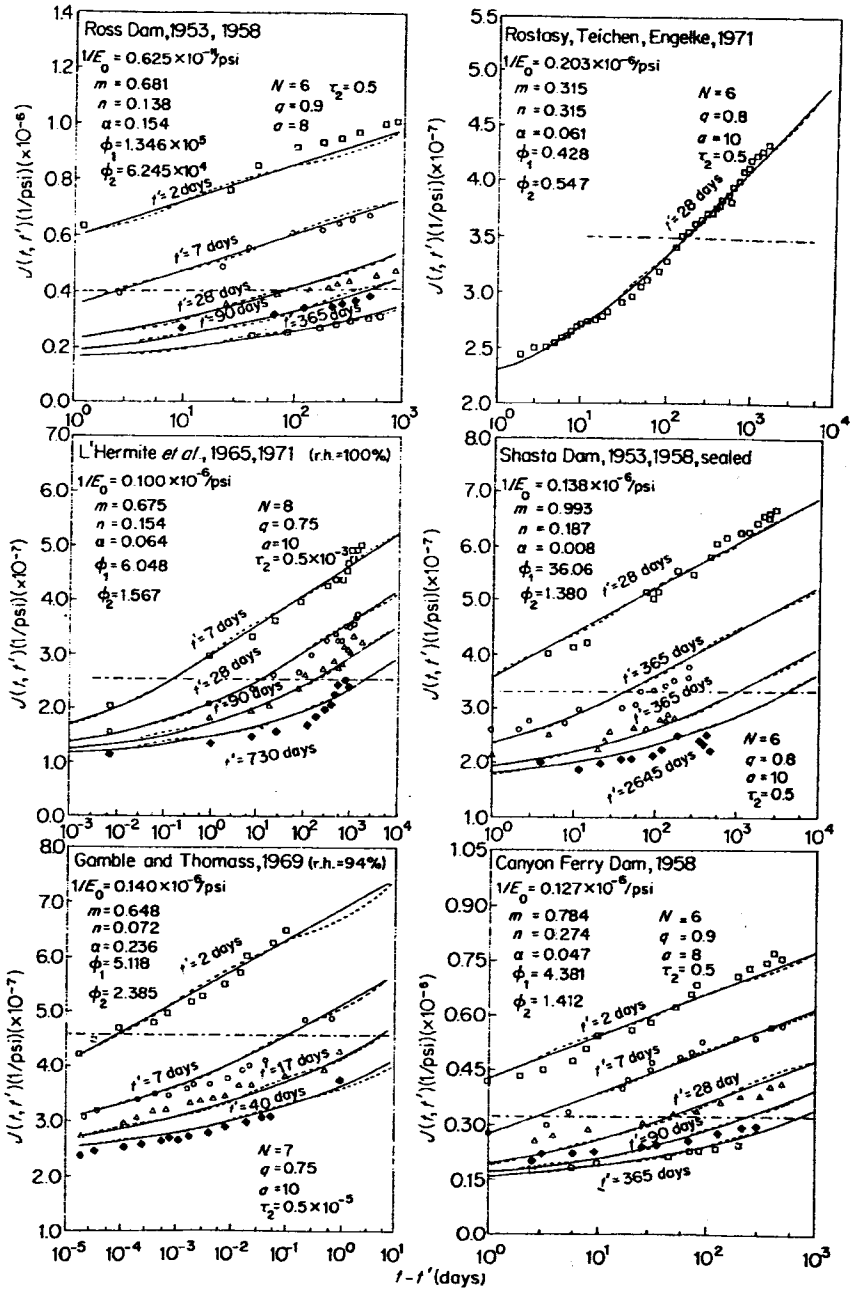

Figure 2.10 Compliance function approximations based on ageing Maxwell chain model (dashed lines), calculated from triple power law fits (solid lines) of various compliance data (after Bažant and Chern, 1985d)

2.2.4 Incremental quasi-elastic stress–strain relations

The most effective approach to numerical step-by-step structural creep analysis is to approximate the stress–strain relation for the time step as an incremental quasi-elastic relation, and then solve the structural creep problem as a sequence of elasticity problems. This can be done both for the integral-type and the differential-type formulations.

Let time t be subdivided by discrete times t_r ($r = 0, 1, 2, \ldots$) into time steps $\Delta t_r = t_r - t_{r-1}$ (Fig. 2.11). Time t_0 coincides with the instant of first loading. If there is an abrupt load change at any time t_s, it is convenient for programming to use a time step of zero (or almost zero) duration, i.e. set $t_{s+1} = t_s$ (or, e.g. $t_{s+1} = t_s + 10^{-4}$ day). Under constant loads, the strains and stresses vary at a rate which decreases roughly as the inverse of time, and for this reason it is advantageous to use progressively increasing time steps Δt_r. They are best chosen so that the time step be kept constant in the $\log(t - t')$ scale. When Bažant's second-order algorithm described below (Eqs 2.31–2.32) is used, normally three or four-steps per decade in log-time suffice.

Using the trapezoidal rule, the error of which is proportional to Δt^2, we may approximate Eq. (2.9) as

$$\boldsymbol{\varepsilon}_r = \sum_{s=1}^{r} \mathbf{B} J_{r,s-1/2}\, \Delta\boldsymbol{\sigma}_s + \boldsymbol{\varepsilon}_r^0 \tag{2.29}$$

where the subscripts refer to the discrete times, and $s - \frac{1}{2}$ refers to the middle of the time step Δ_s; $J_{r,s-1/2}$ may be interpreted either as $(J_{r,s} + J_{r,s-1})/2$, or as $J(t_r, t_{s-1/2})$. Writing Eq. (2.29) also for $\boldsymbol{\varepsilon}_{r-1}$ and subtracting it from Eq. (2.29), Bažant (1972a) obtained the following quasi-elastic incremental stress–strain relation:

$$\Delta\boldsymbol{\varepsilon}_r = \frac{1}{E''}\mathbf{B}\,\Delta\boldsymbol{\sigma}_r + \Delta\boldsymbol{\varepsilon}'' \quad \text{or} \quad \Delta\boldsymbol{\sigma}_r = E''\mathbf{B}^{-1}(\Delta\boldsymbol{\varepsilon} - \Delta\boldsymbol{\varepsilon}'') \tag{2.30}$$

in which

$$E'' = 1/J_{r,r-1/2}, \qquad \Delta\boldsymbol{\varepsilon}'' = \sum_{s=1}^{r-1} \mathbf{B}(J_{r,s-1/2} - J_{r-1,s-1/2})\Delta\boldsymbol{\sigma} + \Delta\boldsymbol{\varepsilon}_r^0 \tag{2.31}$$

Here E'' may be interpreted as the incremental elastic modulus, and $\Delta\boldsymbol{\varepsilon}''$ as the

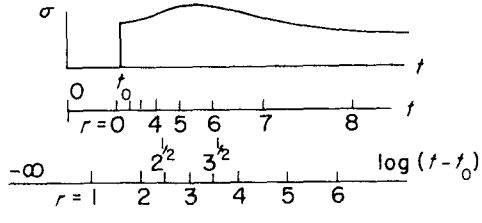

Figure 2.11 Discrete subdivision of time with increasing time steps

column matrix of the incremental inelastic strains because $\Delta\boldsymbol{\varepsilon}''$ can be evaluated before the solution of the time step (t_{r-1}, t_r) begins. The creep structural analysis may thus be reduced to a sequence of elastic analyses performed in the individual time steps. Using the foregoing algorithm, Huet (1980) developed a general computer program for composite beams or frames.

To make programming easy, Madsen (1979) formulated Bažant's second-order algorithm (Eqs 2.30–2.31) as a matrix relation between the column matrices of stresses and strains, such that the column matrix involves the stress or strain values at all discrete times. This formulation represents a matrix version of the elastic–viscoelastic analogy and makes it possible to obtain the solutions for creep simply by replacing the elastic modulus in the formulas of elasticity with the corresponding constitutive matrix (Madsen and Bažant, 1983) (in more detail, see Chapter 3). However, the matrix solution is computationally even more inefficient than the step-by-step solution according to Eqs (2.30) and (2.31) and is suitable only for problems with a few unknowns.

When large time steps are used, the accuracy of the foregoing second-order algorithm may be somewhat improved (Bažant, 1984) by using for the last time step $\Delta\sigma_r$ the effective modulus $E_{\text{eff}} = 1/J_{r,r-1}$. The sum in Eq. (2.29) is then replaced by

$$\boldsymbol{\varepsilon}_r = \mathbf{B}\left(\sum_{s=1}^{r-1} J_{r,s-1/2}\,\Delta\boldsymbol{\sigma}_s + J_{r,r-1}\,\Delta\boldsymbol{\sigma}_r\right) + \Delta\boldsymbol{\varepsilon}_r^0 \tag{2.32}$$

Writing the equation also for $\boldsymbol{\varepsilon}_{r-1}$ and subtracting it, one can obtain instead of Eq. (2.31), the relations

$$\left.\begin{aligned} &E'' = 1/J_{r,r-1} \\ &\text{for } r > 2: \\ &\Delta\boldsymbol{\varepsilon}'' = \sum_{s=1}^{r-1} (J_{r,s-1/2} - J_{r-1,s-1/2})\Delta\boldsymbol{\sigma}_s + (J_{r,r-3/2} - J_{r-1,r-2})\Delta\boldsymbol{\sigma}_{r-1} + \Delta\boldsymbol{\varepsilon}_r^0 \\ &\text{for } r = 2: \\ &\Delta\boldsymbol{\varepsilon}'' = (J_{2,1/2} - J_{1,0})\Delta\boldsymbol{\sigma}_1 + \Delta\boldsymbol{\varepsilon}_2^0; \quad \text{for } r = 1\text{: } \Delta\boldsymbol{\varepsilon}'' = \Delta\boldsymbol{\varepsilon}_1^0 \end{aligned}\right\} \tag{2.33}$$

Algorithms that are based on a quasi-elastic incremental stress–strain relation corresponding to the use of the rectangle rule for the evaluation of the history integral have been used in practice. However, they are not significantly simpler, while their error, being of the first rather than the second order in Δt, is larger, and the convergence at diminishing Δt is markedly slower than for the second-order method (Bažant, 1972a).

An approximation of the impulse memory integral (Eq. 2.9) with a sum leads to an algorithm which was used in some early works. However, this algorithm is computationally less efficient and does not permit increasing Δt to very long intervals as the stress variation is getting slower after a long period under dead load.

The incremental quasi-elastic stress–strain relation based on the history integral has the disadvantage that for each finite element one must store all the preceding values of all stress components, and at each time step one must evaluate long sums from all these values. This requires a very large storage capacity and a very long computing time. For this reason, it is much more efficient to base the incremental quasi-elastic stress–strain relation on the differential-type formulation.

To obtain an efficient algorithm, the key idea is to use for the duration of the time step the exact integral of the differential equation obtained under the assumption that the coefficients of the differential equation and its right-hand side are constant during the time step, while they are permitted to change by jumps between the time steps. Thus, exact integration of Eq. (2.23) for the Maxwell chain yields (Bažant, 1971c; Bažant and Wu, 1974b):

$$\sigma_\mu = \sigma_{\mu_{r-1}} e^{-\Delta y_\mu} + E_{\mu_{r-1/2}} \lambda_\mu \mathbf{B}^{-1}(\Delta\varepsilon - \Delta\varepsilon^0) \tag{2.34}$$

in which

$$\lambda_\mu = (1 - e^{\Delta y_\mu})/\Delta y_\mu \tag{2.35}$$

Substituting this into Eq. (2.20), we may obtain again the quasi-elastic incremental stress–strain relation in Eq. (2.31) in which

$$E'' = \sum_{\mu=1}^{N} \lambda_\mu E_{\mu_{r-1/2}} \qquad \Delta\varepsilon'' = \frac{1}{E''} \sum_{\mu=1}^{N} (1 - e^{-\Delta y_\mu})\sigma_\mu \tag{2.36}$$

Note again that E'' and $\Delta\varepsilon''$ can be evaluated before the solution of the time step (t_{r-1}, t_r) begins. After solving the stress and strain increments in the time step by an elastic structural analysis, the new values of the partial stresses are obtained from Eq. (2.34).

For the Kelvin chain model, exact integration of Eq. (2.29) yields (Bažant, 1971c; Bažant and Wu, 1973a):

$$\gamma_{\mu_r} = \gamma_{\mu_r} e^{-\Delta y_\mu} + \frac{\lambda_\mu}{C_{\mu_{r-1/2}}} \mathbf{B}\,\Delta\sigma \tag{2.37}$$

which then again leads to the quasi-elastic incremental stress–strain relation in Eq. (2.31) with

$$\frac{1}{E''} = \sum_{\mu=1}^{N} \frac{1 - \lambda_\mu}{C_{\mu_{r-1/2}}}, \qquad \Delta\varepsilon'' = \sum_{\mu=1}^{N} (1 - e^{-\Delta y_\mu})\gamma_{\mu_{r-1}} + \Delta\varepsilon^0 \tag{2.38}$$

The computational algorithm based on Eqs (2.30) and (2.34)–(2.36) or (2.37) and (2.38) is called the exponential algorithm. For Δt approaching zero, this algorithm becomes equivalent to the central difference approximation and converges at the same rate as this approximation, i.e. quadratically. The advantage of the exponential algorithms is in the possibility of using time steps that are much longer (even orders of magnitude longer) than the shortest relaxation or retardation time, τ_1, for which the usual central or forward difference formulas would lead to numerical instability. The size of the time steps is subjected to no numerical stability limit. This can be instructively explained by examining the role of coefficient λ_μ as follows.

Among all τ_μ there may be one, say τ_m, which is of the same order of magnitude as the current time step Δt. Then for all $\tau_\mu \leqslant \tau_m$ we have $\Delta y_\mu \gg 1$, $\exp(-\Delta y_\mu) \simeq 0$, and $\lambda_\mu \simeq 0$, whereas for all $\tau_\mu > \tau_m$ we have $\Delta y_\mu \ll 1$, $\exp(-\Delta y_\mu) \simeq 1$, and $\lambda_\mu \simeq 1$. Thus, we see that the chain moduli E_μ which contribute to the instantaneous incremental stiffness E'' are only those for which $\tau_\mu < \tau_m$. This is intuitively obvious because the stress in the Maxwell chain units for which $\tau_\mu \gg \Delta t$ must get almost completely relaxed within a time period less than the step duration. So, the effect of λ_μ as the time step is increased is gradually to 'uncouple' the Maxwell chain units as their relaxation time becomes too small compared to Δt.

A few historical comments are in order. A compliance function in the form of a single exponential was used in structural creep analysis by McHenry (1943), Maslov (1940) and Arutyunyan (1952), although for the purpose of converting the structural problem from integral to differential equations rather than for the purpose of avoiding the storage of stress history in step-by-step solution. The latter advantage of the degenerate kernel in the form of Dirichlet series was utilized by Selna (1967, 1968) and Bresler and Selna (1964); but their algorithm did not allow increasing the time step beyond a fraction of the smallest retardation time. The exponential algorithm which does not have this restriction was developed for non-ageing creep by Zienkiewicz and Watson (1966), Taylor *et al.*, (1970) and Mukaddam (1974). The exponential algorithms for ageing creep based on degenerate forms of the compliance as well as relaxation functions were developed by Bažant (1971c) and were applied in a finite element program by Bažant and Wu (1974a).

Other forms of exponential algorithms which differ in some details were developed by Kabir and Scordelis (1979), Argyris *et al.* (1977, 1978), Pister *et al.* (1976), and Willam (1978) who also used these algorithms in large finite element programs. Based on the second-order differential equation for the stress–strain relation for Arutyunian's compliance function (given in Bažant, 1966b), Haas (1974b), and Schade and Haas (1975) developed a finite element program for spatial beam structures of composite construction, which avoids the storage of stress histories, applies to complex loading histories and to structures built through successive construction stages. This formulation was later improved (Haas, 1978) by introducing an increasing retardation time in order to get a better fit of measured compliance functions.

Anderson (1980, 1982), Smith *et al.* (1977, 1978) implemented Bažant's algorithm (Bažant, 1971c, Bažant and Wu, 1973b) based on a degenerate form of the compliance function in the general-purpose finite element program NONSAP. The same was done for a degenerate form of the relaxation function in the general-purpose finite element program CREEP 80 by Bažant, Rossow and

Horrigmoe (Bažant and Rossow, 1981; Bažant *et al.*, 1981) later refined and applied in various reactor vessel studies by Pfeiffer *et al.* (1985); and also in the finite element program SACAFEM by Jonasson (1977), who applied it in analyses of shrinkage effects in concrete top layers. The algorithm developed by Kabir and Scordelis (1979), also used by Van Zyl and Scordelis (1979), Van Greunen (1979) and Kang (1977), and Kang and Scordelis (1980), has been applied in large finite element programs. This algorithm, which likewise avoids the storage of the previous history by exploiting the Dirichlet series expansion of the compliance function, is similar to Zienkiewicz *et al.*'s (1968) algorithm for non-ageing materials; however, it has a lower order of accuracy than the exponential algorithms just described, since the approximation error is of the first order in Δt rather than the second order (this is because an approximation of the history integral by a rectangle rule is implied). This less accurate approximation nevertheless has the advantage that the same incremental elastic stiffness matrix of the structure may be used in every time step if the age of concrete is the same for all the finite elements, while the aforementioned exponential algorithms require changing the stiffness matrix in each time step. This advantage is lost, however, if the structure is of non-uniform age or if changes of stiffness due to cracking or other effects need to be considered.

2.2.5 Age-adjusted effective modulus

For many practical purposes, the structural creep analysis need not be very accurate. As a matter of fact, it makes no sense to do it accurately if the stochastic nature of creep is ignored and no measures to reduce the statistical uncertainty are taken. Approximate methods of structural creep analysis are then appropriate. The simplest approach is to obtain the time variation from algebraic relations, an approach which is usually formulated as some type of effective modulus.

If the loads are steady, the most attractive method is to use a single, long step $\Delta t = t - t_0$ spanning from the moment of first loading, t_0, up to the current time, t, and consider for this step an effective quasi-elastic stress–strain relation:

$$\Delta\boldsymbol{\varepsilon} = \frac{1}{E''}\mathbf{B}\,\Delta\boldsymbol{\sigma} + \Delta\boldsymbol{\varepsilon}'', \qquad \Delta\boldsymbol{\varepsilon}'' = \mathbf{B}\boldsymbol{\sigma}(t_0)\frac{\phi(t,t_0)}{E(t_0)} + \Delta\boldsymbol{\varepsilon}^0 \tag{2.39}$$

in which $\Delta\boldsymbol{\varepsilon} = \boldsymbol{\varepsilon}(t) - \boldsymbol{\varepsilon}(t_0)$, etc. If the shape of the stress curve from t_0 to t is specified, E'' may be determined on the basis of the compliance function.

It might seem that for determining E'' the best assumption would be a linear stress variation from t_0 to t, for which we would have

$$E'' = E(t_0)/[1 + \phi(t,t_0)/2]$$

Not so, however. A better estimate is to assume that the stress jumps discontinuously right after t_0 and is then constant until the final time. Then one

obtains

$$E'' = E_{\text{eff}} = E(t_0)/[1 + \phi(t,t_0)] = \text{effective modulus}$$

(sustained modulus) (McMillan, 1916; Faber, 1927).

A still better assumption, which is much closer to the assumption that the stress is constant after a jump at t_0 rather than to the assumption that the stress is linearly varying (Fig. 2.12), is to consider that the strain varies from t_0 to t in proportion to the creep coefficient $\phi(t,t_0)$, or to $J(t,t')$. The stress history then is, exactly, a certain linear algebraic function of the relaxation function $R(t,t_0)$, such that the stress–strain relation may be written in the algebraic form of Eq. (2.39) with

$$E'' = \frac{E(t_0) - R(t,t_0)}{\phi(t,t_0)} \tag{2.40}$$

This result (see the theorem in Chapter 3) was proven by Bažant (1970d, 1972b). For a simplified proof, see Bažant (1982b).

It has been numerically demonstrated that, if there is no ageing, the values of E'' for concrete are nearly the same as the values of effective modulus E_{eff}. If there is ageing, the E'' values given by Eq. (2.28) can be considerably larger than the effective modulus. Therefore, as compared to the effective modulus, Eq. (2.40) introduces principally an adjustment for ageing, and therefore, E'' in Eq. (2.40) is called the *age-adjusted effective modulus* (Bažant, 1972b).

Modulus E'' may be regarded as the effective modulus for a modified creep coefficient ϕ, i.e.,

$$E'' = E(t_0)/[1 + \chi(t,t_0)\phi(t,t_0)]$$

where $\chi(t,t_0)$ is a positive coefficient normally les than 1.0. This type of correction to the effective modulus has been introduced by many authors on an empirical

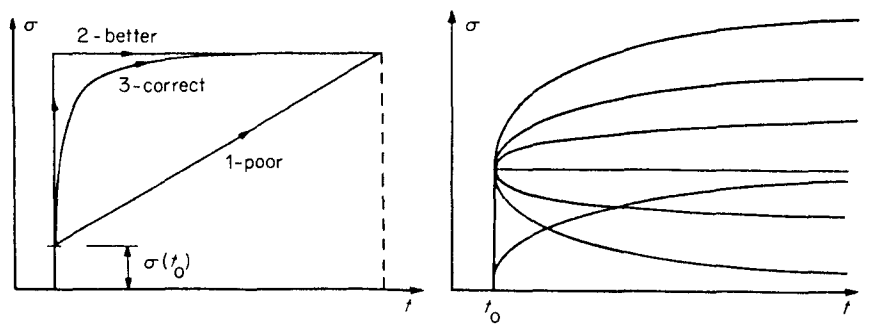

Figure 2.12 Stress history simplifications implied in mean modulus (line 1, $\chi = 0.5$), classical effective modulus (curve 2, $\chi = 1$), and age-adjusted effective modulus (curve 3) (left), and stress histories for which the age-adjusted effective modulus gives exact results (right)

basis. An approximate estimate of coefficient χ has been obtained for relaxation-type stress histories by Trost (1967). Trost's estimate of χ is quite close to the exact value given by Eq. (2.40) provided that the age-dependence of the elastic modulus is neglected. Because $\chi \simeq 1$ in the absence of ageing, coefficient χ introduces principally a correction for ageing and was therefore named by Bažant (972b) the *ageing coefficient*. (Note, however, that χ would not be close to 1 if the exponent n in the power law, Eq. (2.78), were not much less than 1.)

The relaxation function needed in Eq. (2.40) may be calculated with high accuracy using a step-by-step solution. For practical purposes, though, the approximation in Eq. (2.8) may normally be used in Eq. (2.40). Alternatively, a table or graph of the ageing coefficient χ may be set up for any given compliance function. But a table or graph becomes impractical if the dependence of $J(t,t')$ on many parameters is taken into account, as in the BP model.

If the load involves several sudden load changes, then the age-adjusted effective modulus method must be applied separately for each load increment and the results then superimposed.

The effective modulus gives exact results only if the stress is constant in time (curve 2 in Fig. 2.12). For all other stress histories sketched in Fig. 2.12 there is an error. By contrast, the age-adjusted effective modulus gives exact results for all the increasing and decreasing histories sketched in Fig. 2.12, provided they are expressible as linear functions of the relaxation function. The stress histories in structures under constant load are normally quite close to such a time variation. This explains why the age-adjusted effective modulus method gives far better results than the effective modulus method.

The quasi-elastic (algebraic) stress–strain relation based on the age-adjusted effective modulus is the simplest possible approach to linear creep analysis of ageing structures. The method has been endorsed in the latest recommendations of ACI (1982) as well as in CEB–FIP Manual (Chiorino *et al.*, 1984). Excellent results have been obtained in various practical applications (Bažant and Najjar, 1973; Bažant *et al.*, 1975; Brueger, 1974; Bažant and Panula 1980).

2.3 TEMPERATURE AND HUMIDITY EFFECTS

2.3.1 Diffusion theory, residual stresses and cracking

The specific moisture content, w, and its rate of change not only produce shrinkage or swelling but also exert profound influence on creep. The precise law governing this influence, however, is difficult to determine from measurements because test specimens are typically in a non-uniform moisture state, and consequently have non-uniform stress distributions with self-equilibrated residual stresses, and usually undergo tensile cracking or strain-softening as a consequence of these residual stresses. It is because of these complicating aspects that the effect of humidity on creep has been the most argued about property of

concrete, and it is only now, after some 50 years of research, that a clearer picture is emerging.

Measurements on specimens exposed to drying or wetting cannot be interpreted, and the behaviour of structures exposed to the environment cannot be predicted, unless the distributions of water content and pore humidity throughout the specimen are calculated. The movement of moisture through concrete is governed by the diffusion theory. In the early investigations (Carlson, 1937; Pickett, 1946; L'Hermite, 1952) the linear diffusion theory was used, but serious discrepancies have been found in confrontation with measurements. It is now well documented that the diffusion equation that governs moisture diffusion in concrete is highly non-linear, due principally to a strong dependence of permeability λ (as well as diffusivity C) on pore relative humidity. The governing differential equations may be written as (Bažant and Thonguthai, 1978, 1979; Bažant *et al.*, 1981)

$$\frac{\partial w}{\partial t} = -\operatorname{div}\mathbf{J}, \qquad \mathbf{J} = -\frac{a}{g}\operatorname{grad} p \tag{2.41}$$

in which

$$\frac{\partial w}{\partial t} = \frac{\partial w}{\partial p}\frac{\partial p}{\partial t} + \frac{\partial w}{\partial T}\frac{\partial T}{\partial t} - \dot{w}_h, \qquad \dot{w}_h = -\frac{\partial w}{\partial t_e}\frac{\partial t_e}{\partial T} \tag{2.42}$$

Here w = specified water content (kg/m^3), including water that is chemically bound, $w = w(p, T, t_e)$; $\dot{w}_h$ = rate of free water loss from the pores due to hydration (if $\dot{w}_h < 0$, $\dot{w}_h$ represents the rate of free pore water gain due to dehydration, which occurs at temperatures $> 100°$ C, $\mathbf{J}$ = flux of water through concrete (kg/s·m^2), a = permeability, g = gravity acceleration, t_e = equivalent age = $\int \beta_h \beta_T \, dt$ (where β_h, β_T are functions of p and T, see Eq. 2.49), T = temperature, and p = pore water pressure, representing the vapour pressure if the pores are unsaturated, and liquid water pressure if the pores are saturated.

Substitution of Eq. (2.42) into (2.41) and elimination of $\mathbf{J}$ yields a differential equation for p, coupled with the variation of temperature and of the degree of hydration. Alternatively, the diffusion problem can be formulated in terms of w instead of p. This is, however, inconvenient when the temperature is variable because the water flux at non-uniform temperature is still governed by grad p as the single driving force (Bažant and Thonguthai, 1978). When w is used as the basic variable, it means that $\mathbf{J}$ depends on both grad w and grad T, and not just on grad w; this is a mathematical complication. (The flux caused by grad w is called the Fick flux, and the flux caused by grad p the Soret flux or the thermal moisture flux.)

At constant temperature below 100 °C, it is convenient to reformulate Eqs (2.41) and (2.42) in terms of pore (relative) humidity $h = p/p_{sat}(T)$, where $p_{sat}(T)$ = saturation vapour pressure at temperature T (Bažant and Najjar, 1971, 1972).

$$\frac{\partial h}{\partial t} = -k \operatorname{div}\mathbf{J} + \frac{\partial h_s}{\partial t}, \qquad \mathbf{J} = -\lambda \operatorname{grad} h \tag{2.43}$$

where $k = (\partial h/\partial w)_{T,t_e}$ = inverse slope of the desorption or sorption isotherm of concrete at constant T and t_e, λ = permeability-type coefficient depending on T and t_e, and $h_s = h_s(t_e)$ = self-desiccation humidity, representing the variation of h with the age in a sealed specimen. For normal concretes, h_s decreases gradually from 1.0 to between 0.96 and 0.98. This variation is quite small and may be neglected as an approximation, which represents an advantage of the formulation in terms of h.

It is also possible to formulate the diffusion problem at constant T in terms of the free (evaporable) water content $\bar{w}$, but then the source term in the diffusion equation, representing the loss of free water consumed by the hydration reaction, is large and must be included. This is an inconvenience in such an approach.

The basic assumption underlying Eq. (2.41) is that local thermodynamic equilibrium always exists in each pore of concrete. This implies that w, p, and T are not related by a differential equation but simply by a function, representing the set of empirical desorption or sorption isotherms.

The material properties are characterized by empirical coefficients λ, β_h, β_T and isotherms $w = w(p, T, t_e)$, or coefficients k, a, and function $h_s(t_e)$. Their direct measurement is not an easy task. Generally it is physically simpler, albeit mathematically more complicated, to deduce these material characteristics by fitting transient data on h or p from drying or wetting tests with a finite element program (e.g. Bažant and Wu, 1974b).

For desorption at room temperature, slope k may often be considered as approximately constant, in which case Eq. (2.43) becomes

$$\frac{\partial h}{\partial t} = \operatorname{div}(C \operatorname{grad} h) + \frac{\partial h_s(t_e)}{\partial t} \tag{2.44}$$

where $C = kc$ = diffusivity of concrete. The assumption of constant slope k, however, is not very accurate for many concretes, and it is then preferable to use separate k and c (Eq. 2.41) instead of their product, C (Eq. 2.44). Especially at $h \to 1$, the slope k may vary between the mean slope of isotherm and an almost infinite value.

An important fact about moisture transport in concrete is that it is essentially uncoupled from the stress-deformation problem. This is confirmed by the fact that loading has no appreciable effect on the water loss due to drying, as observed by Maney (1941), Hansen (1960b) and others. However, an exception is the formation of large cracks due to stress, which were experimentally observed to increase permeability diffusivity significantly (Bažant, Şener and Kim, 1987). In that case, there is a two-way coupling with the stress-deformation problem.

The diffusion equation of moisture transfer (Eqs 2.41, 2.43 or 2.44) is strongly non-linear because of the dependence of λ (or C) on p (or h). It has been found (Bažant and Najjar, 1971, 1972) that λ (or C) decreases to about 1/20 as h drops from 0.95 to 0.50 (Fig. 2.13). This is probably due to the fact that at a high degree of saturation the moisture transfer occurs mainly in the capillary phase of water,

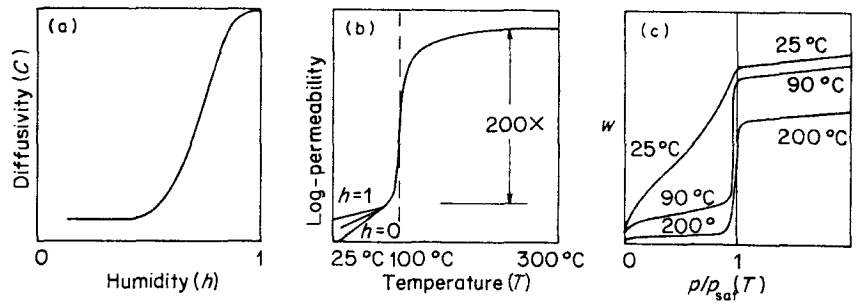

Figure 2.13 Theoretical dependences of diffusivity on pore humidity, permeability on temperature, and specific water content on pore relative vapour pressure, verified by comparisons with test results

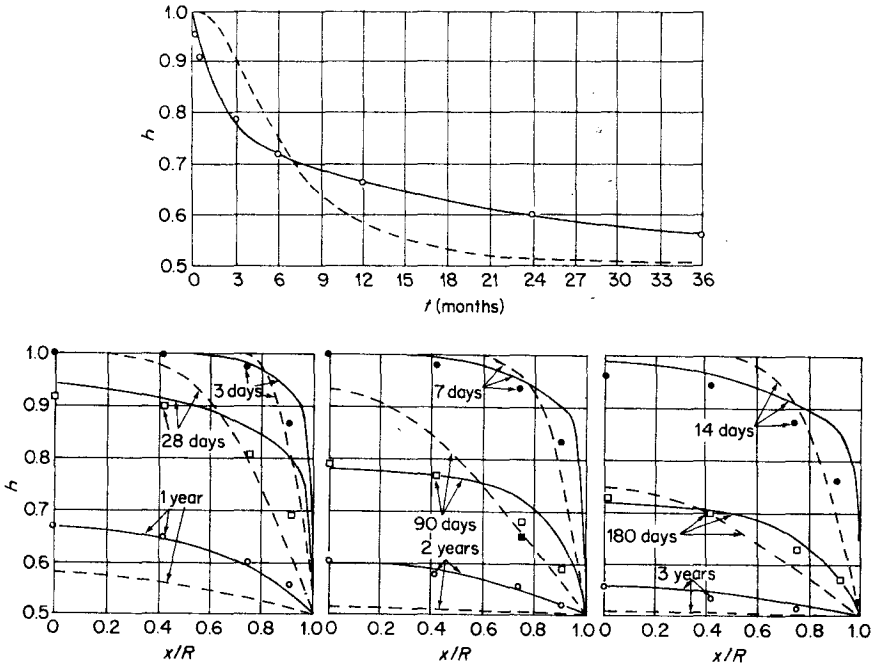

Figure 2.14 Example of measurements (by Monfore) of pore humidity distributions in a drying cylinder which lead to the dependence of diffusivity on the humidity shown in Fig. 2.13, for which the calculation yields the solid curves. The dashed curves represent the best fits possible with a constant diffusivity (top—evolution of humidity in the centre of cylinder; after Bažant and Najjar, 1971)

while at a low degree of saturation the moisture transfer probably involves surface diffusion along adsorption layers of water on the pore walls, as well as vapour movements (see Chapter 1). A suitable empirical expression, which was determined from drying data (Fig. 2.14) under the assumption of a constant value of k and was used by many authors in finite element analysis, is as follows (Bažant

and Najjar, 1972) (Fig. 2.13):

$$C = k\lambda \simeq C_1(T, t_e)\{0.05 + 0.95[1 + 3(1-h)^4]^{-1}\} \tag{2.45}$$

in which C_1 is the diffusivity value at $h = 1$; C depends strongly on temperature and the degree of hydration, which may be described by the semi-empirical formula (Bažant, 1975):

$$C_1(T, t_e) = C_0\left[0.3 + \left(\frac{13}{t_e}\right)^{1/2}\right]\frac{T}{T_0}\exp\left(\frac{Q}{RT_0} - \frac{Q}{RT}\right) \tag{2.46}$$

in which Q = activation energy of diffusion, R = gas constant, T = absolute temperature; $Q/R \simeq 4700$ K.

Below 100° C, drying of concrete is a very slow process, orders of magnitude slower than heating or cooling. A standard 6 in diameter cylinder of normal concrete requires over ten years to almost equilibrate pore humidity with a constant environment.

Equations (2.41)–(2.44) apply, of course, for both drying and wetting. Note, however, that diffusivity C greatly increases as concrete becomes oversaturated, i.e. $h > 1$ or $p > p_{sat}(T)$. This is because the inverse slope of the isotherm, $\partial p/\partial w$ or $\partial h/\partial w$, greatly decreases. As the boundary conditions, for a sealed surface the normal water flux $\mathbf{J}_n$ cannot be 0. For an exposed surface we may usually assume perfect moisture transfer, in which case we have at the surface $p = p_{en}$, where p_{en} is the environmental vapour pressure (this is apparently true even if the environmental and surface temperatures differ). In reality, the vapour pressure in the environment and in the pores at concrete surfaces differ. This is important only for very thin specimens, and one must then formulate the boundary condition with the help of the surface transmissivity coefficient for moisture.

The initial condition consists of a prescribed spatial distribution of h. The initial condition for concrete as cast is that $h \simeq 1$ everywhere.

Due to non-linearity of the diffusion equation, solutions must be obtained numerically. This can be easily accomplished using a finite element formulation in space and step-by-step integration in time. For the latter, the Crank–Nicolson algorithm appears to be most efficient (Bažant and Thonguthai, 1978, 1979; Bažant *et al.*, 1981). The finite element formulation may be developed using the Galerkin-type variational procedure (Bažant and Thonguthai, 1978, 1979).

Consider now the basic physical consequences for shrinkage and creep. One simple consequence of the diffusion theory is that geometrically similar specimens or structures of different sizes have similar distributions and time histories of pore humidity h. Using linear as well as non-linear diffusion equations, it may be shown (e.g. Bažant, 1982b) that, at the same relative location in geometrically similar bodies of different sizes, the pore humidity is a function of the non-dimensional time:

$$\theta = (t - t_0)/\tau_s \quad \text{with } \tau_s = D^2/C_1 \tag{2.47}$$

in which t_0 = age at the start of drying, D = characteristic dimension of the body (e.g. thickness), and τ_s = a coefficient which may be called the drying half-time. The time required for drying to reach the same pore humidity at the same relative location is proportional to τ_s, which in turn is proportional to the square of the dimension (thickness) of the concrete specimen or structure. Generally, the drying (or wetting) times of geometrically similar bodies are proportional to their size (dimension, thickness) squared.

The size-square dependence (Eq. 2.47) is useful for the modeling of shrinkage and has been introduced in a recent shrinkage prediction model (Bažant and Panula, 1978). However, this property is exactly true only if self-desiccation and the age dependence of permeability (Eq. 2.45) are neglected, and if the temperature is either constant or varies in a self-similar way for specimens of different sizes. On the other hand, non-linearity of the diffusion equation does not spoil the size-square dependence. Experimental data agree with this property quite closely.

Another simple basic property which follows from the diffusion theory characterizes the rate of penetration of the drying front into concrete from the surface. It can be shown (Bažant, Wittmann, Kim, Alou, 1987) that the penetration depth δ_p of the drying front is initially (for short $t - t_0$) given by

$$\delta_p = [12C_1(t - t_0)]^{1/2} \tag{2.48}$$

So, the penetration depth δ_p is proportional to the square root of the drying time, $t - t_0$. This property is again exactly true only if the self-desiccation and the age dependencies of permeability and of the slope of the sorption diagram are neglected. However, the non-linearity due to the dependence of diffusivity or permeability (Bažant and Najjar, 1971, 1972) on h does not invalidate Eq. (2.48). For a typical diffusivity value $C_1 = 0.1$ cm^2/day, the drying front penetrates the depth of 1 mm in 12 min, 1 cm in 20 hours, 10 cm in 83 days, and 1 m in 23 years. The drying times needed to reach a nearly uniform humidity distribution up to this depth are about a hundred times longer.

An important consequence of Eq. (2.48) for the penetration depth is that the shrinkage curves (for constant surface humidity) must be initially (i.e. asymptotically for short times) proportional to $(t - t_0)$ ($t - t_0$ = drying time) (see Eq. 2.84). This property, which is true not merely for the linear diffusion theory but also for the non-linear one (Bažant, Wittmann, Kim, Alou, 1987), closely agrees with carefully controlled experiments.

As a consequence of non-uniform humidity distributions, the shrinkage strains, as well as the creep strains at drying, are non-uniformly distributed throughout the specimen. Consequently, additional elastic and creep deformations are always produced such that the total strains become compatible. For the drying of a wall, the pore humidity distributions at various times, the associated free shrinkage strains, and the stress distributions produced are illustrated in Fig. 2.15. The strains produced by non-uniform drying normally greatly exceed the strain value for the tensile strength limit of concrete (i.e., f'_t/E). Therefore, they

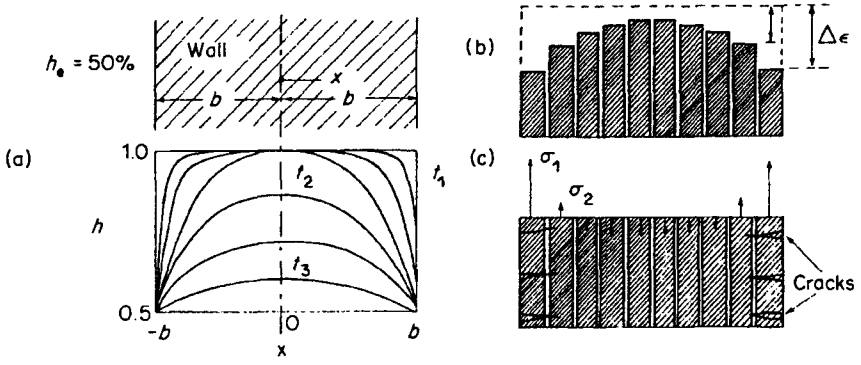

Figure 2.15 Typical subsequent humidity distributions in a wall exposed to drying (a), the corresponding shrinkages at various layers imagined as unrestrained (b), and shrinkage stresses with cracking caused by restoration of compatibility (c) (after Bažant, 1982b)

cause tensile strain softening and cracking. This means that the deformations measured in the standard tests of shrinkage and creep at drying or wetting merely represent the apparent shrinkage and creep of the specimen but not the true shrinkage and creep. They must be analysed and fitted with the help of a finite element program (Bažant and Wu, 1974a) in order to infer indirectly the true material properties.

2.3.2 Temperature and humidity dependence of creep viscosities and aging

Pore relative humidity h and temperature T affect creep and shrinkage in two ways: (1) directly, by altering the viscosity coefficient η_μ, and (2) indirectly, through the effect on the rate of ageing (hydration). Consider the latter effect first.

The rate of hydration strongly decreases as h decreases; at $h = 0.3$ the hydration rate is almost zero, and then there is no ageing. This may be conveniently described by means of a change of the time-scale, considering that the age-dependent material parameters, i.e. E_μ and η_μ, rather than being functions of the actual age of concrete t, are functions of a certain equivalent hydration period t_e; thus we may write

$$t_e = \int \beta_h \, dt, \qquad E_\mu = E_\mu(t_e), \qquad \eta_\mu = \eta_\mu(t_e) \tag{2.49}$$

in which β_h is an empirical function of h, which may be approximately considered as $\beta_h = [1 + (a - ah)^4]^{-1}$ (Bažant and Najjar, 1972). Calibration by test data yields $a \simeq 5$. For $h = 1$, we have $\beta_h = 1$ and $t_e = t$.

Similarly, an increase of temperature accelerates hydration, provided the temperature is below 100° C. Since the rate of chemical reactions generally follows the activation energy concept (rate-process theory) (Glasstone *et al.*,

1941), it is logical to use this concept for the rate of hydration or ageing; accordingly, the definition of the equivalent hydration period (or maturity) may be extended as

$$t_e = \int \beta_T \beta_h \, dt \tag{2.50}$$

in which

$$\beta_T = \exp\left[\frac{U_h}{R}\left(\frac{1}{T_0} - \frac{1}{T}\right)\right] \tag{2.51}$$

Here T is the absolute temperature (in kelvins), T_0 is the reference temperature (in kelvins, normally 296 K) (for $T = T_0$, $\beta_T = 1$), R is a gas constant, and U_h = activation energy of hydration; Bažant and Wu (1974a) found $U_h/R \simeq 2700$ K (Fig. 2.16). Strictly speaking, Eq. (2.51) ignores the fact that hydration consists of several simultaneous chemical reactions, each governed by a different activation energy. So deviations from Eq. (2.51) may be expected, and Jonasson (1984) finds that the empirical relation $U_h/R = 4600[30/(T - 263)]^{0.39}$ agrees with the test data better.

According to studies of non-linear creep (Bažant *et al.*, 1983), it seems that the rate of hydration (or ageing) might also depend on stress, as if compression promoted the rate of formation of new bonds. In particular, Eq. (2.50) would thus be generalized as

$$t_e = \int \beta_T \beta_h \beta_\sigma \, dt \tag{2.52}$$

in which β_σ is a function of the hydrostatic pressure component in concrete, such that β_σ increases with the magnitude of pressure. This effect might be even more complex in that each principal stress could affect the rate of hydration separately for each direction.

Now consider the direct effect of temperature and pore humidity on the rate of creep. This effect may be described as (Bažant *et al.*, 1981; Bažant and Chern, 1985a)

$$\frac{1}{\eta_\mu(t_e)} = \frac{\phi_T \phi_h}{\tau_\mu E_\mu(t_e)} \qquad (\mu = 1, 2, \ldots, N) \tag{2.53}$$

ϕ_T and ϕ_h are functions of T and h, which increase when T or h increase. The effect of temperature may again be based on the fundamental concept of activation energy, which implies that

$$\phi_T = \exp\left[\frac{U_c}{R}\left(\frac{1}{T_0} - \frac{1}{T}\right)\right] \tag{2.54}$$

in which U_c is the activation energy of creep; $U_c/R \simeq 5000$ K. The activation energy of creep could have different values for different τ_μ (i.e. for components of different relaxation or retardation times); however, the existing data do not indicate any need for such a refinement.

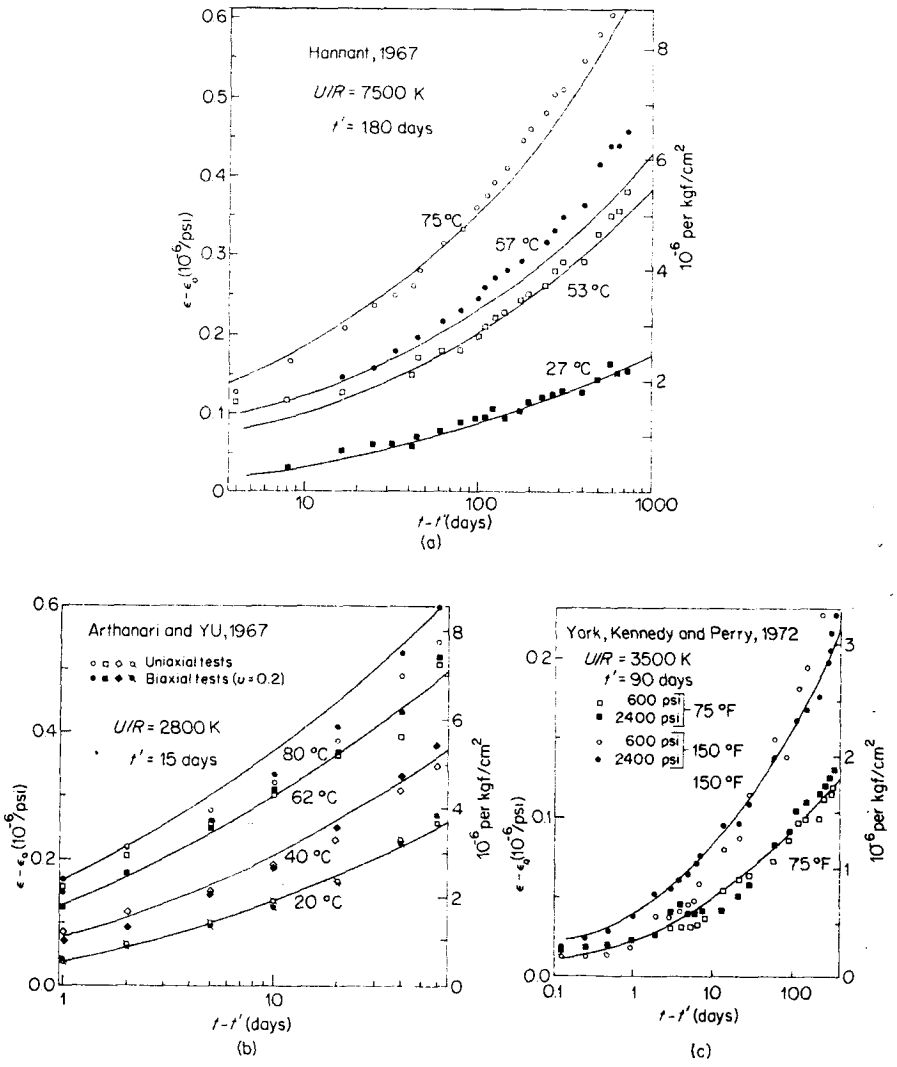

Figure 2.16 Compliance measurements for various temperatures, and fits (solid lines) by ageing Maxwell chain model with viscosities and reduced time which depend on temperature according to activation energies (Bažant and Wu, 1974b)

The effect of pore humidity on the creep rate may be described by the empirical equation (Bažant and Chern, 1985a) $\phi_h = \alpha_h + (1 - \alpha_h)h^2$, which indicates that the creep rate decreases if pore humidity decreases. According to some data for cement paste specimens predried in an oven and then rewetted (Wittmann, 1968), $\alpha_h \simeq 0.1$. However, the preheating might have made this effect too severe. Tests with drying at constant temperature (Bažant *et al.*, 1976) indicate a larger value,

$\alpha_h \simeq 0.5$ (Bažant *et al.*, 1976) which seems to work well for concrete (Bažant and Chern, 1985a).

The aforementioned humidity dependence of the creep rate may seem to go against the established notion that the creep at simultaneous drying is higher than the creep of sealed specimens. For this reason, it first appeared surprising when, during the 1960s, it was experimentally discovered that creep is lower at lower humidity (Wittmann, Ruetz, Cilosani, Ishai, etc.). However, when normal size specimens are drying while loaded, this effect is normally overridden by transient effects of stress-induced shrinkage and of cracking or strain-softening due to shrinkage stresses. These additional effects will be discussed later in this chapter.

2.3.3 Shrinkage, thermal expansion, and their stress dependence

Shrinkage as a material property, called true shrinkage, is the shrinkage of a material element at zero stress and variable humidity. Unfortunately, the true shrinkage of concrete cannot be measured directly because it is impossible to obtain a specimen with no residual stresses. This is because of the extremely slow process of drying of concrete at normal temperatures (extremely low diffusivity). To measure true shrinkage, it is necessary to use thin-walled specimens and vary the environmental humidity sufficiently slowly so that the pore humidity distribution throughout the wall of the specimen remains nearly uniform at all times. The wall thickness must be roughly 1 mm to permit changing the environmental humidity from 100 per cent to 50 per cent within about one day (Bažant and Raftshol, 1982). Specimens of this thickness can be prepared from cement paste (Bažant *et al.*, 1976), but not from concrete. For the thinnest possible wall of concrete, roughly 1 in., the aforementioned humidity change would have to be carried out gradually over a period of about 2 years, and for a 6 in. thickness, over a period of about 100 years. Therefore, the true shrinkage must be inferred indirectly from observations of specimens in which there are significant residual stresses. These stresses normally produce cracking, although the cracks are often invisible because they are too fine.

The total shrinkage (or swelling) of concrete may be expressed as $\varepsilon_s + \varepsilon_{sh}^a + \varepsilon_{sh}^c$, where ε_{sh}^a is the autogeneous shrinkage caused by volume changes due to chemical reactions during hydration, ε_{sh}^c is the carbonation shrinkage due to the reaction of calcium hydroxide from the cement paste with atmospheric carbon dioxide, and ε_s is the drying shrinkage (or swelling). The autogeneous shrinkage is normally quite small, about 5 per cent of the maximum drying shrinkage, and can be neglected. So can the carbonation shrinkage, since carbon dioxide penetrates only a very thin surface layer (perhaps 1 mm) in a good-quality concrete. From now on, we consider only the drying shrinkage (or swelling).

As shown by Carlson (1937), Pickett (1946) and others, drying shrinkage is approximately proportional to the loss of water from concrete, i.e. to w (the

specific water content of concrete). However, although this dependence is very simple, it seems usually more convenient to consider ε_s as a function of pore humidity h because the changes of h produced by hydration are very small (only a few per cent) while the changes of the evaporable water content are large. Shrinkage as a material property may be best described incrementally,

$$d\varepsilon_s = \kappa\, dh \tag{2.55}$$

in which κ is the shrinkage coefficient (incremental). Its values depend on h, T, and t_e, and are different for drying ($dh < 0$) and wetting ($dh > 0$). Because h is a function of the specific water content w, Eq. (2.55) is equivalent to $d\varepsilon_s = k_1\, dw$ where k_1 is a constant.

The shrinkage coefficient (at zero stress) depends on pore humidity and the age of concrete (degree of hydration). This may be approximately described as

$$\kappa = \varepsilon_s \psi, \qquad \psi = g_s(t_e)\frac{df_s(h)}{dh} \tag{2.56}$$

Here one may perhaps approximately introduce $g_s(t_e) = E(t_0)/E(t_e)$ and $f_s(h) = 1 - h^3$ (for $h \leqslant 0.99$, since for $h = 1$ swelling results). According to Jonasson, $1 - h^3$ is good only for $h \geqslant 0.4$, and for $h < 0.4$ shrinkage is much larger. Bažant suggests $h \simeq 1 - h^3 + c_b(1-h)^5$, $c_b \simeq 1$, for $0 < h \leqslant 0.99$.

In structures, shrinkage always occurs simultaneously with elastic deformations and creep. The previously given constitutive equation for linear ageing creep at various humidities and temperatures may then be generalized as

$$\frac{1}{E_\mu(t_e)}\mathbf{B}\dot{\boldsymbol{\sigma}}_\mu + \frac{1}{\eta_\mu(t_e)}\mathbf{B}\boldsymbol{\sigma}_\mu = \dot{\boldsymbol{\varepsilon}} - \boldsymbol{\kappa}\dot{h} - \boldsymbol{\alpha}\dot{T} \tag{2.57}$$

in which $\boldsymbol{\kappa}$ and $\boldsymbol{\alpha}$ are the column matrices of the shrinkage coefficients and thermal expansion coefficients, defined as $\boldsymbol{\kappa} = (\kappa_{11}, \kappa_{22}, \kappa_{33}, \kappa_{12}, \kappa_{23}, \kappa_{31})^T$, $\boldsymbol{\alpha} = (\alpha_{11}, \ldots)^T$. If the shrinkage and thermal expansion coefficients were independent of stress, they would be expressed as $\kappa_{ij} = \varepsilon_s^0 \psi \delta_{ij}$, $\alpha_{ij} = \alpha^0 \delta_{ij}$. However, these coefficients are not independent of stress, as has been recently established.

In the presence of stress, the shrinkage and thermal expansion coefficients may be approximately considered as linear functions of the stress tensor defined as follows (Bažant and Chern, 1985a)

$$\kappa_{ij} = \varepsilon_s^0 \psi(\delta_{ij} + r\sigma_{ij}\operatorname{sign}\dot{H}), \qquad \alpha_{ij} = \alpha^0(\delta_{ij} + \rho\sigma_{ij}\operatorname{sign}\dot{H}) \tag{2.58}$$

in which r and ρ are material constants and $\dot{H} = \dot{h} + c\dot{T}$ where c is a positive constant. A general linear dependence would also include terms $\sigma_0\delta_{ij}$ (where $\sigma_0 = \sigma_{kk}/3$ = volumetric stress); however, these terms appear to be negligible. Coefficient r is normally between $0.1/f_t'$ and $0.6/f_t'$, and coefficient ρ is about, $2.5/f_t'$ (Bažant and Chern, 1985a). Equation (2.58) means that at constant T the drying shrinkage is increased by compression stress and decreased by tensile stress, while the opposite is true of swelling (Bažant and Chern, 1986).

What is the physical mechanism that causes the stress dependence of κ and α? A definite answer does not yet exist; nevertheless, the following explanation seems logical. In hardened cement paste there exist two classes of pores: the macropores or capillary pores, and the micropores or gel pores. Their sizes differ by several orders of magnitude. The passages of the macroscopic water transport through concrete (drying or wetting process) pass mostly through the macropores and traverse probably only very little of the micropore space, although they must traverse at least some of it because capillaries in good-quality concretes are known to be discontinuous (Copeland *et al.*, 1960). The macro-diffusion process governs the pore relative humidities, h. When h (or T) changes, thermodynamic equilibrium of water between a macropore and adjacent micropores is disturbed, and micro-diffusion of water, i.e. the exchange of water with the adjacent micropores, is produced. This micro-diffusion process passes through molecule-size pores across which large stresses (resisting the applied load) are no doubt transmitted, due to the surface roughness and probable presence of some solid particle bridging the micropores. (The word 'micropore' is used here in the loose, relative sense of mechanics rather than in the sense of cement physics, in which it has a more precise meaning—pores $\leqslant 25$ Å in width; see Chapter 1.)

Now, although consensus on the details of the creep mechanism does not exist at present, it is agreed by most that creep must consist of some sort of debonding and rebonding of solid particles in the cement gel. It is reasonable to assume that this process of bond ruptures and reformations is promoted by the movement of water through the micropores. Thus, it seems physically justified to make the hypothesis that the creep rate, or the creep viscosity η, is a function of the flux of micro-diffusion of water, j; i.e. $\eta = \eta(j)$. Moreover, since the direction of flux j should not matter, η ought to depend only on $|j|$.

The macro-diffusion cannot be supposed to affect the creep rate since it bypasses most of the micropores which are significantly stressed by the applied load. Indeed, tests showed that a steady-state permeation of water through a wall does not appreciably affect creep.

The micro-diffusion transports water over extremely small distances, perhaps of the order of 10^{-5} or 10^{-6} m. From this, it may be estimated that the micro-diffusion process approaches equilibrium within a time with the order of magnitude of 10 sec. Thus, the micro-diffusion process may be considered to be infinitely fast. From this conclusion, and from the fact that diffusion is driven by a difference in the specific Gibbs free energy of water (chemical potential), it can be shown that the dependence of η on j is equivalent to a dependence of η on the quantity $|\dot{H}| = |\dot{h} + c\dot{T}|$. The dependence of $1/\eta$ on $|\dot{H}|$ is no doubt smooth and may be expanded in the Taylor series. If the series is truncated after the linear terms, i.e. $(1/\eta) = (1/\eta_0) + \kappa_1|\dot{H}|$, then, if we consider a single Maxwell unit, we may write

$$\frac{\dot{\sigma}}{E} + \left(\frac{1}{\eta_0} + \kappa_1|\dot{H}|\right)\sigma = \dot{\varepsilon} - \kappa_0\dot{h} - \alpha_0\dot{T} \tag{2.59}$$

κ_1, κ_0, η_0, and α_0 are positive coefficients independent of $\dot{h}$ and $\dot{T}$. Noting that $|\dot{H}| = \dot{H}\,\text{sign}\,\dot{T}$, this equation may be rearranged as

$$\frac{\dot{\sigma}}{E} + \frac{\sigma}{\eta_0} = \dot{\varepsilon} - (\kappa_0 + \kappa_1 \sigma\,\text{sign}\,\dot{H})\dot{h} - (\alpha_0 + \alpha_1 \sigma\,\text{sign}\,\dot{H})\dot{T} \qquad (2.60)$$

where $\alpha_0 = c\kappa_1$. Thus, we see that viscosity dependence on $\dot{h}$ and $\dot{T}$ is equivalent to *stress-induced shrinkage* and *stress-induced thermal expansion*, defined by the stress-dependent parts of the shrinkage coefficient and the thermal expansion coefficient. Equation (2.60) is then generalized by referring its left-hand side to a single Maxwell unit as in Eq. (2.23).

It may be noted that the formulation in Eq. (2.57) with stress-induced shrinkage and stress-induced thermal dilatation is a special, greatly simplified case of Bažant's original thermodynamic theory (Bažant, 1969, 1970a, 1972a; Bažant and Wu, 1974c), which was shown capable of describing the bulk of test data on creep at variable humidity. In that theory, several unnecessary hypotheses about the cement paste micro-structure and the mechanism of creep and shrinkage were introduced. The special case just described does not depend on these hypotheses, and it yields similar agreement with test data.

The stress dependence of the shrinkage coefficient and the thermal expansion coefficient was introduced by Bažant and Chern (1985a). Modeling creep of concrete at temperatures over 100° C, Thelandersson (1983) independently deduced the stress dependence of the thermal expansion coefficient on the basis of the test data of Schneider *et al.*, Bažant and Chern fitted with their theory the test data of L'Hermite *et al.*, (1965), L'Hermite and Mamillan (1968a, b), Troxell *et al.*, (1958), Hansen and Mattock (1966), McDonald (1972), Mamillan (1969), Brooks and Neville (1977), Ward and Cook (1969), Pickett (1946), Domone (1974), Bažant *et al.* (1976), and others. Some of the fits of these data are exhibited in Fig. 2.17.

The stress-dependence of shrinkage and thermal expansion coefficients means that these deformations are not simply additive to creep. Rather, one affects the other, contrary to what the current practical formulations for design imply. From the thermodynamic viewpoint this constitutes a cross effect, whose presence is normally to be expected whenever a phenomenon involves more than one irreversible thermodynamic process.

2.3.4 Effect of strain-softening (cracking)

The residual stresses produced by shrinkage (as well as non-uniform creep) are large enough to produce tensile cracking. These cracks may be either continuous and visible, or discontinuous and so fine and densely spaced that they are better described in a smeared, continuous manner as strain-softening. The latter case appears to be typical of concrete, with the exception of very thick unreinforced walls. This agrees with visual observations as well as theoretical calculations

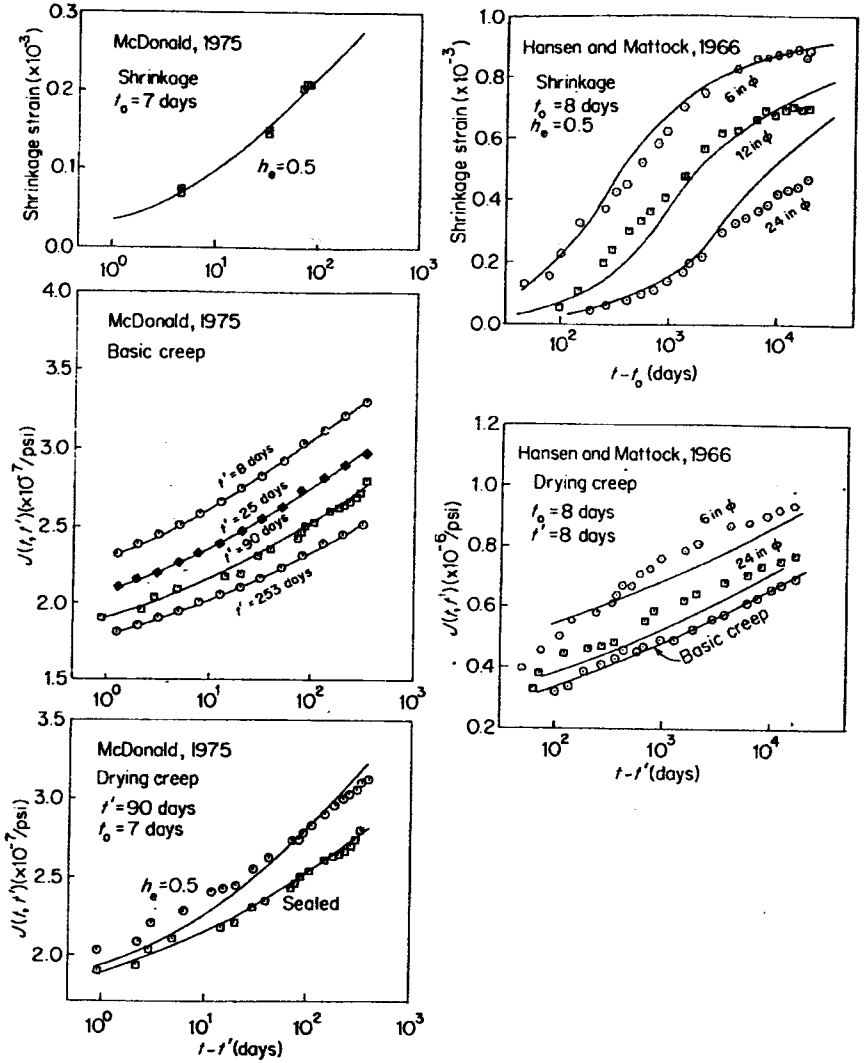

Figure 2.17 Basic data on compliance function at various environmental humidities h_e and ages at loading t', and the corresponding shrinkage, compared with calculations (Bažant and Chern, 1985a) taking into account stress-induced shrinkage, strain-softening (cracking), ageing, and pore humidity effect on viscosities and ageing (solid lines ——— calculated).

of crack width and spacing which were based on stability analysis of a parallel crack system (Bažant and Roftshol, 1982).

The constitutive relation for creep with tensile strain-softening must satisfy three requirements:

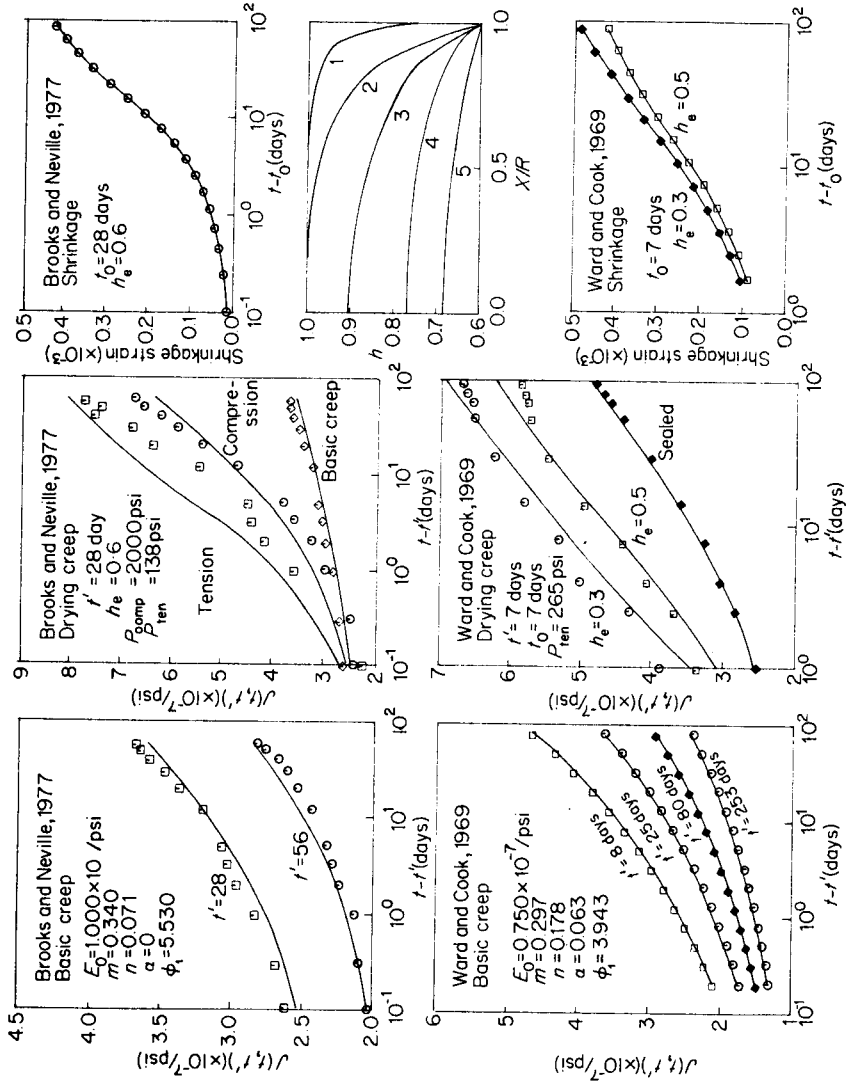

Figure 2.17 (*cont.*)

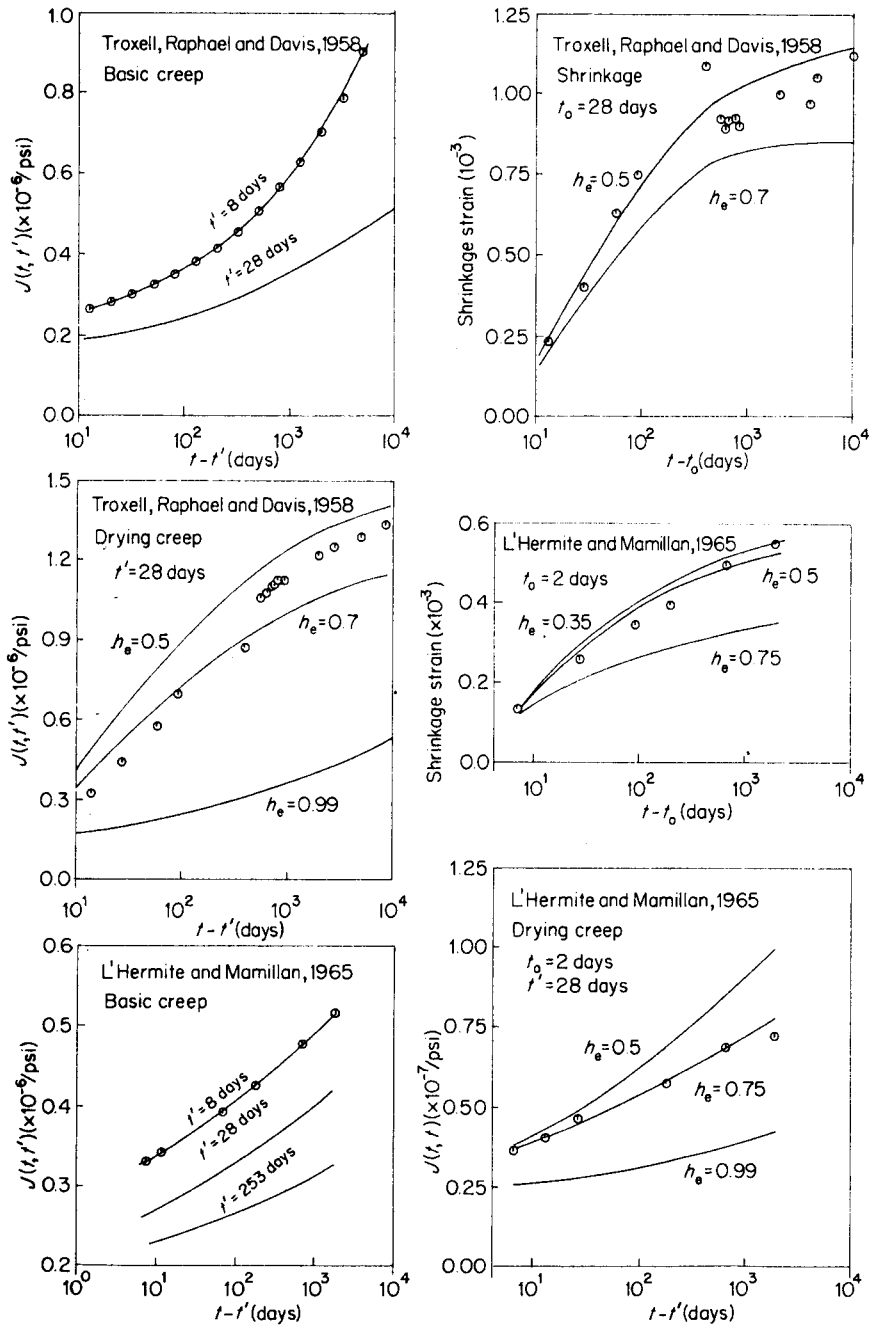

Figure 2.17 (*cont.*)

1. In the absence of strain-softening (cracking), it must reduce to linear viscoelasticity with ageing, augmented by shrinkage and thermal expansion terms.
2. In the absence of creep (as approximately true for very fast deformations), the constitutive relation must reduce to a strain-softening law, which is best described by an algebraic relation.
3. Irrespective of creep, ageing, shrinkage, and the loading path and history, the maximum principal tensile stress must reduce at very large tensile strain exactly to zero.

The third requirement is essential. It makes it difficult to use various incremental laws, such as those patterned after the theory of plasticity with loading surfaces. The reason is that such laws are path-dependent, whereas the final value of stress must be exactly zero regardless of the path. The uniqueness and path-independence of the zero final stress value can be easily achieved if the stress–strain relation for the part of strain, ξ, which is due to strain softening is algebraic, i.e.

$$\sigma = C(\xi)\xi \tag{2.61}$$

in which $C(\xi)$ is the variable secant modulus for strain-softening (Fig. 2.18). In particular, the simple expression $C = B_s \xi^{q-1} \exp(-C\xi^s)$ is found to give a reasonably shaped curve (B_s, q, s, c = constants, $s \geqslant 1$, $0 < q < 1$).

A special case of strain-softening is an abrupt stress drop, which has been extensively used in finite element simulation of cracking. Gradual strain-softening, however, describes the real behaviour of concrete much better than an abrupt stress drop.

How should the strain-softening relation be coupled with the stress–strain relation for creep? The aforementioned requirements (1) and (2) can be satisfied if these stress–strain relations correspond to a series coupling in the

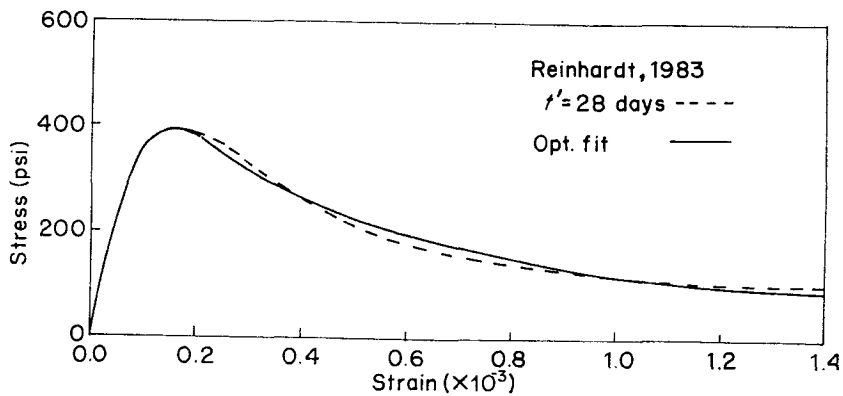

Figure 2.18 Tensile stress–strain diagram of concrete measured by Reinhardt and Cornellissen (1984), showing strain-softening due to invisible microcracking (dashed), and its fit by a formula (solid curve)

rheologic model (Fig. 2.9(c)). Thus, the strains (and strain rates) are assumed to be additive, i.e.

$$\dot{\boldsymbol{\varepsilon}} = \dot{\mathbf{e}} + \dot{\boldsymbol{\varepsilon}}^0 + \dot{\boldsymbol{\xi}} \tag{2.62}$$

in which $\mathbf{e}$, $\boldsymbol{\varepsilon}^0$, $\boldsymbol{\xi}$ = column matrices of strains due to creep with elastic deformation, shrinkage and thermal expansion, and strain-softening due to cracking.

A difficult aspect is the modeling of progressive cracking under general stress histories. A simple approach, which gives reasonable results if the principal stress directions do not significantly rotate during cracking, is to permit only certain fixed orthogonal crack directions which are fixed for each numerical integration point of each finite element when its maximum principal tensile stress first exceeds the tensile strength. A more realistic, but more complicated approach is the microplane model, an analogue of the slip theory of plasticity, in which cracking is modelled separately for all spatial directions and interaction of various directions is handled by kinematically constraining the strain for each crack direction to the same macroscopic strain (Bažant and Chern, 1985a).

When strain-softening occurs, particular attention must be paid to numerical approximation. Incremental quasi-elastic stress–strain relations may be based on central difference time-step formulas. However, such formulas require very small time steps, especially during strain-softening.

A much more efficient procedure is possible using the same idea as in the exponential algorithm for rate-type creep based on Maxwell or Kelvin chain, and applying that idea separately to the cracking strain ξ. A separate quasi-elastic stress–strain relation for the strain-softening part of deformation may be obtained if the equation $\sigma = C\xi$ is differentiated, i.e. $\dot{\sigma} = C\dot{\xi} + \dot{C}\xi = C\dot{\xi} + \dot{C}\sigma/C$, which may be rewritten as $\dot{\sigma} + \beta\sigma = C\dot{\xi}$ in which $\beta = -\dot{C}/C$. Now, this differential equation looks the same as that for the Maxwell unit, and for $\dot{\xi} = 0$ its solution describes stress relaxation. Stress relaxation always eventually leads to a reduction of stress exactly to zero, which conveniently satisfies the aforementioned requirement (3) no matter how long the time step is. An exact solution of this differential equation may be exploited to obtain incremental quasi-elastic stress–strain relations which permit very long time steps. To this end, the differential equation for $\dot{\sigma}$ is integrated exactly under the assumption that β and $C\dot{\xi}$ are constant during the time step although they may change discontinuously between the time steps. This leads to the incremental stress–strain relation (Bažant and Chern, 1985a)

$$\Delta\xi = \frac{\Delta\sigma}{D} + \Delta\xi'' \tag{2.63}$$

in which

$$D = \frac{1 - e^{-\Delta z}}{\Delta z}\bar{C}, \qquad \Delta\xi'' = (1 - e^{-\Delta z})\frac{\sigma}{D}, \qquad \Delta z = -\frac{\Delta C}{\bar{C}} \tag{2.64}$$

Here, $\bar{C}$ is the mean value of $C(\xi)$ for the time step. Equation (2.63) is then

combined in the manner of series coupling with a similar quasi-elastic stress-strain relation based on the Maxwell chain mentioned above (Eqs 2.31, 2.36). The resulting formulas are numerically quite accurate and stable even for very long time steps (Bažant and Chern, 1985a).

Whenever strain-softening (or an abrupt stress drop) is considered, questions arise with regard to localization of deformation, stability, sensitivity to the mesh size, and convergence as the mesh is refined. These questions border on fracture mechanics and are beyond the scope of this chapter.

2.3.5 Pickett effect (drying creep)

Having expounded the mathematical models for moisture diffusion, viscoelasticity with ageing, stress-induced shrinkage and thermal dilatation, and tensile cracking or strain-softening, we are now in a position to discuss the Pickett effect—probably the most intriguing phenomenon exhibited by concrete, named after the man who was first to clearly document this effect and analyse it (Pickett, 1942). The Pickett effect consists of the fact that, at simultaneous drying, the deformation of a concrete specimen under sustained load exceeds, usually by a large amount, the sum of the drying shrinkage deformation of a load-free specimen and of the deformation of a specimen that does not dry, i.e. is sealed (Fig. 2.19). The excess deformation may be regarded either as drying-induced creep (in short, drying creep) or as stress-induced shrinkage. The Pickett effect is also called the drying creep, or the stress-induced shrinkage, or the mechanosorptive effect (the last term prevails in the literature on wood).

Pickett (1942), in his original explanation, assumed that shrinkage stresses put creep into the non-linear range, in which the creep per unit stress is larger, thus producing excess deformation. This explanation is still in principle correct; however, it is far from complete. After extensive analyses of numerous test data pertaining to this phenomenon (Bažant and Chern, 1985a), it now appears that there are essentially four mechanisms causing the Pickett effect. They are, in the order of decreasing significance, as follows:

1. Stress-induced shrinkage (representing a thermodynamic cross effect).
2. Tensile strain softening due to cracking.
3. Irreversibility of unloading (i.e. resistance to contraction) after tensile cracking.
4. Increase of material stiffness with age.

Mechanism (2) is an extension of Pickett's hypothesis from non-linear hardening behaviour to non-linear softening behaviour. Tensile cracking of concrete specimens exposed to drying during creep was analysed by finite elements by Bažant and Wu (1974a) who noticed a significant influence of cracking on the response. Similar analysis was made by Jonasson (1978), and a

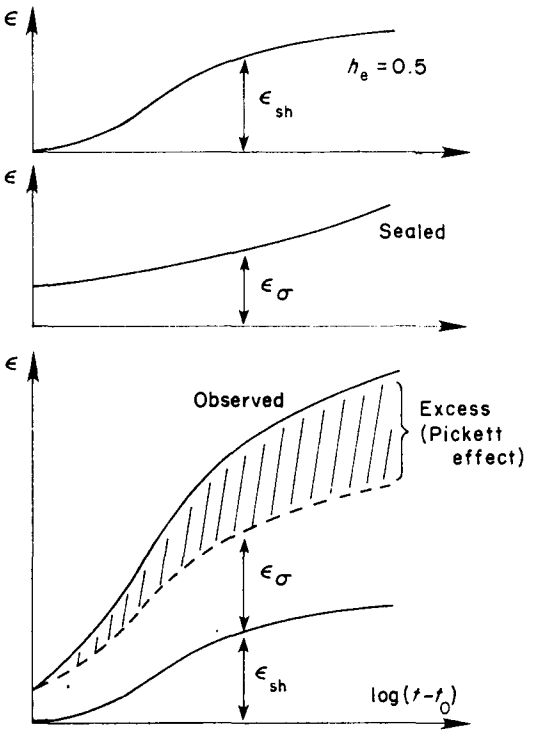

Figure 2.19 Excess deformation produced by simultaneous drying (Pickett effect)

similar conclusion about the importance of cracking was reached by Becker and Bresler (1977) and Iding and Bresler (1982).

A more penetrating examination of this effect was made by Wittmann and Roelfstra (1980) who suggested that tensile cracking might perhaps explain all of the excess deformation at drying. They emphasized that the observed overall shrinkage of load-free drying specimens is much less than the true material shrinkage, due to the effect of cracking. The consequence is that the deformation difference between the loaded and load-free specimens is magnified, and thus may falsely appear as creep according to the traditional definition of creep. However, when long-time compression creep, or creep in tension or bending, are considered, it appears that the phenomenon of cracking alone is insufficient to obtain agreement with experimental data. Compared to the assumption of a sudden crack drop, a significantly improved agreement with long-term measurements can be obtained when strain-softening is considered, as was done by Bažant and Chern (1985a). Yet an additional effect such as the stress-induced shrinkage appears inevitable for modeling the observed behaviour in its entirety.

The various influences on creep during drying may be illustrated in Figs 2.20 and 2.21. As shown in Fig. 2.20, the observed specimen shrinkage is considerably less than the true material shrinkage between the cracks. Because the creep with elastic deformation is determined by subtracting the deformation of a companion

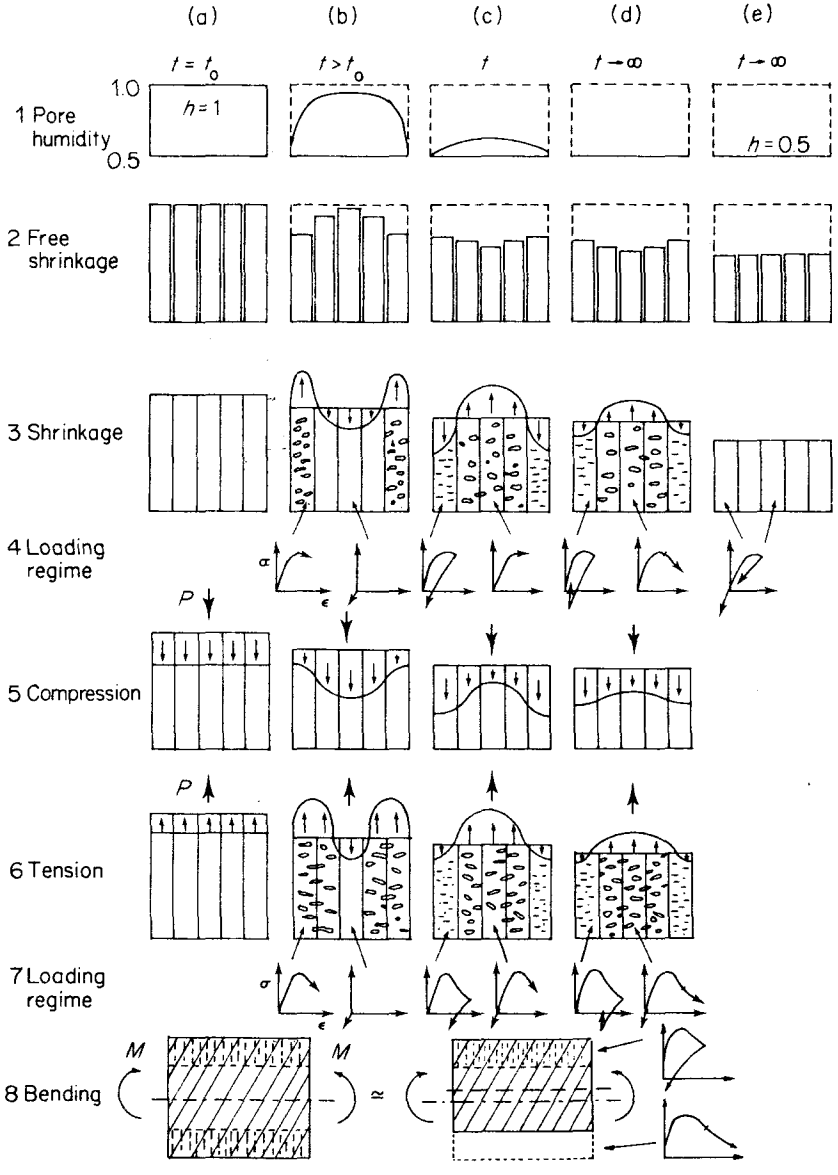

Figure 2.20 Evolution of deformations at various layers of a cross-section, with induced stresses and cracking, and stress–strain paths at various layers

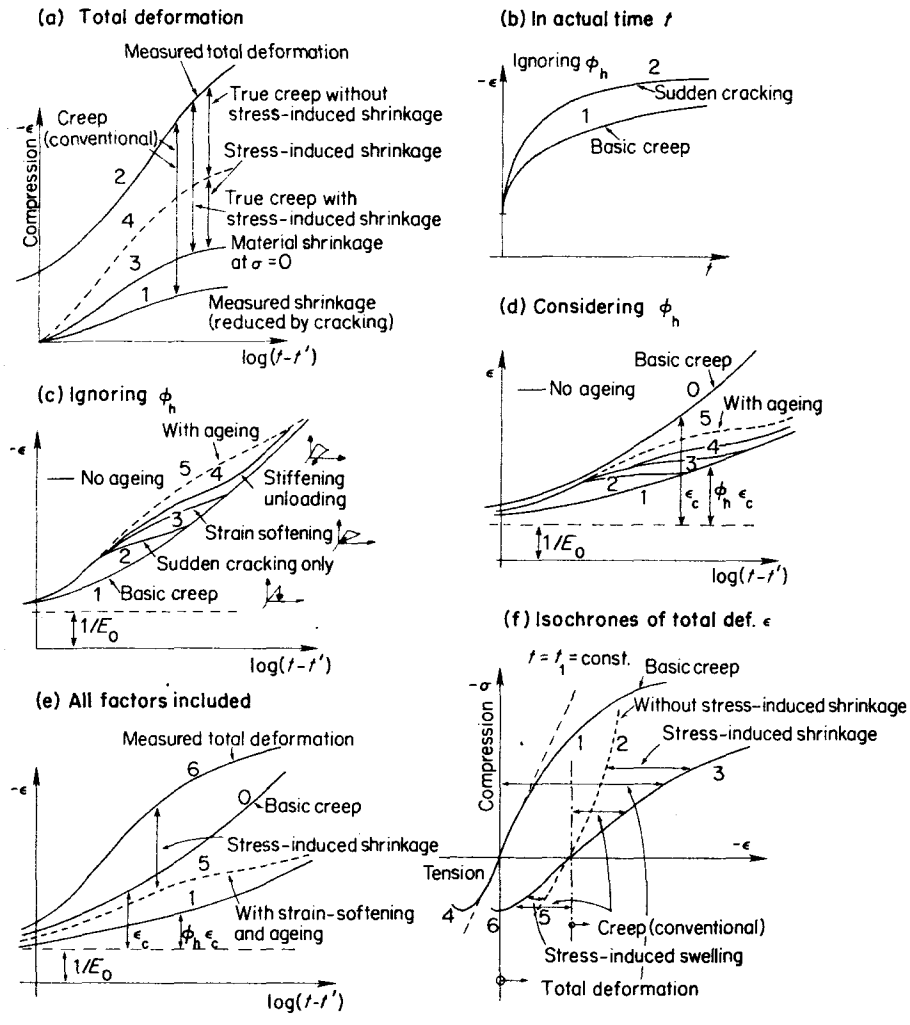

Figure 2.21 Various components explaining the excess creep at simultaneous drying

load-free specimen from the deformation of the loaded specimen, the observed (apparent) creep is considerably larger than that which would be obtained by subtracting the true (but unknown) material shrinkage. If the stress-induced shrinkage is included in the calculation (curve 4 in Fig. 2.21(a)), the true creep becomes even smaller.

If mechanisms (1), (3), and (4) are ignored, along with the coefficient α_h (giving a viscosity decrease as the water content decreases, and if the strain-softening is modelled as a sudden drop of stress to zero, then typically the curve shown in Fig. 2.21(b) is obtained (when plotted in the actual time-scale). Thus it might seem

that a sudden stress drop due to cracking might alone suffice to explain the Pickett effect. Not so, however. When the same curve is plotted in the logarithm of load duration, the excess deformation (curve 2 in Fig. 2.21(c)) is seen to disappear after about one decade in the log-time scale. The calculated excess deformation can be made to last considerably longer if the tensile strain softening is considered as gradual (curve 3, Fig. 2.21(c)). Eventually, though, the excess deformation still vanishes. But if one further includes irreversible unloading that does not return to the origin (Fig. 2.20, lines 4 and 7), the calculated excess deformation never vanishes (curve 4 in Fig. 2.21(c)). If the stiffening of unloading due to ageing is included as well, the calculated excess deformation becomes still more significant at long times (curve 5, Fig. 2.21(c)). This is because in the later stage of drying, when the core of the specimen shrinks, the outer layer, previously cracked in tension, is forced to contract, which it resists (column c, curves 3–4, Fig. 2.20).

These explanations become insufficient, however, if ϕ_h, i.e. the reduction of creep viscosities due to reduced water content, and the dependence of creep on stress are included (Fig. 2.21(d), (f)). Then the curves 2–5 in Fig. 2.21(d) which are in excess of curve 1 for the steady-state creep of a specimen in thermodynamic equilibrium at a certain reduced humidity, cannot be made to exceed the basic creep curve 0. This is one strong argument in support of the stress-induced shrinkage. Only then one can obtain curve 6 (Fig. 2.21(c)) passing significantly above the basic creep curve 0. An important aspect is that, since the stress-induced shrinkage is defined incrementally and is irreversible, the calculated excess deformation remains large for infinitely long times, while the contribution from tensile cracking or strain-softening tends to die out (Fig. 2.21(c)).

A second argument for the stress-induced shrinkage arises from the stress dependence of creep (Fig. 2.21(f)). Without the stress-induced shrinkage, the isochrone for the total deformation at drying (curve 2 in Fig. 2.21(f)) rises with a gradually increasing slope, approaching the basic creep curve 1 at higher compressive stresses. By contrast, existing tests (Mamillan and Lelan, 1970) yield the isochrone 3 in Fig. 2.21(f), which has a smaller slope than isochrone 1 for the basic creep, and which is diverging from the basic creep isochrone as the compressive stress magnitude increases. The reason that curve 2 (Fig. 2.21(f)) does not diverge from the isochrone 1 for basic creep is that the contribution to the excess deformation which is due to tensile cracking arises totally in the load-free companion shrinkage specimen, because the compression-loaded specimen does not crack (curve 5 in Fig. 2.20). So this contribution is essentially constant, independent of stress, and a stress-dependent contribution, as provided by the stress-induced shrinkage, must be superimposed.

A third argument for the stress-induced shrinkage comes from tensile creep. For tension, the compliance is generally observed to be at least as large as for uniaxial compression, but usually larger (Brooks and Neville, 1977; Davis *et al.*, 1937; Illston, 1965). This is also true for drying. Thus, the Pickett effect is at least

as intense in tension as in compression, and usually it is more intense. The part of creep increase per unit stress due to cracking is larger for tension than for compression, according to the present theory, while the part due to the stress dependence of shrinkage coefficient is about the same; see curve 6 in Fig. 2.20. Thus, the isochrone of total deformation (curve 6 in Fig. 2.21(f)), has a smaller slope than the basic creep isochrone in tension (curve 4). Without the stress-induced shrinkage, however, the total deformation isochrone at drying, obtained from computer simulations, has about the same slope as the basic creep isochrone (curve 5). This is because the cracking caused by tensile loading in addition to the cracking caused by shrinkage is not large enough, and also because the additional cracking produced by tensile load does not increase much with time.

In this context it should be observed that for concrete specimens in water, which swell, the self-equilibrated stresses are opposite to those in line 3 of Fig. 2.20. Yet, an increased creep is again observed during swelling (Domone, 1974; Gamble and Parrott, 1978), which was initially considered paradoxical. The explanation is that since tensile stress σ reduces the value of the shrinkage (swelling) coefficient κ, the swelling in a tensile-loaded specimen is less than the swelling at no stress, thus making the deformation difference between the loaded and load-free specimens larger.

A fourth argument for the stress-induced shrinkage is furnished by bending creep tests, through which the drying creep effect was in fact first unambiguously demonstrated by Pickett (1942). The bending creep test has the advantage that shrinkage in a load-free specimen produces no bending, so that no companion deformation needs to be subtracted. This eliminates the uncertainties due to inevitable random differences between two specimens, as well as the difficulty due to different cracking patterns and different residual stress distributions in the loaded and load-free specimens. Pickett (1942) explained the excess creep deflections by non-linearity of the tensile stress–strain diagram, with irreversible elastic unloading. Drying produces microcracked layers near the surface (Fig. 2.20(f)). As the bending moment M is applied, the lower microcracked layer is further extended while the upper microcracked layer is forced to contract back. The incremental stiffness for further extension is much less than that for reverse contraction. This is true even in Pickett's sense, i.e. without the strain-softening. However, if strain-softening is taken into account, the differences in incremental stiffness between the top and bottom microcracked layers become much more pronounced, which is needed to fit the data on bending creep during drying while at the same time the analytical model can represent compression and tension creeps during drying (for which sufficient data were unavailable to Pickett.

As for the effect of the stress-induced shrinkage, the compressed side of the beam shrinks more and the tension side shrinks less than the true material shrinkage at no stress. Evidently, this causes additional curvature in the sense of

the applied bending moment. In computer simulations (Bažant and Chern, 1985a), this in fact appears to be the most important contribution of drying to the excess deflections.

Fits of numerous test data pertaining to these effects are given by Bažant and Chern (1985a) along with plots of residual stress distributions in test specimens at various times.

The use of an extensive data set is important for being able to reach the foregoing conclusions. History teaches us that limited test data can be fitted in more than one way, sometimes using radically different theories. Determination of a constitutive equation from test data becomes unambiguous only when the complete set of information on the material is considered.

2.3.6 Behaviour at high temperatures

Due to applications of concrete in nuclear power plants and concern about their safety in regard to various hypothetical nuclear accidents, behaviour of concrete at temperatures over 100° C has recently been in the forefront of interest. Predictions of response require a realistic constitutive relation for high-temperature creep, shrinkage and swelling, as well as a realistic model for the coupled heat and water transport through concrete. A reasonable mathematical model is now emerging.

It appears that the formulations for normal temperatures can mostly be extended to high temperatures, with some significant differences. For moisture transfer, the most significant difference is that the permeability as well as diffusivity of concrete for water increases about two hundred times as the temperature exceeds 100° C. Another important aspect, not quite well understood at present, is the interchange of water between the capillary, adsorbed, and chemically bound (hydrated) states, along with the description of dehydration and the consequent release of free water into the pores of concrete.

A curious aspect is that high pore pressures (in excess of 10 atm) have never been measured in experiments, although calculations of pressures from the thermodynamic properties of water yield much larger pressures, under the assumption that the pore space is constant and completely filled. The only explanation is that significant increases in pore space available to free water result from heating. The determination of pore pressure is very important for predicting explosive spalling of concrete. All the existing experiments have been limited to concrete at constant or decreasing water content. It could be that the increase of the water content (oversaturation) which must arise when water is pushed into the heated concrete layer ahead of the drying front, may result in much larger pressures than those measured so far.

The aforementioned properties have been incorporated in the sorption–desorption isotherms at high temperature, along with the thermodynamic properties of water based on the well-known equation of state. The analytical

results for pore pressures and water loss can then be brought in agreement with measured data (Bažant and Thonguthai, 1978, 1979).

As for the stress–strain relation, the chief question remains with regard to the effect of drying. All tests carried out so far pertain to specimens which were losing moisture when heated over 100° C, except for some limited tests on small cement paste specimens. From these tests it appears that the relation of creep at constant water content and creep at drying is reversed compared to the situation at room temperature. This may be due to the sharp increase in permeability, causing water diffusion phenomena to be short-lived, with a very short half-time. Thus, the transient aspect such as the stress-induced shrinkage, which is explained by the effect of the microdiffusion flux on the creep viscosities, is important only at the beginning of creep, while afterwards the reduction of creep viscosities due to the decrease of water content prevails. This may explain why the existing tests (Maréchal, 1970a, b, 1972a) indicate for dried concrete at high temperatures a much lower creep than that at constant water content (Bažant *et al.*, 1982).

Furthermore, significant difference is found at high temperatures between the creep at constant water content and the creep in water immersion (Bažant *et al.*, 1976; Bažant and Prasannan, 1986). Apparently, the latter condition causes a sort of microstructure conversion similar to autoclaving which is known to reduce creep.

As for the triaxial properties, it is of interest to note that the creep Poisson ratio at high temperatures has been observed at Northwestern University (Bažant *et al.*, 1976) to be much higher than for room temperature (0.46 compared to 0.18). But this observation is limited to cement paste. The difference is much smaller for concrete for which the Poisson ratio value is dominated by the aggregate skeleton.

The phenomenon of stress-induced thermal expansion, mentioned above, has been detected for temperatures above 100° C and mathematically formulated by Thelandersson (1983), based on the test data of Schneider and Kordina (1975), Schneider (1982) and others (Bažant *et al.*, 1982). A logical conclusion from this result is that stress-induced shrinkage must also exist at high temperatures above 100° C, and the stress-induced thermal expansion at temperatures below 100° C.

Mathematical models for concrete creep at high temperature and the associated coupled heat and mass transport have been developed and implemented in computer programs at Northwestern University (Bažant and Chern, 1985a; Bažant *et al.*, 1981), Argonne National Laboratory (Lau, Acker *et al.*, 1986; Lazić, 1985), Technical University of Lund (Thelandersson, 1983), and Gesamthochschule Kassel (Schneider, 1982, 1986).

2.4 NON-LINEAR EFFECTS AND THERMODYNAMIC ASPECTS

2.4.1 Deviations from linearity (principle of superposition)

The linearity of creep, synonymous to the principle of superposition, is applicable for stresses within the service stress range, i.e. up to about one-half of the strength

limit. Even within this range, however, there are deviations. The deviations may be described as the phenomenon of adaptation (not to be confused with the phenomenon of adaptation in cyclic plasticity). Concrete subjected to a sustained compressive stress appears to adapt to the stress, getting stronger, as indicated by increases of strength and stiffness observed at subsequent load changes, both short-time and long-time. Thus, it appears that after a long period of compression creep, the recovery is significantly less than that predicted by the principle of superposition, and the additional creep due to a later compressive stress increment is also significantly less (Fig. 2.22).

It seems that the phenomenon of adaptation may be adequately described by generalizing the equivalent hydration period t_e so as to represent an acceleration of ageing due to compressive stress, and by introducing a stiffness adjustment coefficient $a(t)$ for which a separate evolution equation (a first-order differential equation) is written (Bažant and Kim, 1979b). A model of this type permits the representation of the test data of Komendant *et al.* (1976), Freudenthal and Roll (1958), Roll (1964), Brettle (1958), Meyers and Slate (1979), Aleksandrovskii and Popkova (1970), Aleksandrovskii and Kolensnikov (1971) and others.

The existing data on the deviations from linearity in the service stress range may be also described in a different manner, admitting that the law governing creep is inherently non-linear although at low stress it exhibits a proportionality property for creep under various constant stress values. This formulation (Bažant *et al.*, 1983) has a form of a simple non-linear differential equation for the case of constant stress, which may be explained in terms of the rate-process theory (activation energy concept). For variable stress, this equation is gen-

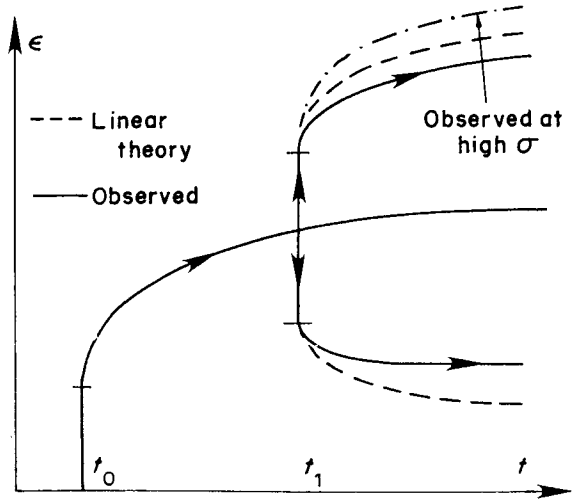

Figure 2.22 Typical observed deviations from superposition principle in service stress range

eralized by a history integral which is singular in terms of the creep strain. This formulation also gives good agreement with the existing test data.

The most important deviations from linearity (principle of superposition) within the service stress range are caused by humidity changes simultaneous with creep. The non-linearity is due to tensile cracking or strain-softening. The stress-induced shrinkage is linear in stress, to the first order of approximation considered here.

Creep in the high-stress range at constant stress may be described quite well by the simple differential equation $\dot{\varepsilon}_c = a\sigma^r(t-t')^u\varepsilon_c^s$ in which a, r, u, and s are material constants and ε_c is the creep strain. However, the proper generalization of this equation to arbitrary stress histories is complicated and leads to a singular history integral for creep strain (Tsubaki *et al.*, 1982). A non-linear constitutive law for concrete of a different type, which involves multiple history integrals, was developed by Huet, Gaucher *et al.*

Remark

After completion of the committee's work, Bažant and Prasannan (1987) discovered a new model which describes both the high-stress non-linearity (increased creep) and the reduced recovery (Fig. 2.22) in a manner that is close to test data, simpler and physically better justified. See the Addendum to this chapter.

2.4.2 Viscoplasticity and cyclic creep

Another important non-linear phenomenon arises for cyclic or pulsating loads with many repetitions. According to the principle of superposition, the creep due to cyclic stress should be approximately the same as the creep due to a constant stress equal to the average of the cyclic stress. In reality, a higher creep is observed. The larger the amplitude of the cyclic stress component, the larger the excess creep.

The time-average compliance function for cyclic creep at constant stress with amplitude Δ and a constant mean stress σ may be reasonably well described by an extension of the double power law (see Section 2.5.3) in which $(t-t')^n$ is replaced by the expression $[(t-t')^n + 2.2\phi_\sigma\Delta^2N^n]$, where N is the number of uniaxial stress cycles of amplitude Δ and ϕ_σ is a function of mean stress σ (Bažant and Panula, 1978, **12**). For stresses beyond the service stress range, both the short-time and the long-time responses of concrete become strongly non-linear.

The short-time response may, within certain limitations, be described by three-dimensional constitutive relations of plasticity. Accordingly, the non-linear long-time response needs to be described by viscoplastic constitutive relations.

At present, the question of short-time three-dimensional non-linear constitutive models still remains unsettled, and so it is difficult to consider the three-dimensional long-time non-linear behaviour. Except for some attempts to

generalize certain existing non-linear multiaxial constitutive models for the influence of strain rate, no models are available for non-linear triaxial long-time creep. Some models have been formulated, however, for uniaxial loading. From these it transpires that the hereditary aspect (history dependence) of creep becomes weaker at high stresses, and the creep may be largely described as flow, understood as the time-dependent deformation described by the Maxwell model with a non-linear dashpot (Bažant and Kim, 1979b).

2.4.3 Cracking and strain-softening

While the non-linear creep properties under compressive stresses may be described as viscoplasticity (flow), the non-linear creep under tensile stress states requires a different description. For such loading, there is significant additional deformation caused by cracking (frequently so finely distributed that it is invisible) and strain-softening in tension. This aspect has already been discussed in Section 2.3.4 in relation to drying. Nevertheless, the discussion pertains also to cracking in the absence of drying, caused solely be applied loads.

2.4.4 Thermodynamics of constitutive relations

The constitutive equation for creep and shrinkage must satisfy certain thermodynamic restrictions. For non-ageing materials, these restrictions are well understood (Biot, 1955; Rice, 1971), but for ageing materials there has been much misunderstanding.

Not every function of two variables is acceptable as the compliance function $J(t,t')$. Certain thermodynamic restrictions, such as $\partial J(t,t')/\partial t \geqslant 0$, $\partial^2 J(t,t')/\partial t^2 \leqslant 0$, and $[\partial J(t,t')/\partial t']_{t-t'} \leqslant 0$ are intuitively obvious. Some further restrictions, however, are necessary to express certain aspects of the physical mechanism of ageing.

At present we know how to guarantee fulfilment of such thermodynamic restrictions only if we first convert the constitutive relation to a differential-type form and then make the hypothesis that these restrictions should be applied to internal variables such as the partial strains or partial stresses in the same way as they would be applied to the strains and stresses. If we did not accept this hypothesis, we could say nothing about thermodynamic restrictions. It might be possible that no thermodynamic restrictions are violated by the stresses and strains even though they may be violated by the partial stresses or partial strains. But we cannot guarantee it. It is certainly a matter of concern if violations occur. It has been found (Bažant, 1979) that such violations do in fact happen for certain existing creep laws. On the other hand, if the thermodynamic restrictions are satisfied by the partial stresses or partial strains, it is guaranteed that they are also satisfied by the total stresses and strains. This is one basic advantage of the thermodynamic method (Section 2.4.4).

If we reduce the compliance function to a rate-type form corresponding to a spring-dashpot model, fulfilment of the second law of thermodynamics can be guaranteed by certain conditions on spring moduli E_μ and viscosities η_μ. (The second law might of course be satisfied by the compliance function even when some of these conditions are violated, but again the point is that we cannot be certain of it.) Two obvious conditions are $E_\mu \geqslant 0$ and $\eta_\mu \geqslant 0$. However, the second law leads to a further condition when the spring moduli are age-dependent (Bažant, 1974).

$$\dot{\sigma}_\mu = E_\mu(t)\dot{\varepsilon}_\mu \quad \text{for } \dot{E}_\mu \geqslant 0 \tag{2.65}$$

$$\sigma_\mu = E_\mu(t)\varepsilon_\mu \quad \text{for } \dot{E}_\mu \leqslant 0 \tag{2.66}$$

where σ_μ and ε_μ are the stress and the strain in the μth spring. The first relation pertains to a solidifying material, such as an ageing concrete, while the second relation pertains to a disintegrating (or melting) material, such as concrete at high temperatures (over 150° C) which cause dehydration.

If Eq. (2.66) is used, it can be shown that the expression $\dot{D}_{ch} = -\sigma_\mu^2 \dot{E}_\mu / 2E_\mu^2$ represents the rate of dissipation of strain energy due to the chemical process (particularly due to disappearance of bonds) which proceeds while the material is in a strained state (i.e. a state in which the energy of chemical bonds differs from its initial value at zero macroscopic strain). Thus, to ensure that $\dot{D}_{ch} \geqslant 0$ we must have $\dot{E}_\mu \leqslant 0$. So the dissipation inequality is violated if Eq. (2.66) is used (or if its use is implied) for an ageing (solidifying, hardening) material.

Equations (2.65) and (2.66) can be also derived from the fact that the new bonds formed in a solidification process must be in a stress-free state when they form (e.g. due to hydration). By contrast, for dehydration the bonds are in a stressed state when they are lost (e.g. due to dehydration). (Section 2.4.4).

Various differential-type forms of the creep law are possible. One form can be obtained by expanding the memory function $L(t,t')$ into the Dirichlet series:

$$L(t,t') = \sum_{\mu=1}^{N} \frac{1}{\eta_\mu(t')} \exp[-(t-t')/\tau_\mu] \tag{2.67}$$

Substitution into Eq. (2.5) yields:

$$\varepsilon = \sum_{\mu=1}^{N} \varepsilon_\mu + \varepsilon^0, \qquad \varepsilon_\mu(t) = \int_0^t \frac{\sigma(t')}{\eta_\mu(t')} \exp[-(t-t')/\tau_\mu]\,dt' \tag{2.68}$$

By differentiating $\varepsilon_\mu(t)$ and denoting $E_\mu(t) = \eta_\mu(t)/\tau_\mu$, one can readily verify that $\varepsilon_\mu(t)$ satisfies the differential equation

$$\sigma = E_\mu(t)\varepsilon_\mu + \eta_\mu(t)\dot{\varepsilon}_\mu \tag{2.69}$$

From this, the non-viscous part of stress σ is $\sigma_\mu = E_\mu(t)\varepsilon_\mu$. Now we notice that this represents an elastic relation that is admissible only for a disintegrating (melting, dehydrating) material (Eq. 2.66). Thus, Eq. (2.67), which has been used as the

basis of one large finite element program for creep of reactor vessels, implies violation of the dissipation inequality by the internal variables. This puts the practical applicability in question.

We may note that Eq. (2.69) along with $\varepsilon = \Sigma_\mu \varepsilon_\mu$ corresponds to a Kelvin (or Kelvin–Voigt) chain model (Bažant, 1979), the springs of which are, however, governed by an incorrect equation (Eq. 2.66). If the correct equations for the springs are used ($\dot{\sigma}_\mu = E_\mu \dot{\varepsilon}_\mu$), then the Kelvin chain is characterized by second-order rather than first-order differential equations (Eq. 2.26). The reason for violation of the dissipation inequality by Eqs (2.67) or (2.68) can be traced to the fact that the equation for partial strains (Eq. 2.69) is of the first order. One can show (Bažant, 1979) that even if a non-linear rate-type creep law is considered such that $\varepsilon = \Sigma_\mu \varepsilon_\mu$ and $\dot{\varepsilon}_\mu = f_\mu(\sigma, \varepsilon_\mu)$, Eq. (2.66), which violates the dissipation inequality, is still implied as long as these equations are of the first order. This is one inherent difficulty of using Kelvin chain-type models (i.e. decomposing ε into partial strains ε_μ) for ageing (hardening) materials. By contrast, the differential equations for the ageing Maxwell chain are of the first order, which is an advantageous property. (*Remark*: The model in the Addendum, discovered after the completion of the committee's work, however, shows that a non-ageing Kelvin chain can be used for ageing creep if ageing is modelled by a separate transformation of variables.)

From the physical viewpoint, ageing is not admissible as the property of a substance in a thermodynamic system. Rather, ageing must be treated as an increase of the ratio of mass of the solidified component (hydrated cement) to the mass of the unsolidified components (water and unhydrous cement grains), each of which undergoes no ageing (see Section 2.4.4 and the Addendum).

Ageing Kelvin chain models have another interesting property. Consider the degenerate creep compliance in Eq. (2.14). We calculate $\partial^2 J/\partial t\, \partial t'$ and substitute

$$C_\mu(t') = [(C(t') - E_\mu(t')]\dot{y}_\mu(t') \quad \text{and} \quad C_\mu(t') = \eta_\mu(t') y_\mu(t')$$

according to Eq. (2.27) for the Kelvin chain. This yields

$$\frac{\partial^2 J(t,t')}{\partial t\, \partial t'} = \sum_{\mu=1}^{N} \frac{\dot{y}_\mu(t)}{\dot{y}_\mu(t')} \frac{E_\mu(t')}{[\eta_\mu(t')]^2} \exp[y_\mu(t') - y_\mu(t)] \tag{2.70}$$

Here we must always have $\dot{y}_\mu > 0$ and $E_\mu \geqslant 0$. Consequently, thermodynamically admissible Kelvin chain models always yield a compliance function such that

$$\frac{\partial^2 J(t,t')}{\partial t\, \partial t'} \geqslant 0 \tag{2.71}$$

Now, what is the meaning of this inequality? Geometrically, it means that the slope of a unit creep curve would become greater as t' increases, which means that two creep curves for different t', plotted versus time t (not $t - t'$) would never diverge as t increases. Is this property borne out by experiment? Due to the large scatter of creep data we cannot answer this question with complete certainty. A few test data exhibit slight divergence of adjacent creep curves beginning with a certain creep duration $t - t'$ (Bažant and Kim, 1978; Bažant, 1979), but most data do not. As for the creep formulas, the double power law, Eq. (2.72), as well as the ACI formulation, always exhibit divergence after a certain value of $t - t'$, whereas the improved Dischinger model (CEB–FIP 1978 formulation) does not. (Neither does the new model in the Addendum.)

So the ageing Kelvin chain models cannot closely approximate a compliance function with divergence without violating the thermodynamic restrictions $E_\mu \geqslant 0$, $\eta_\mu \geqslant 0$, $\dot{E}_\mu \geqslant 0$. Indeed, the previously described algorithms for determining $E_\mu(t)$ yield negative E_μ for some μ and some (albeit short) time intervals whenever $J(t,t')$ with divergent creep curves is fitted.

For ageing Maxwell chain models, by contrast, it has been demonstrated (Bažant, 1979) that it is possible to violate inequality (2.71) without violating any of the thermodynamic restrictions. Therefore, the ageing Maxwell chain models are more general in the range of ageing creep forms that they can describe. The equivalence of Maxwell and Kelvin chains to each other as well as to any other rheologic model (Roscoe, 1950) does not quite apply in the case of ageing.

The ageing Maxwell chain model, however, is not entirely trouble-free either. As numerical experience with the fitting of long-time creep data indicates, the condition $E_\mu \geqslant 0$ can be easily satisfied but it has not been possible to identify the condition that $\dot{E}_\mu \geqslant 0$ for all μ and all t. The violations, though, were found to occur only for short time periods and for those Maxwell units which are inactive at the time, i.e. have not started relaxing as yet or have already fully relaxed.

Note that we merely evade the question if we restrict ourselves to an integral-type creep law, for without its conversion to a differential-type form we cannot know whether our formulation of ageing is thermodynamically admissible. We also evade the answer by introducing a differential-type model without recourse to a rheologic spring-dashpot model. (Every differential-type model can be associated with some such rheologic model.)

It should be noted that the rheologic model corresponding to a given compliance function is not unique (Roscoe, Meixner). If we find that a certain creep function $J(t,t')$ leads to one unsatisfactory differential-type model, we are not sure whether the same creep function might also be represented by some other differential-type model that is satisfactory.

To summarize, we have two kinds of differential-type formulations based on ageing rheologic models: (a) those whose form is fundamentally questionable (e.g. Eq. 2.66) because it always violates the dissipation inequality for the internal variables; and (b) those which are of correct form (e.g. Eq. 2.65) and can represent the ageing creep curves for various t' over a limited time range but cannot do so for a broad time range without numerically violating some thermodynamic restrictions ($E_\mu \geqslant 0$ or $\dot{E}_\mu \geqslant 0$) for some period of time. Although for the second kind of models the problems are less severe, no rheologic model with age-dependent $E_\mu(t)$ and $\eta_\mu(t)$ is entirely satisfactory. (*Remark*: Recognition of this fact

has led to a new model described in the Addendum, which describes ageing creep on the basis of a non-ageing rheologic model.)

2.4.5 Thermodynamics of creep mechanism

Valuable information on the form of the constitutive equation for creep and shrinkage can be obtained from mathematical modeling of the processes in the microstructure. This approach, however, is hampered by the fact that knowledge of the microstructural processes is still quite limited at present.

To illuminate the nature of the ageing effect in creep, an attempt was made to deduce the constitutive equation from an idealized micromechanics model of the solidification process in a porous material, describing the increase in stiffness due to the volume growth of the solidified component (Bažant, 1977). This approach led to a certain form of the compliance function, of which the triple-power law (Bažant, 1977; Bažant and Chern, 1985d) is one possible special case. (For a successful application of this approach, see the Addendum to this chapter.)

Thermodynamics has also helped understanding of the equilibrium of various phases of water in concrete and their possible role in creep. This aspect was discussed in Section 2.3.3 in relation to the humidity-rate dependence of creep viscosities and the stress-induced shrinkage.

2.5 FORMULATION OF COMPLIANCE FUNCTION AND SHRINKAGE

2.5.1 Separation of instantaneous deformation and creep

Separation of the stress-produced strain (mechanical strain) into the instantaneous or elastic strain ε_E and the creep strain ε_C is, unfortunately, ambiguous because significant creep exists even for extremely short load durations; see the typical curves at constant stress plotted in Fig. 2.1 in the log-time scale, in which the left-hand-side horizontal asymptote represents the true instantaneous deformation (since $\log 0 = -\infty$). This asymptotic value is difficult to determine experimentally, and it corresponds to load durations that are too short for practical use. Therefore, the deformation which corresponds to some load duration between 1 min and 1 day (Fig. 2.23) is usually considered as the instantaneous or elastic strain.

Regretfully, there is no general agreement as to the definition of the conventional elastic strain. The conventional elastic modulus obtained from the formulas of ACI or CEB–FIP recommendations (e.g. $E = 57\,000\sqrt{f'_c}$) represents approximately one-half of the true instantaneous modulus and corresponds to a load duration of approximately two hours. (The reason for this choice seems to be that it gives good deflection predictions for the load test of a bridge or other structure, which usually takes about two hours.) On the other hand, some

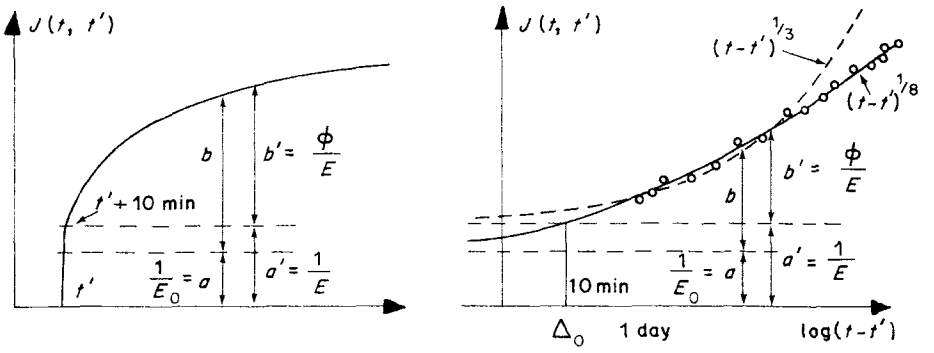

Figure 2.23 Ambiguity in the definition of elastic deformation $1/E$ or $1/E_0$ (left and right), and fits of creep data by power curves corresponding to various values adopted for initial elastic deformation

experimentalists use or tacitly imply the instantaneous deformation to be that for 1–10 min duration (the typical duration of a static strength test in the laboratory), while others use 0.001 sec (rapid loading achieved, e.g., by gas released from an accumulator tank by a valve).

Practically, there would be no problem if one would always base the analysis on the experimentally determined (or predicted) values of the total deformation, i.e. the compliance function $J(t, t')$, because the subdivision of $J(t, t')$ into the elastic and creep parts is artificial and only the total $J(t, t')$-values matter for structural analysis. Much confusion and error, however, has been caused by carelessly combining incompatible values of the elastic modulus $E(t')$ and the creep coefficient $\phi(t, t')$ (e.g. combining a with b' or b with a' in Fig. 2.23). Such practice ought to be avoided, if not outlawed.

There is, of course, no objection to characterizing creep by the creep coefficient $\phi(t, t')$; however, the creep coefficient and the elastic modulus must both be determined from the same compliance function $J(t, t')$, using the same load duration Δ for the initial 'elastic' deformation. This is done by using the relations

$$E(t') = 1/J(t' + \Delta, t') \quad \text{and} \quad \phi(t, t') = [J(t, t')/J(t' + \Delta, t')] - 1$$

Of course, Δ cannot be chosen longer than the shortest creep duration of interest (usually one day) or longer than about 0.3 of the smallest concrete age considered, but otherwise its choice is arbitrary.

2.5.2 Influencing factors

A number of factors influence creep and shrinkage. They may be divided into intrinsic factors and extrinsic factors. The intrinsic ones are those which are fixed once for all when the concrete is cast. They include the design strength, the elastic modulus of aggregate, the volume fraction of aggregate in the concrete mix, the maximum aggregate size, the water–cement ratio, the grading and mineralogical

properties of aggregate, the type of cement, etc. The extrinsic factors are those which can be changed after casting; they include temperature, specific pore water content, age at loading, etc.

Among the extrinsic factors, one must distinguish those which represent state variables and those which do not. The former ones are those which can be treated as a point property of a continuum, and they are the only ones which can legitimately appear in a constitutive equation. The temperature, age, degree of hydration, pore humidity (or pore-water content), and stress represent state variables. On the other hand, the size and shape of cross-section and the environmental humidity are not admissible as state variables in a constitutive equation, even though they have a great effect on creep of a concrete specimen. Properly, the latter variables must be expressed through the boundary conditions for the partial differential equation governing pore humidity. Creep depends directly on the pore humidity, not on the environmental one. These two values are normally quite different because moisture diffusion in concrete is a very slow process.

The effects of state variables, documented by many experimental studies (Neville 1973, 1981; L'Hermite *et al.* 1965; 1968a, b, Wagner, 1958; Lambotte *et al.*, 1976; Hanson, 1953; Hanson and Harboe, 1958; Troxell *et al.*, 1958; Neville *et al.*, 1983; Neville and Dilger, 1970) are as follows. Creep decreases as the age of concrete at the instant of loading increases, which is actually the effect of an increased degree of hydration, and increases as the temperature increases, although this effect is to some extent offset by the acceleration of hydration caused by heating, which tends to reduce creep. The lower the pore-water content, the smaller is creep (see the tests of Ruetz, 1968; Wittmann, 1974; Bažant *et al.*, 1976; Cilosani, 1964 (above 100° C, Bažant and Prasannan, 1987). In most practical situations, however, this local effect is overwhelmed by the effect of the changes in environmental humidity (an extrinsic factor) upon the overall creep of the specimen or structural member. This effect is usually opposite—the creep of a specimen is usually increased, not decreased, by a decrease of environmental humidity (Troxell *et al.*, 1958; L'Hermite, 1965; L'Hermite and Mamillan, 1968a, b). Another extrinsic factor which is not a state variable is the specimen size. The larger the size, the slower the drying process, and the smaller the creep increase due to simultaneous drying (Hansen and Mattock, 1966).

2.5.3 Constitutive properties

The compliance function may be defined by a table of values directly based on experimental data. An interpolation subroutine may then be used to yield any desired value of the compliance function in a computer program. It is, however, more convenient to define the compliance function by a formula. This has the beneficial effect of smoothing rough and randomly scattered test data.

Among simple formulas, the creep of concrete at constant moisture and

thermal state (also called the basic creep) may be well described by power curves of load durations $t - t'$, and by inverse power curves of age t' at loading. This leads to the double power law (Bažant, 1975; Bažant and Osman, 1976; Bažant and Panula, 1978)

$$J(t,t') = \frac{1}{E_0} + \frac{\phi_1}{E_0}(t'^{-m} + \alpha)(t - t')^n \tag{2.72}$$

Approximately, $n \simeq \frac{1}{8}, m \simeq \frac{1}{3}, \alpha \simeq 0.05, \phi_1 \simeq 3$ to 6 (if t' and t are in days), and $E_0 =$ asymptotic modulus (for $\log(t - t') \to -\infty$). $E_0 \simeq 1.5$ times the conventional elastic modulus for concrete 28 days old. These coefficients can be relatively simply determined from test data. For example, by using the foregoing estimates for E_0, m, and α, and plotting $y = \log[(E_0 J - 1)/(t'^{-m} + \alpha)]$ versus $\log(t - t')$, one gets a straight-line plot whose slope is n and y-intercept is ϕ_1. Comparisons with test data are exemplified in Bažant and Panula (1978, 1980).

Since $(t - t')^n = e^{nx}$ where $x = \ln(t - t')$, the power curves of $(t - t')$ appear on a log-time scale as curves of ever-increasing slope and with no bounded final value (Fig. 2.1). The question whether there exists a bounded final value of creep (at $t \to \infty$) has been debated for a long time and no consensus has yet been reached. It is nevertheless clear that if a final value exists it would be reached at times far beyond those of lifetimes of structures. All measurements of creep of sealed or immersed specimens indicate, except for what appears to be statistical scatter, a non-decreasing slope on a log-time scale for the entire test duration. There is *no* evidence of a final value.

For design purposes, however, the question of existence of a bounded final value is not too important because the creep increase from 50 to 100 years is, according to extrapolations of test data (or Eq. 2.72), relatively insignificant (since at very long times the creep curve is approximately a straight line in $\log(t - t')$). Most structures are being designed for 40- or 50-year service lives.

The power law of load duration, first proposed by Straub (1930) and Shank (1935), follows theoretically from certain reasonable hypotheses about the microstructural creep mechanism, e.g. the rate process theory (Wittmann, 1971b, 1974) as well as a statistical model of creep mechanism (Çinlar *et al.*, 1977) or some micromechanics models (Bažant, 1979). Until recently the power law had been used in conjunction with the conventional elastic modulus for the elastic term ($1/E$ instead of $1/E_0$ in Eq. 2.72; see Section 2.5.1). However, this definition of the elastic term greatly restricts the range of applicability. Namely, by choosing the left-hand-side horizontal asymptote to be too high (Fig. 2.23), a higher curvature of the power curve, i.e. a higher exponent (about $n \simeq \frac{1}{3}$), is required in order to fit the creep data for durations from 3 to 100 days. Then the excessively large curvature due to too high an exponent ($\frac{1}{3}$ instead of $\frac{1}{8}$) causes the curve to pass well above the creep data for longer creep durations (over 100 days); see Fig. 2.23. It was for this reason that in the older works the power law was deemed to be applicable only for relatively short times. (For extremely long times,

though, a logarithmic law is no doubt more realistic than a power law; see Eq. 2.75.)

To be able to fit the creep test data with a power law up to many years of duration, the elastic term ($1/E_0$ in Eq. 2.72) must be taken as the true instantaneous value, i.e. as the left-hand-side horizontal asymptote on the log-scale, and the exponent then turns out to be around $\frac{1}{8}$. The double power law thus acquires a rather broad range of applicability. It agrees reasonably well with the known data for creep up to 30 years of duration, and at the same time it describes quite well the test data for load durations under 1 day and as short as 1 sec. It even gives approximately correct values for the dynamic modulus E_{dyn} when one substitutes as the load duration the typical duration of acoustic period, $t - t' \simeq 10^{-7}$ day.

The conventional elastic modulus, along with its age dependence, may be considered as the value of $1/J(t,t')$ for $t - t' = 0.001$ day, for which Eq. (2.72) yields:

$$E(t') = \frac{E_0}{1 + \phi_1'(t'^{-m} + \alpha)}, \qquad \phi_1' = 10^{-3n}\phi_1 \tag{2.73}$$

However, the value obtained by substituting $t - t' = 0.1$ day agrees better with the ACI formula ($E = 57\,000\sqrt{f_c'}$). Note that since four parameters (E_0, m, α, ϕ_1') are needed to describe the age dependence of the elastic modulus, there is only one additional parameter, namely the exponent n, which suffices to describe creep.

Many other expressions for the compliance function have been proposed (Wittmann, 1971b; Bažant *et al.*, 1976). Ross (1937) and Lorman (1940) proposed a hyperbolic expression

$$C(t,t') = \bar{t}/(a + b\bar{t}), \quad \bar{t} = t - t'$$

which is convenient for fitting of test data but unfortunately does not apply to long creep durations (Bažant and Chern, 1982). Neither does Dischinger's (1937) formula, $1 - \exp[-a(t-t')]$. Hanson (1953) proposed a logarithmic law, $C(t,t') = \phi(t')\log(1+\bar{t})$, which does not approach any final value and gives good predictions for rather long creep durations, (see Eq. 2.75) but for short durations is not as good as the double power law. Mörsch (1947) proposed the expression

$$C(t,t') = \phi\{1 - \exp[-(bt)^{1/2}]\}^{1/2}$$

and Branson *et al.* (1970a, b, 1971) proposed the expression $C_u[1 + 10/(t-t')^{0.6}]^{-1}$; these exhibits a final value. The expressions of Ross and Mörsch work somewhat better for creep at drying (see Section 2.5.4). McHenry (1943), Maslov (1941), Arutyunian (1952), Bresler and Selna (1964), Selna (1967, 1969), and Mukaddam and Bresler (1972, 1974), used a sum of exponentials of $t - t'$ with coefficients depending on t'. Such a sum can be closely adapted to any test data (as discussed in Section 2.2.3) if there are at least four exponential terms in the sum.

Various expressions have been introduced with the particular purpose of enabling a certain simplified method of creep structural analysis. These include the expressions of Whitney (1932), Glanville (1930), Dischinger (1937, 1939), England and Illston (1965), and Nielsen (1970, 1977), which all lead to the rate-of-creep (Dischinger's) and rate-of-flow methods for structural analysis and will be mentioned later, and other expressions (Chiorino and Levi, 1967; Arutyunian, 1952; Levi and Pizzeti, 1951).

The double power law exhibits a certain questionable property which was recently discussed in the literature (Bažant and Kim, 1978; Bažant, 1979). It is the property that the creep curves for different ages t' at loading diverge after a certain creep duration, i.e. there exists a time $t - t' = t_D$ (function of t') after which the difference between these curves increases while up to this time it decreases (of Section 2.4.1). This property, which is shared with the ACI recommendation (1971, 1982) but not with the CEB–FIP Model Code (1978), is equivalent to the condition that $\partial^2 J(t,t')/\partial t\,\partial t'$ changes its sign from positive to negative (it is non-negative if there is no divergence). One objection was that the creep recovery curves obtained by the principle of superposition do not have a decreasing slope at all times if the creep curves exhibit the divergence property. This argument, however, is not quite realistic because the principle of superposition does not apply to creep recovery anyway. Further it was thought that the divergence property might violate the second law of thermodynamics but it was proven that this is not so (Bažant and Kim, 1978, 1979b) (see Section 2.4.4). So, whether the divergence property is real depends strictly on experimental observations. The evidence from test data is not without ambiguity; some data do exhibit the divergence, but most do not. It could be that the observed instances of divergence property are due to random scatter or to some non-linear effect. If so, divergence would not belong to function $J(t,t')$. (See also Eq. 2.108.)

Careful examination shows that the double power law exhibits certain deviations from experimental data which seem to be systematic rather than random. In particular, for a short age at loading and a very long load duration, the final slope of the creep curve obtained from the power law is too high. The measured creep curves appear to approach in the $\log(t-t')$ scale a constant slope for very long $t - t'$. An improvement can be obtained by the recently proposed triple power law (Bažant and Chern, 1985d), which specifies the unit creep rate, i.e. the time derivative of the compliance function, as follows:

$$\frac{\partial J(t,t')}{\partial t} = \dot{J}(t,t') = \frac{\psi_1}{E_0}\frac{t'^{-m} + \alpha}{(t-t')^{1-n}(t/t')^n} \tag{2.74}$$

This formula contains one more constant, ψ_1, than the double power law. Some optimum fits of test data from the literature obtained with the triple power law in Bažant and Chern (1985d) are exhibited in Fig. 2.24.

For short load durations, $t - t' \ll t'$, we may substitute $t/t' = 1$, upon which Eq. (2.74) becomes identical to the derivative of the double power law. For load

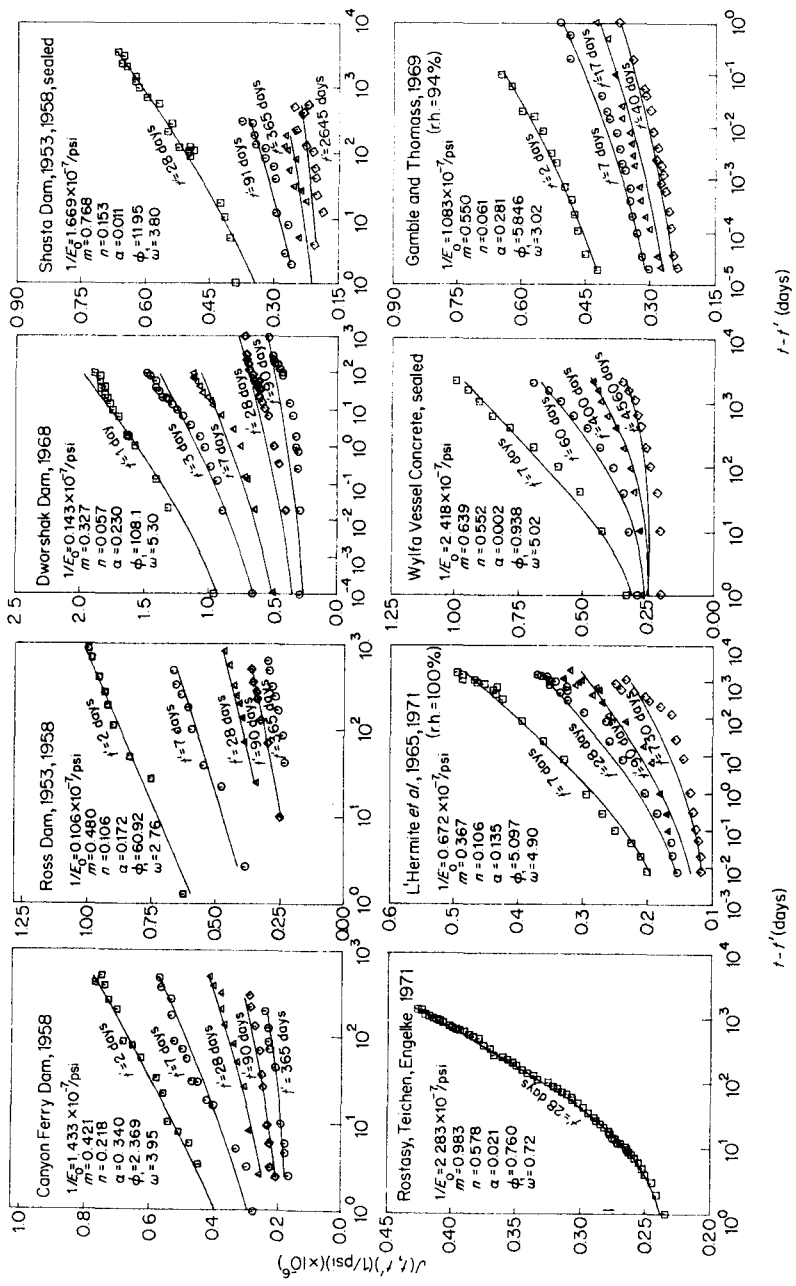

Figure 2.24 Triple power law fits (solid lines) of principal existing measured data for basic creep (Bažant and Chern, 1985d)

durations that are long compared to the age at loading, $t - t' \gg t'$, we may approximately replace $t - t'$ in Eq. (2.74) with t, and upon integration Eq. (2.74) then yields

$$J(t,t') = E_0^{-1}[1 + \psi_1(t'^{-m} + \alpha)t'^n \ln t + f_0(t')] \tag{2.75}$$

This equation represents the logarithmic law, initially proposed by Hanson (1953); it is represented by an inclined straight line in the $\log t$ scale. The compliance function corresponding to the triple power law is obtained by integrating Eq. (2.74):

$$J(t,t') = \frac{1}{E_0} + \frac{\phi_1}{E_0}(t'^{-m} + \alpha)[(t-t')^n - B(t,t';n)] \tag{2.76}$$

in which

$$B(t,t';n) = n\int_{\xi=0}^{t-t'}\left[1 - \left(\frac{t'}{t'+\xi}\right)^n\right]\xi^{n-1}\,d\xi, \qquad \xi = t - t' \tag{2.77}$$

Function $B(t,t';n)$, representing the deviation from the double power law, is a binomial integral, which cannot be expressed in a closed form for realistic values of exponent n. Nevertheless, this integral may be easily evaluated in terms of a convergent power series, or by step-by-step integration in log t scale. A table of values of this integral as well as a graph have also been presented (Bažant and Chern, 1985d).

The triple power law represents a smooth transition from the double power law, applicable for short load durations, to the logarithmic law, applicable for long load durations. The higher the age at loading, the longer is the load duration at which the transition is centred.

Although numerical evaluation of the binomial integral is easy, its use may be avoided by another formula which also represents a smooth transition from the double power law to the logarithmic law and is called the log-double power law (Bažant and Chern, 1985b):

$$J(t,t') = \frac{1}{E_0} + \frac{\psi_0}{E_0}\ln[1 + \psi_1(t'^{-m} + \alpha)(t-t')^n] \tag{2.78}$$

in which $\psi_0 = \phi_1/\psi_1$. Compared to the triple power law, however, Eq. (2.78) has the disadvantage that it is not applicable for very short loading times (below about 0.1 day). Especially, it is not applicable for the dynamic range, because the plot in the log-time scale has initially much too high a curvature, thus yielding too high compliance values.

This last drawback may be avoided, still without the use of binomial integral, by a two-part formula with discontinuous curvature (but continuous slope). This formula uses the double power law for $t - t' \geqslant \theta_L$ where (Bažant and Chern, 1984b)

$$\theta_L = \left(\frac{\phi_L}{\phi_1(t'^{-m} + \alpha)}\right)^{1/n} \tag{2.79}$$

and after this transition time it uses the logarithmic law given by the expression

$$J(t,t') = \frac{\eta\phi_L}{E_0}\ln\frac{t-t'}{\theta_L} + \frac{1+\phi_L}{E_0} \tag{2.80}$$

This expression yields the same compliance value and slope at transition time $t - t' = \theta_L$ as does the double power law (Eq. 2.72) (Bažant and Chern, 1984b).

Compared to the double power law, the triple power law, as well as Eqs (2.78)–(2.80), offers only a relatively modest improvement, as measured by the reduction of the coefficient of variation of the deviations from the bulk of experimental data in the literature. However, this is partly due to the fact that very long loading periods are scant among the existing data. Statistics of the final slope of long-time creep curves compared to the existing observations indicate a significant improvement. Thus, the use of the triple power law is recommended particularly when short-time data are to be extrapolated to long times. (*Remark*: The creep law in the Addendum, however, found after the completion of the committee's work, is superior to triple-power and log-double power laws.)

For extrapolating short-time creep data to long durations, Ross's hyperbola $C(t,t') = \bar{t}(a + b\bar{t})$ (Ross, 1937) has been popular since it makes it possible to obtain the 'final' creep value by linear regression in the plot of $\bar{t}/C$ versus $\bar{t}$. It has been shown, however, that such extrapolation greatly underestimates the long-time value (Bažant and Chern, 1982). Worse yet, due to transformation of variables, the type of regression plot used here obscures the errors and deceives the analyst by an illusion of a good fit.

Consider now the temperature effect. Although it is best introduced only after the compliance function is converted into a differential-type form (Section 2.3.2), the effect of various values of a constant temperature may be also represented in the double power law or the triple power law. The double power law is generalized as

$$J(t,t') = \frac{1}{E_0} + \frac{\phi_T}{E_0}(t_e'^{-m} + \alpha)(t-t')^{n_T} \tag{2.81}$$

in which $t_e' = \int \beta_T(t')\mathrm{d}t'$ represents the age corrected for the effect of temperature on the rate of hydration and is called the reduced age or the equivalent hydration period (or maturity). Coefficients ϕ_T, n_T, and β_T are empirical functions of temperature (Bažant *et al.*, 1976; Gamble and Parrott, 1978) introduced such that, at reference (room) temperature T_0, $\phi_T = \phi_1, n_T = n$, and $\beta_T = 1$. For temperature history that equals T_0 up to time t_0 and then jumps to another constant value T, we have $t_e' = t_0 + \beta_T(t - t_0)$.

2.5.4 Mean cross-section behavior at drying

The best way to represent creep at variable humidity and temperature is to first obtain a differential-type creep law from the compliance function at constant

humidity and temperature, and then to introduce the effect of variable humidity and temperature into the differential-type creep law as well as the boundary conditions. Nevertheless, for many practical applications it is desirable, and probably sufficient for crude calculations, to use a compliance function $\bar{J}(t,t')$ which describes the mean properties of the cross-section of a structural member exposed to drying environment ($h < 1$). The mean compliance function at drying, of course, does not represent a constitutive property of the material; rather, it represents a property of the cross-section as a whole. This property is not really applicable to cross-sections of different sizes or shapes, or other structures. Of course, strictly speaking, different mean compliance functions should be considered for different loading modes, e.g. axial compression, tension, bending, compression combined with bending, torsion, etc.

Since drying is a process governed by diffusion theory, some fundamental laws which result from the diffusion theory must be obeyed by the expressions for shrinkage and the mean compliance function. The first such law concerns the size effect. The diffusion theory (linear as well as non-linear) indicates that the drying times are proportional to the square of the size when geometrically similar specimens or bodies are compared (Fig. 2.25). This same type of size dependence

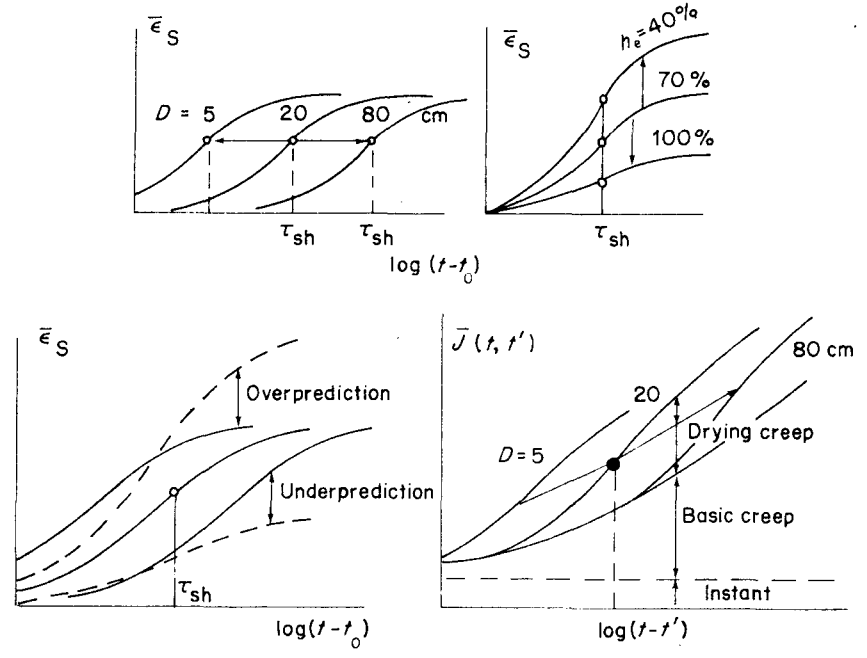

Figure 2.25 Horizontal shift of shrinkage curves due to change of thickness D (top left), vertical scaling of shrinkage curves due to change in environmental humidity h_e (top right), errors in shrinkage prediction when thickness effect is not treated as a horizontal shift in log-time (bottom left), and mean compliance with drying creep for various thicknesses D (bottom right)

must apply to shrinkage since the free shrinkage strain is a function of the pore-water content, which in turn is a function of the pore humidity. In practice, the size-square dependence is not exact, being spoiled by the effects of continuing hydration and microcracking, but it agrees with measurements reasonably well. It also satisfies the obvious limiting conditions due to diffusion theory, namely that if the size of the cross-section tends to infinity the shrinkage must tend to zero (autogenous shrinkage excluded), and so must the additional creep due to the lowered environmental humidity. (Carbonation shrinkage is also a diffusion-type phenomenon, but in good-quality concrete it affects only a thin surface layer.)

For shrinkage, in particular, we have

$$\bar{\varepsilon}_s(t, t_0) = \varepsilon_{sh_\infty} k_h S(\theta) \tag{2.82}$$

where

$$\theta = \frac{t - t_0}{\tau_{sh}}, \qquad \tau_{sh} = c_s \frac{(k_s D)^2}{C_1} \tag{2.83}$$

Here τ_{sh} is the shrinkage square half-time (i.e. the drying time needed for the square of shrinkage strain to reach about 1/2 of its final value); ε_{sh} is a parameter characterizing the final shrinkage which depends on the mix ratios and the strength (typically 0.0005–0.0013). Parameter k_h is a function of environmental humidity h_e; empirically $k_h = 1 - h_e^3$ for $h_e < 0.99$, while for $h = 1.00$, $k_h = -0.2$ may be used to describe swelling. According to Jonasson, k_h should be larger than this when $h_e < 0.4$, and Bažant suggests for the entire range $0 < h_e \leqslant 0.99$ the expression $h_e = 1 - h_e^3 + c_b(1 - h_e)^5$ with $c_b \simeq 1$. Function S gives the evolution of shrinkage in non-dimensional time θ; t_0 is the age at the start of drying; C_1 is the drying diffusivity of concrete at the start of drying (10 mm^2/day, as the order of magnitude); k_s is the shape parameter, which can be calculated from the diffusion theory ($k_s = 1$ for slab, 1.15 cylinder, 1.25 square prism, 1.30 sphere, 1.55 cube); D is the effective thickness of cross-section (in mm), defined as $D = 2v/s$, where v is the volume and s the surface area exposed to drying (for a slab, D represents the actual thickness); and c_s is an empirical constant (taken as 0.267 mm^2).

The second physical law, which results from the diffusion theory, linear as well as non-linear (Bažant, Wittmann, Kim and Alou, 1977), concerns the initial shape of the shrinkage curves:

$$\varepsilon_{sh} \sim D^{-1}\sqrt{(t - t_0)} \quad \text{for small } t - t_0 \tag{2.84}$$

where $\sim$ is the proportionality sign. This law, which is confirmed by careful measurements very well (ibid.), restricts the choice of empirical expressions for the shrinkage curve.

The two physical restrictions in Eqs (2.83) and (2.84) are satisfied by the formula (Bažant, 1986; Wittmann, Bažant, Kim and Alou, 1987):

$$S(\theta) = \left[1 + \left(\frac{\tau_{sh}}{t - t_0}\right)^r\right]^{-1/2r} \tag{2.85}$$

where r is a constant. The original BP model used $r = 1$. It seems, however, that values of r between 0.75 and 0.95 are slightly better.

A further consequence of the diffusion theory is that the effects of temperature T and of the age at the start of drying on shrinkage may be described by means of diffusivity, C_1, and have the form $C_1 = C_0 k'_T k_1$, where C_0 is a constant, k_1 is an empirical function of age t_0; and k'_T is a function of temperature, which may be based on the activation energy theory.

Examples of a comparison between calculated shrinkage curves (for different cylinder diameters and different environmental humidities) and test data from the literature are given in Fig. 2.17. Figure 2.25 illustrates the effect of a change in environmental humidity, h_e, which causes a vertical scaling of the shrinkage ordinates, and the effect of changing the size from D_0 to D, which does not cause a vertical scaling but a horizontal shift of the shrinkage curve in the log-time scale; the shift is by the distance $2\log(D/D_0)$, because $\log\theta = \log(t - t_0) + 2\log D + \text{constant}$ (see Fig. 2.25).

In some other practical formulae (Branson *et al.*, 1970a, b, Branson, 1971; ACI, 1971; Ali and Kesler, 1963), the size effect on shrinkage is handled by scaling the ordinates. This disagrees, however, with the diffusion theory, is not supported by measurements, and leads to under-prediction of long-time shrinkage for thick structural members (Fig. 2.25). The size-square dependence of shrinkage times is the simplest and the most essential property of shrinkage.

The mean compliance function $\bar{J}(t, t')$ of the cross-section in the presence of drying may be expressed approximately as (Bažant *et al.*, 1976; Bažant and Panula, 1978, 1980, 1982).

$$\bar{J}(t, t') = J(t, t') + \bar{C}_d(t, t') \tag{2.86}$$

where $J(t, t')$ is the compliance function for basic creep, i.e. for constant pore humidity (e.g. Eqs 2.72 or 2.76), and $\bar{C}_d(t, t')$ is the mean additional compliance due to drying (including the indirect effect of simultaneous shrinkage).

For a lower humidity, the drying is more severe, and thus the drying creep magnitude is larger when the environmental humidity is lower. When the size tends to infinite, there is no drying in the limit. So the drying creep term $\bar{C}_d$ must decrease with increasing size and approach zero as the size tends to infinity. Yet, some practical models (ACI, 1971, 1982; Branson *et al.*, 1970a; Branson and Christianson, 1971) disregard this condition.

Since drying follows the size-square dependence, the same should be expected of the drying creep term. So we may write, in analogy to Eqs (2.82) and (2.83) for shrinkage,

$$\bar{C}_d(t, t') = \frac{f_d(t')}{E_0} k'_h \bar{S}(\bar{\theta}), \qquad \bar{\theta} = \frac{t - t'}{\tau_{sh}} \tag{2.87}$$

where τ_{sh} is the shrinkage-square half-time (same as in Eq. 2.83), $t - t'$ is the duration of load; k'_h is an empirical function of environmental humidity

($k'_h \simeq 1 - h_e^{1.5}$); $\bar{S}(\bar{\theta})$ is an empirical function of $\bar{\theta}$ similar to $S(\theta)$; and $f_d(t')$ is a decreasing empirical function of age at loading t' (Bažant *et al.*, 1976; Bažant and Panula, 1978). An important property of Eq. (2.87) is that the drying creep term actually represents a shrinkage influence, thus reflecting the fact that shrinkage affects creep and is not simply additive to creep, as the experimentalists have always been emphasizing.

An essential feature is that the size-square dependence is again embodied in Eq. (2.87). A change in size causes a horizontal shift of the curve for the drying creep term in the log-time scale. Thus, superimposing this term on the basic creep, $J(t,t')$, we may imagine the drying term curve to slide on top of the basic creep curve as shown in Fig. 2.25. A change of environmental humidity, on the other hand, causes a vertical scaling of the ordinates of this term. In this manner, many different shapes of the creep curves can be generated. This property is not reflected in the older formulae in which both the humidity and size effects are handled by a multiplicative factor, i.e. vertical scaling of the creep curve. This then leads to underprediction of long-time creep for very thick structural members, and overprediction for very thin ones (as in Fig. 2.25).

The fact that in log-time the slope of the creep curves for a drying environment begins to decline after a certain time period (which depends on the size) appears to be due to the drying creep term. From this decline, however, we may not infer that the creep curves approach a final value since the basic creep term does not approach one.

It must be emphasized that the drying term $\bar{C}_d$ is strictly a cross-section property. No such term is admissible in the constitutive equation or as part of the compliance function characterizing the behaviour at a point of the continuum that approximates concrete.

2.5.5 Rate-of-creep method and related formulations

Until step-by-step computer methods enabled solution of ageing creep problems using a general constitutive law given by any compliance function, it had been necessary to impose upon the compliance function a form that permits a simple analytical solution of typical creep and shrinkage problems. Several such formulations were conceived before the computer era.

One of them uses the compliance function due to Whitney (1930) (Eq. 2.88) for which the stress–strain relation can be reduced to a first-order differential equation corresponding to a Maxwell solid with age-dependent viscosity and elastic modulus. This differential equation, introduced by Glanville (1930) and first extensively applied in structural creep analysis by Dischinger (1937, 1939), was widely used by German, Central European, and Russian engineers. At the same time, US and British engineers favoured the effective modulus method, based on the effective modulus $E_{\text{eff}} = 1/J(t,t')$ proposed by McMillan (1915) and Faber (1927–1928). The structural analysis is simpler for the effective modulus

method since the stress–strain relation is algebraic (quasi-elastic) and no differential equations in time need to be solved, while the rate-of-creep method leads to differential equations in time.

The rate-of-creep method, also called the Dischinger method, gives better predictions for loads applied at a young age, and the effective modulus for loads applied at old age. Generally the errors of both approaches can be quite large, and are overall about equally large for both methods. These errors tend to be on the opposite sides of the exact solution of linear ageing viscoelasticity. So a practically sensible way is to carry out the structural analysis by both methods and then make sure that the design satisfies both of them.

The compliance function used in the rate-of-creep method, which corresponds to an ageing Maxwell solid, has the form

$$J(t,t') = \frac{1}{E(t')} + \frac{\psi(t) - \psi(t')}{E_c} \tag{2.88}$$

in which E_c is a constant, and $\psi(t)$ is a function of one variable, chosen such that $\psi(t) = \phi(t,t_0)$, t_0 being the age at first loading. Obviously, the creep curves for various ages at loading, as defined by Eq. (2.88), are of the same shape and are vertically shifted relative to each other (Fig. 2.1). This property is acceptable for small ages at loading but very poor for old ages at loading.

The advantage of Eq. (2.88) is that when it is substituted into the superposition integral (Eq. 2.6), the integral equation reduces to the differential equation

$$\dot{\varepsilon}(t) = \frac{1}{E(t)}\dot{\sigma}(t) + \frac{\sigma(t)}{E_c}\dot{\psi}(t) \tag{2.89}$$

according to which the creep rate is independent of the past stress history. Structural analysis based on this equation is called the rate-of-creep method or Dischinger method. Structural analysis problems may then be reduced to differential equations which can be solved particularly easily if the elastic modulus $E(t)$ is replaced by a constant. It is now known, however, that the error due to the rate-of-creep method can be quite large (Bažant and Najjar, 1973) and exceed even 50 per cent of the exact results, although in many situations useful results can still be obtained.

Under stress relaxation regimes (declining stress), the solutions based on Eq. (2.89) overestimate the stress changes due to creep, and under increasing stress regimes (e.g. creep buckling), they underestimate the changes due to creep. These errors are opposite to the errors of the effective modulus method. A particularly severe limitation is the fact that Eq. (2.88) yields almost no creep for loads applied at very high ages. Nevertheless, when the stress change from t_0 to t is small, the results of both methods are good.

To remedy the aforementioned problems, a certain combination of the rate-of-creep method and effective modulus method, known as the improved Dischinger method, was proposed by Fuglsang Nielsen (1970), Rüsch *et al.* (1973),

and others on the basis of England and Illston's (1965) rate-of-flow method. These formulations introduce the compliance function in the form

$$J(t,t') = \frac{1}{E(t')} + \frac{1}{E_{ef}^{d}} + \frac{\psi(t) - \psi(t')}{E_c} \tag{2.90}$$

in which E_{ef}^{d} is assumed to represent an additional elastic deformation imagined as delayed. Properly, this additional deformation is a function of $t - t'$. For the sake of simplification, however, this dependence is neglected in computations and E_{ef}^{d} is treated as the effective modulus for the delayed elastic deformation.

This treatment of the delayed elastic deformation would have a small error if its final value were independent of the age at loading, t', and if the delayed elastic deformation reached its final value in a relatively short time (about 100 days was assumed). Subsequent comparisons with extensive test data, however, indicated that these assumptions are not very close to reality. According to many data (Jessop, 1969, 1971; England and Illston, 1965; Roll, 1964; Jordan and Illston, 1971; Hanson, 1953; Ross, 1958a; Glucklich, 1959; Ishai, 1964; Kimishima and Kitahara, 1964), the strains identified as delayed elastic deformations are in fact strongly dependent on the age at loading, representing from 15 to 90 per cent of the initial elastic strain after a period of a few months (Bažant and Osman, 1975). Moreover, the recovery curves tend to be essentially straight lines in the logarithmic time-scale for a long period of time (Bažant and Osman, 1975), indicating that the final value of the delayed elastic strain is not reached very soon.

From the thermodynamic viewpoint, the separation of the total creep strain into a reversible component (delayed elasticity) and an irreversible component (flow, corresponding to the dashpot of the Maxwell model) is not justified if the material undergoes ageing. In the presence of ageing, separation of irreversible and reversible strains is in a strict sense possible only for the strain increments, but not for the total strains (see Addendum to this chapter).

Nevertheless, the rate-of-flow method or improved Dischinger method (Eq. 2.90) represented in the 1960s a great improvement compared to the previously used rate-of-creep method (Dischinger method) or the effective modulus method. It significantly reduced the error of creep calculations compared to these two previous methods. However, the age-adjusted effective modulus method, which was in approximate terms proposed by Trost (1967) and was rigorously formulated by Bažant (1970d, 1972b) based on his proof of a mathematical theorem (see Chapter 3), has an even smaller error compared to the exact solutions according to the principle of superposition if an arbitrary form of $J(t,t')$ is used (this principle is assumed or implied in all the existing practical simplified methods of creep analysis). When $J(t,t')$ is given in the special form of Eq. (2.90), then of course the error of neither method is large. The age-adjusted effective modulus is applicable to any experimentally determined form of the compliance function, and does not force the analyst to describe his creep data by

any particular formula, such as Eq. (2.90). Thus, although the rate-of-flow method or improved Dischinger method was a historically important development, the subsequently developed age-adjusted effective modulus method can now give overall better results compared to the exact solutions of linear ageing viscoelasticity (Bažant and Najjar, 1973).

Various expressions for the compliance function, including Eq. (2.90), have been thoroughly evaluated in comparison to the numerous creep data existing in the literature (Bažant and Osman, 1975; Bažant and Thonguthai, 1976; Bažant and Panula, 1978, 1980; Bažant *et al.*, 1983). It was found that Eq. (2.90) does not permit close approximation of long-time creep curves for the data that involve a wide range of the ages at loading, especially not for the basic creep (constant humidity and temperature). The main reason is that Eq. (2.90) can be fully calibrated according to the creep curve for one small age at loading and one creep recovery test, the creep curves for other (higher) ages at loading representing superfluous information. It has often been argued that one is rewarded with a better description of the creep recovery. This is, however, not quite true for long-time recovery tests and recovery tests after very different durations of the previous constant load and at very different ages at loading and unloading. Moreover, it is of questionable merit to base the compliance function on creep recovery tests, for two reasons: (1) most practical applications do not involve sudden unloading; and (2) the principle of superposition is inapplicable to unloading anyway; see Addendum. (This does not exclude stress relaxation at which the strain is constant, although the stress decreases; for stress relaxation the principle of superposition applies very well.)

2.5.6 Practical creep prediction models

Since experimental data on creep and shrinkage for the particular structure to be designed are often lacking and are at best only limited, the creep and shrinkage characteristics must be predicted from various influencing factors known in advance, such as the design strength, water–cement ratio, temperature, etc. Two types of prediction must be distinguished.

1. Prediction of constitutive properties for creep and shrinkage

This is the type of prediction that needs to be used as the input for finite element computer programs. The practical prediction models contained in the recommendations of engineering societies (ACI, 1971, 1982; CEB–FIP, 1978) do not predict constitutive properties but mean cross-section properties when environmental humidity or temperature changes are involved, as is usually the case. Even for the case of constant humidity and temperature these prediction models are inappropriate because they are intended to describe primarily concrete structures exposed to moderate climatic conditions and do not work

well for basic creep (i.e. creep at constant humidity and temperature, or creep of mass concrete). Neither are these models intended for harsh climates (e.g. tropical, desert, continental, or arctic); they have been calibrated for moderate climates. These models from the current society recommendations, utilizing among material parameters the environmental humidity rather than the pore humidities inside concrete, are incapable of providing stress and strain distributions throughout the cross-sections of beams and walls. Their purpose is the calculation of the distribution of bending moments and deflections in structures.

A comprehensive creep and shrinkage prediction model which gives cross-section properties as well as constitutive properties and can be used for finite element programs has been developed by Bažant and Panula (1978) (with a later extension to high strength concrete, Bažant and Panula, 1984; and to cyclic humidity, Bažant and Wang, 1985a). Only that part of the model which gives the compliance function for constant humidity and temperature (basic creep) and the final shrinkage coefficient with drying diffusivity, may be used for the prediction of constitutive properties. The compliance function is then converted by a special input subroutine (Bažant, 1982; Bažant *et al.*, 1981; Ha *et al.*, 1984; Section 2.5.7) to a differential-type form. The effect of variable pore humidity and temperature is then brought in through the dependence of the viscosities of the rate-type model on temperature and humidity and through the stress-induced parts of shrinkage and thermal expansion, as described in Sections 2.3.2 and 2.3.3.

It is impossible to characterize the constitutive properties for variable pore humidity and temperature in terms of the compliance function, because the differential-type stress–strain relation cannot be explicitly integrated if the pore humidity or temperature is arbitrarily variable. The integration is possible only for specified temperature and humidity histories, but then a different compliance function would be obtained for each different history. Moreover, the compliance function would depend on the stress level because the humidity effect is non-linear due to cracking.

2. *Prediction of mean cross-section properties*

This is the only type of prediction that is addressed by the engineering societies in their current design recommendations. This type of prediction is intended mainly for the analysis of bending moments and deflections of beam structures for which the stress distributions within the cross-section are not particularly needed. The objective of describing the cross-section creep and shrinkage properties as a whole introduces inevitably a large additional error, and also restricts the applicability of the prediction model to a narrow range of conditions (e.g. narrow range of cross-section sizes, of temperature, of climates, etc.). Furthermore, the prediction of cross-section properties in the mean is usually designed to work for axial compression (since it is based on test data for compression creep) and does not apply very well to bending or combinations of axial force and bending moment because for each different combination a different set of prediction formulas would be needed, which is ignored for practical reasons. If a greater range of applicability is intended, as in the BP model, a considerably more complex set of formulas inevitably results.

Although a reasonable prediction of creep and shrinkage properties for a certain range of typical conditions is intended, the committees of engineering societies have required that their prediction models must be relatively easy to evaluate from the available empirical data, and that their formulas must be simple so as to make the numerical evaluations straightforward. The requirement of simplicity should, however, be viewed in proper perspective. Generally, the effort spent on determination of the material properties should be commensurate to that devoted to the structural analysis itself. Since inaccuracies in material characterization usually cause by far the most serious errors in the results of structural analysis, it makes no sense if the analyst spends, say, only four hours on predicting the compliance function and shrinkage formula, and then spends one week to carry out the structural analysis. He should spend equal time on both tasks. In this perspective, the widespread desire to keep the prediction of material properties trivially simple appears to be misguided. No doubt this tendency is due mainly to the fact that the task is handled by structural analysts who are well trained to carry out structural analysis (and do not mind spending much time for this purpose), rather than materials engineers. (Perhaps if this task were handled by material scientists, they would wish to spend only one hour on structural analysis and would not mind devoting a week to material parameter determination; simply, the bias due to narrow professional training is part of the problem.)

The error of the current prediction models by the committees of engineering societies is enormous; the 95 per cent confidence limits are around $\pm$ 80 per cent! (Bažant and Panula, 1978, 1980; Bažant and Zebich, 1983). This magnitude of error in fact makes computer analysis meaningless. Even a substitution of the simple portal frame analysis formulas for a statically indeterminate analysis of a frame structure involves much less error than do these current prediction models of engineering societies. Without drastic improvement, computer analysis of creep and shrinkage hardly makes sense for these prediction models.

Several practical models for predicting mean cross-section creep and shrinkage exist at present. They differ in their degree of accuracy and simplicity, and naturally one of these must be traded for the other. These models are:

1. Model of ACI Committee 209 (1971, 1982), and Branson *et al.* (1970a, b, Branson, 1971).
2. Model of CEB–FIP Model Code (1978), and Rüsch *et al.* (1973).
3. BP Model, either its complete version or its simplified version (Bažant and Panula, 1978, 1980), with extensions in Bažant and Panula (1984) and Bažant and Wang (1985a).

The ACI Model is the simplest one, while the BP model is the most

comprehensive one, being applicable over the broadest time range (of t, t', and t_0) and covering a number of influencing factors neglected by the other two models. It should be remembered that all three models are at least partially empirical, albeit to various extents, and are all based on the fitting of data obtained in laboratory controlled tests. Attempts at verification by measurements on structures in the field have so far been inconclusive, for three reasons: (1) the difficulties in sorting out various influencing factors, which are much more numerous than in laboratory tests; (2) the large statistical scatter due to outdoor environment; and (3) the fact that many important influencing factors were not reported or not even determined.

ACI model. Based on the works of Branson *et al.* (1970a, b, 1971), the ACI Committee 209 (1971, 1982) recommended the expressions:

$$\bar{J}(t,t') = \frac{1}{E(t')}\left(1 + \frac{(t-t')^{0.6}}{10+(t-t')^{0.6}}\right)C_u, \qquad \bar{\varepsilon}_s(t,t_0) = \varepsilon_u^s \frac{t-t_0}{f_c+(t-t_0)} \tag{2.91}$$

in which t' is the age at loading in days, t is the current age in days, t_0 is the age of concrete in days at the completion of curing; f_c is a constant; C_u is the ultimate creep coefficient defined as the ratio of the (assumed) creep strain at infinite time to the initial strain at loading; and ε_u^s is the ultimate shrinkage strain after infinite time. Coefficients C_u and ε_u^s are defined as functions of six factors: environmental humidity, minimum thickness of structural member, slump, cement content, per cent fines, and air content.

CEB–FIP model (1978). According to the CEB–FIP Model Code (1978, Annexe e; see also Rüsch *et al.*, 1973, with corrections in CEB, 1981, and Chiorino *et al.*, 1984, Appendix B):

$$\bar{J}(t,t') = F_i(t') + \frac{\phi_d \beta_d(t-t')}{E_{c28}} + \frac{\phi_f[\beta_f(t)-\beta_f(t')]}{E_{c28}} \tag{2.92}$$

$$\bar{\varepsilon}_s(t,t_0) = \varepsilon_{s_0}[\beta_s(t)-\beta_s(t_0)] \tag{2.93}$$

in which E_{c28} is the elastic modulus of concrete at age 28 days; $\phi_d = 0.4$; ϕ_f is a coefficient depending on the environmental humidity and the effective thickness of member; β_t and β_s are functions of the age and the effective thickness; β_d is a function of the load duration $t-t_0$; $F_i(t')$ (representing the sum of instantaneous strain and initial creep strain over a period of several days) is a function of the age at loading. These functions are defined by graphs consisting of sixteen curves. Formulas approximating these graphs were published in Appendix D of Chiorino *et al.* (1984).

BP model. This model utilizes Eqs (2.72) and (2.82)–(2.87), whose basic forms ensue from diffusion theory and activation energy theory, as already explained.

The coefficients in these equations are expressed by empirical formulas determined from test results. For the case of drying, these formulas are relatively complicated. This is, however, at least partly due to consideration of many influencing factors and to a broad range of applicability. A program for computer evaluation of the BP model and its fitting to given data is available; see the full program listing in Bažant (1982) and its improvement with a manual by Ha *et al.* (1984). Extensions of the BP model were later developed for high-strength concretes (Bažant and Panula, 1984) and cyclic humidity (Bažant and Wang, 1985a). The long-time creep predictions of the BP Model may be improved by replacing in the basic creep term the double power law with the triple power law (Bažant and Chern, 1985d).

Comparison of existing models

For basic creep, the BP model and the ACI model have in common the product form of the compliance function, in which a function of the age at loading multiples a function of the stress duration. In the ACI model, however, the multiplicative factor C_u introduces not only the effect of age at loading but also the effect of humidity and size. This is very simple but not quite realistic. As stressed in Section 2.5.4, the diffusion theory leads to a different form of the size effect, which amounts to translation in log-time rather than vertical scaling of the ordinates. The same deficiency characterizes the ACI shrinkage formula (Eq. 2.91).

Likewise, the CEB–FIP model (1978) does not follow the size effect of the diffusion theory. In this model, the basic form of $\bar{J}(t,t')$ is based on the idea of reversibility of deformation. The second term in Eq. (2.92) is considered to represent the so-called reversible (or delayed elastic) creep, and the last term the so-called irreversible creep. It must be noted, however, that in the case of ageing the concept of a reversible creep component lacks theoretical (thermodynamic) justification because this component cannot be defined uniquely (only reversible creep increments can, Bažant, 1979).

The fact that in the CEB–FIP model the so-called 'reversible' component of $\bar{J}(t,t')$ was calibrated by fitting the creep recovery curves obtained from the superposition principle to recovery test data has been questioned (Bažant and Osman, 1975; Bažant and Thonguthai, 1976; Bažant and Panula, 1980). The reason was that linear superposition does not hold in the case of unloading, as has been conclusively demonstrated by tests. The domain of approximate validity of the principle of superposition includes only non-decreasing strain histories within the service stress range. Thus, only the creep curves for various ages at loading and the relaxation curves, which belong to this domain, appear to be suitable for calibrating the compliance function.

The fact that the second term in Eq. (2.92) is assumed to be independent of t and the last one independent of $t-t'$ is also questionable in regard to test data

(Bažant and Osman, 1975; Bažant, 1979). Another aspect which was criticized on the basis of test data is that the humidity and size influences in Eq. (2.92) appear only in the irreversible term (Bažant and Panula, 1982), and that the size effect in the shrinkage term does not agree with the observations, whereas the prediction of a model based on the diffusion theory is in agreement.

It has often been claimed that for structures exposed to outdoor environment the creep prediction formulas need not fit the basic creep data (sealed specimens) and need to be calibrated only according to the creep data for standard cylinders (15 cm diameter) exposed to about 65 per cent relative humidity. This view, however, is unjustified, because structures often involve walls over 30 cm thick, whose creep is actually closer to the creep of sealed specimens (basic creep) then to the creep of drying standard specimens; see the reply to the discussion of Bažant and Zebich (1983).

The BP model is the only one which involves the influence of temperature. It describes this influence for shrinkage, basic creep, and drying creep. It also gives the effect of the load cycling (pulsation), cyclic variation of environmental humidity (Bažant and Wang, 1985a), the effects of the delay of the start of loading after the start of drying, the time-lag of loading after heating, the decrease of creep after drying, swelling in water, autogenous shrinkage of sealed concrete (Honk *et al.*, 1969), etc. The price paid for this broader range of applicability is greater complexity.

The BP model differs from the ACI and CEB–FIP models also by the absence of a final (asymptotic) value of creep, as it has already been commented upon.

The BP model was obtained by computer analysis and fitting of 80 different data sets on different concretes from different laboratories (over 800 creep and shrinkage curves involving about 10000 data points). Based on this quite complete, computerized data bank (Bažant and Zebich, 1983), the 95 per cent confidence limits (i.e. the relative deviations from the mean that are exceeded with a probability of 2.5 per cent on the plus side and 2.5 per cent on the minus side) were found for the BP Model to be $\omega_{95} = \pm 37$ per cent. For the ACI model, comparisons with the same data indicated $\omega_{95} = \pm 77$ per cent, and for the CEB–FIP model $\omega_{95} = 92$ per cent (Bažant and Panula, 1980). The effects which are ignored by the ACI and CEB–FIP models, such as temperature effects, could not be included in the calculation of these statistics, although the BP model describes them quite well.

The majority of the existing test data that could be used for these comparisons pertained to small-size specimens and to a limited time range, i.e. $t - t'$ ranging from one week to one year and t' from one week to six months. The ACI and CEB–FIP models describe this limited range better than the data for large specimens or long times. For very long creep durations (> 10 years), for very high or very small ages at loading (> 10 years, < 10 days), for thick specimens (> 30 cm), and for the final slopes of creep curves (which matter for extrapolation), the comparison is even more favourable to the BP model.

For drying creep alone, however, the confidence limits of the BP model ($\omega_{95} = \pm 35$ per cent) are only slightly better than those of CEB–FIP model (± 39 per cent) and not much better than those of ACI model (± 51 per cent). These two models are of course intended mainly for not too massive (average size) structures in a moderate climate.

Although the foregoing error statistics are probably the best that can be inferred from the presently available test data, it should be recognized that corrections to these numbers should be made to eliminate the errors due to the conduct of tests, e.g. to unreliable load control, zero drift over long times, gauge instability, inadequate environmental control, etc. These measurement errors (which are, of course, not 'felt' by structures), could possibly be quite large, but it is difficult to estimate their magnitudes, especially retroactively, after the tests. So these corrections to the error values given above cannot be determined at present. On the other hand, noting that the total coefficient of variation ω can be approximately written as $\omega \simeq (\omega_0^2 + \omega_m^2)^{1/2}$, we have $\omega_0 \simeq \omega[1 - (\omega/\omega_m)^2]^{1/2}$ (where ω and ω_m are the coefficients of variation due to the material and to the measurement), we can see that even measurement errors as large as $\omega_m = 0.25\omega$ (i.e. about 11 per cent of mean strain when ω for the ACI model is considered) would reduce ω only by 3 per cent, i.e. to $\omega_0 = 0.97\omega$ (for $\omega_m = 0.1\omega$, $\omega_0 = 0.995\omega$). Simply, the coefficients of variation of errors are not added linearly; only the largest errors matter. Thus, the measurement errors have little effect unless their magnitudes were comparable to the magnitude of material scatter, which is unlikely. Moreover, the hand-smoothing of raw test data, made before the aforementioned statistics were calculated, eliminates a part of the measurement error which is of a randomly fluctuating nature. Hence, the aforementioned confidence limits are probably reasonably good estimates.

The foregoing statistics were determined from laboratory data. For structures in outdoor environment, further errors due to the random fluctuations of environmental humidity and temperature would have to be added, making the uncertainties even larger (cf. Chapter 5, and Bažant and Wang, 1984a).

In view of the large magnitude of error of the existing models, there is no doubt much room for improvement. The greatest part of the error results from the effects of composition of concrete. This is documented by the fact that the prediction errors can be greatly reduced when the initial elastic deformation or one short-time shrinkage value is measured (Bažant and Panula, 1980; Bažant *et al.*, 1987), provided that a correct theory is used (e.g. size effect agreeing with the diffusion theory). Finite element analysis hardly makes sense if the error in $J(t, t')$ exceeds 20 per cent, and so availability of some short-time tests is a requirement for practical applications, in addition to the use of a physically correct theory. Also preferable are such creep and shrinkage prediction formulas which are easily amenable to statistical extrapolation from given short-time values by regression (Bažant and Panula, 1980; Bažant *et al.*, 1987; Bažant and Zebich, 1983).

At present no consensus on the proper form of the compliance function $J(t,t')$

or $\bar{J}(t,t')$ has yet been reached. Much of the disagreement is due to the great statistical scatter of the available test data, which obscures the underlying mean trend. But it may be also due to the fact that a linear theory is used for a phenomenon which is not really linear, i.e. necessitates a non-linear theory. A linear theory can be adequate only within a limited range, and specialists still disagree as to what is this range, in particular what is the type of tests to be used for determining the compliance function for a linear theory. Some include only creep or relaxation tests for all ages at loading, which alone define the compliance function completely, while others include information from creep recovery tests (without analysing them by a non-linear theory) at the cost of sacrificing a good fit of the measured creep curves for high ages at loading and long times. Because a non-linear theory is not at present considered appropriate for building codes, the question is which form of the compliance function can give the best results in practical problems over the broadest possible range.

Since prediction of the long-time creep is of main interest, efforts have been made to compare the creep prediction models with the final creep values deduced directly from creep measurements. Such comparisons, however, suffer by the error which inevitably occurs in deducing such final values from the test data. This error may be just as large as the error of the creep model that is supposed to be checked.

For example, it has become almost traditional for the experimentalists to use the Ross hyperbola (Ross, 1937; Neville, 1973, 1981; Neville and Dilger, 1970, Nevile *et al.*, 1983): $C = \bar{t}/(a + b\bar{t})$, where $\bar{t} = t - t'$ and $C = J(t,t') - 1/E(t')$. This relation may be written as $\bar{t}/C = a + b\bar{t}$. So, if one plots the measured data as $\bar{t}/C$ versus $\bar{t}$ and approximates this plot by a straight regression line, the slope of the line is b, its intercept with the vertical axis is a, and the value of inverse slope $1/b$ is the extrapolated 'final' value of creep ($\bar{t} \to \infty$). Alternatively, one may also write $1/C = b + a/\bar{t}$ and plot $1/C$ versus $1/\bar{t}$, in which case the slope of the regression line is a and its vertical intercept is b. Either of these plots looks very satisfactory if the creep data span over a limited time period such as from $\bar{t} = 1$ week to 1 year, and consequently one is induced to believe that the 'final' creep value obtained from this plot is good. Only such limited data were available in the early investigations in the 1930s, and so the use of Ross's hyperbola appeared adequate and became standard practice.

At present, however, long-range creep measurements of basic creep are available, and then gross deviations from Ross's hyperbola are found (Bažant and Chern, 1982). Worse yet, regression plots of Ross's hyperbola have the property of concealing errors. Even when the errors are blatant in the plot of $J(t,t')$ versus $\log \bar{t}$, they are barely noticeable in the plot of $\bar{t}/C$ versus $\bar{t}$. In the plot of $1/C$ versus $1/\bar{t}$, the inverse scales of $1/C$ and $1/\bar{t}$ obscure the errors for long times by crowding together the points for large C and large $\bar{t}$. The plot of $C/\bar{t}$ and $1/\bar{t}$ is dominated by the deterministic dependence of $1/\bar{t}$ on $1/\bar{t}$, and is little influenced by the scatter of C. Still another element of error and ambiguity was

already discussed, namely the value to be used for $E(\bar{t})$, which must be decided before the regression plot can be constructed. To sum up, the use of Ross's hyperbola for long-time creep extrapolation ought to be abandoned.

The extrapolated final values of certain creep tests obtained from creep test data on the basis of Ross's hyperbola were recently compared by a CEB committee with various models for creep prediction. The committee concluded that the agreement was best for the CEB–FIP 1978 Model Code. From the preceding analysis (Bažant and Chern, 1982), however, it is clear that such a method of comparison of various models is questionable. The final value found by extrapolating the test data strongly depends on the choice of the expression for the creep curve, in this case the Ross hyperbola, and the error of the long-time values of Ross's hyperbola compared to more realistic expressions, such as the double power law, is easily 50 per cent.

2.5.7 Input of material parameters for structural analysis computer programs

Different characterizations of creep and shrinkage may be appropriate in various situations. For the input of material properties, subroutine MATPAR, used in finite element program CREEP 80 (Bažant and Rossow, 1981; Bažant *et al.*, 1981) and listed in full in Bažant (1982a) is very effective. This subroutine was further improved and is available form Ontario Hydro (Ha *et al.*, 1984). The subroutine has the following options:

1. $J(t,t')$ is specified as an array of values; no drying.
2. $\bar{J}(t,t')$ and $\varepsilon_s(t,t_0)$ are specified as an array. Drying.
3. $J(t,t')$ is given by the double power law, for which all parameters are given; no drying.
4. Same as (3) but all double power law parameters except E_{c28} are generated from the given strength and composition parameters.
5. Same as (4) except that E_{c28} is also predicted from the strength and composition parameters.
6. $\bar{J}(t,t')$ is defined by the double power law plus the drying term $C_d(t,t')$ and shrinkage is given by a formula. All parameters are given.
7. Same as (6) but all parameters except E_{c28} and ε_{sh} are predicted from the strength and composition.
8. Same as (6) but all parameters except E_{c28} are predicted from the strength and composition.
9. Same as (6) but all parameters are predicted from the strength and composition.
10. The double power law parameters E_0 and ϕ_1 are determined by the best fit of the given array of values $J(t,t')$ which may be of limited range; m, n, α are given. No drying. Coefficient of variation for the deviations from given $J(t,t')$ is computed and printed.